Chaos via torus destruction in models of dengue fever and predator-prey systems, implications for data analysis

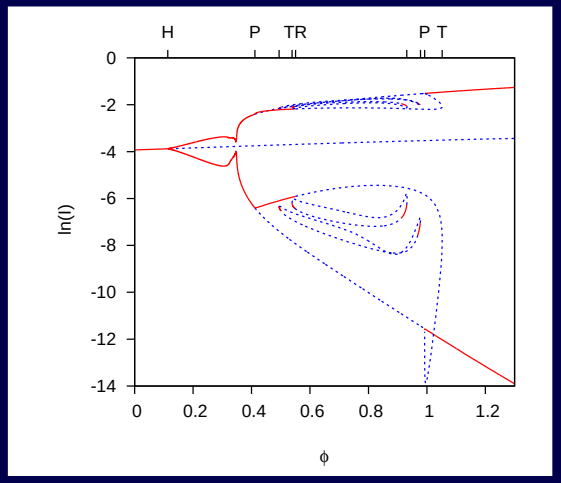

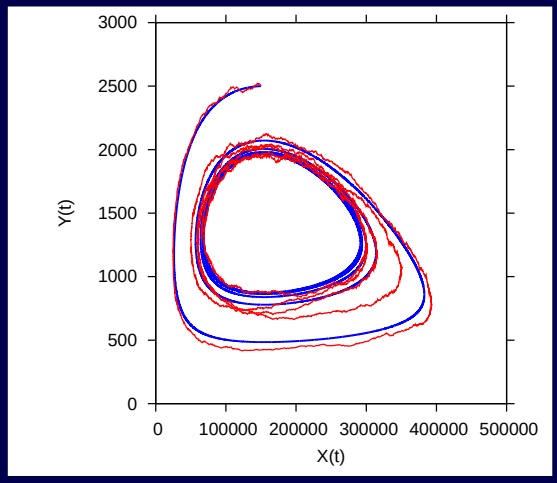

Nico Stollenwerk, Pablo Fuentes Sommer, Bob Kooi, Luís Mateus, Peyman Ghaffari, Maíra Aguiar

Biomathematics and Statistics Group

Centro de Matemática, Aplicações Fundamentais e Investigação Operacional (CMAF-CIO), Univ. Lisboa, Department of Theoretical Biology, Vrije Universiteit Amsterdam

Explicit multi-strain models:
example: dengue fever

simplest example: two-strain SIR model
including antibody dependent enhancement (ADE)

=> chaos only for large ADE parameter ϕ

biologically motivated extension
including temporary cross immunity

=> chaos for much wider ϕ–region
(also for "inverse ADE")

Explicit multi-strain models:
example: dengue fever

simplest example: two-strain SIR model
including antibody dependent enhancement (ADE)

=> chaos only for large ADE parameter ϕ

biologically motivated extension
including temporary cross immunity

=> chaos for much wider ϕ–region
(also for "inverse ADE")

via Hopf, torus bifurcations and torus destruction

Antibody dependent enhancement, ADE

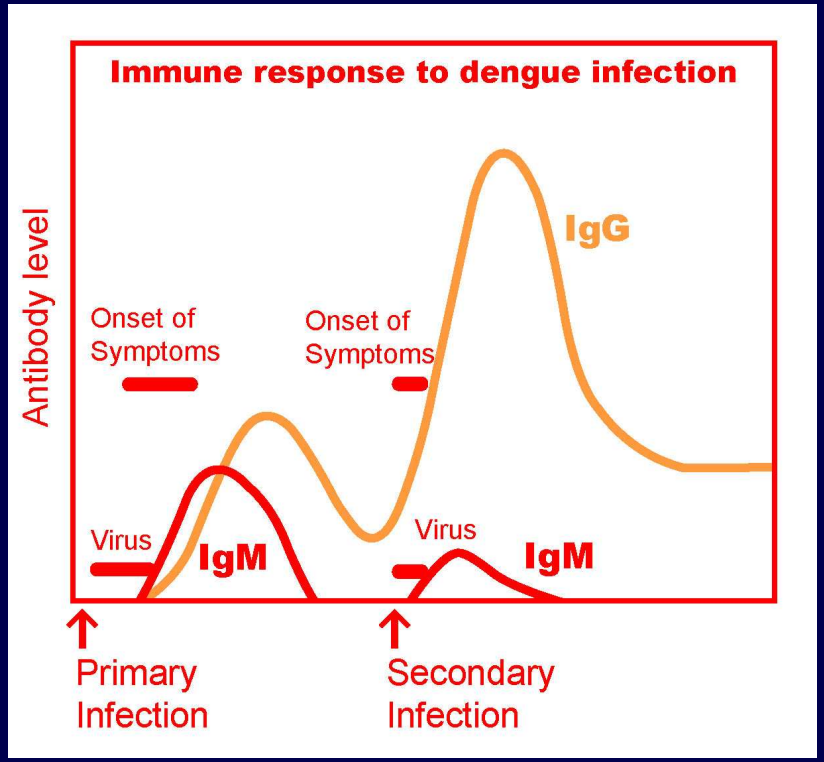

... and temporary cross-immunity

Transition rates for two-strain SIR model with ADE and temporary cross immunity

$$
\begin{aligned}
S + I_1 &\xrightarrow{\beta_1} I_1 + I_1 \\
S + I_{21} &\xrightarrow{\phi_1\beta_1} I_1 + I_{21} \\
I_1 &\xrightarrow{\gamma} R_1 \\
R_1 &\xrightarrow{\alpha} S_1 \\
S_1 + I_2 &\xrightarrow{\beta_2} I_{12} + I_2 \\
S_1 + I_{12} &\xrightarrow{\phi_2\beta_2} I_{12} + I_{12} \\
I_{12} &\xrightarrow{\gamma} R
\end{aligned}
$$

Transition rates for two-strain SIR model with ADE and temporary cross immunity

$$
\begin{aligned}
S + I_1 &\xrightarrow{\beta_1} I_1 + I_1 \\
S + I_{21} &\xrightarrow{\phi_1\beta_1} I_1 + I_{21} \\
I_1 &\xrightarrow{\gamma} R_1 \\
R_1 &\xrightarrow{\alpha} S_1 \\
S_1 + I_2 &\xrightarrow{\beta_2} I_{12} + I_2 \\
S_1 + I_{12} &\xrightarrow{\phi_2\beta_2} I_{12} + I_{12} \\
I_{12} &\xrightarrow{\gamma} R
\end{aligned}
$$

Transition rates for two-strain SIR model with ADE and temporary cross immunity

$$
\begin{aligned}
S + I_1 &\xrightarrow{\beta_1} I_1 + I_1 \\
S + I_{21} &\xrightarrow{\phi_1\beta_1} I_1 + I_{21} \\
I_1 &\xrightarrow{\gamma} R_1 \\
R_1 &\xrightarrow{\alpha} S_1 \\
S_1 + I_2 &\xrightarrow{\beta_2} I_{12} + I_2 \\
S_1 + I_{12} &\xrightarrow{\phi_2\beta_2} I_{12} + I_{12} \\
I_{12} &\xrightarrow{\gamma} R
\end{aligned}
$$

Multi-strain model for dengue fever

$$
\begin{aligned}
\frac{dS}{dt} &= -\frac{\beta_1}{N} S(I_1 + \phi_1 I_{21}) - \frac{\beta_2}{N} S(I_2 + \phi_2 I_{12}) + \mu(N - S) \\
\frac{dI_1}{dt} &= \frac{\beta_1}{N} S(I_1 + \phi_1 I_{21}) - (\gamma + \mu) I_1 \\
\frac{dI_2}{dt} &= \frac{\beta_2}{N} S(I_2 + \phi_2 I_{12}) - (\gamma + \mu) I_2 \\
\frac{dR_1}{dt} &= \gamma I_1 - (\alpha + \mu) R_1 \\
\frac{dR_2}{dt} &= \gamma I_2 - (\alpha + \mu) R_2 \\
\frac{dS_1}{dt} &= -\frac{\beta_2}{N} S_1(I_2 + \phi_2 I_{12}) + \alpha R_1 - \mu S_1 \\
\frac{dS_2}{dt} &= -\frac{\beta_1}{N} S_2(I_1 + \phi_1 I_{21}) + \alpha R_2 - \mu S_2 \\
\frac{dI_{12}}{dt} &= \frac{\beta_2}{N} S_1(I_2 + \phi_2 I_{12}) - (\gamma + \mu) I_{12} \\
\frac{dI_{21}}{dt} &= \frac{\beta_1}{N} S_2(I_1 + \phi_1 I_{21}) - (\gamma + \mu) I_{21} \\
\frac{dR}{dt} &= \gamma(I_{12} + I_{21}) - \mu R
\end{aligned}
$$

Bifurcations for changing ϕ

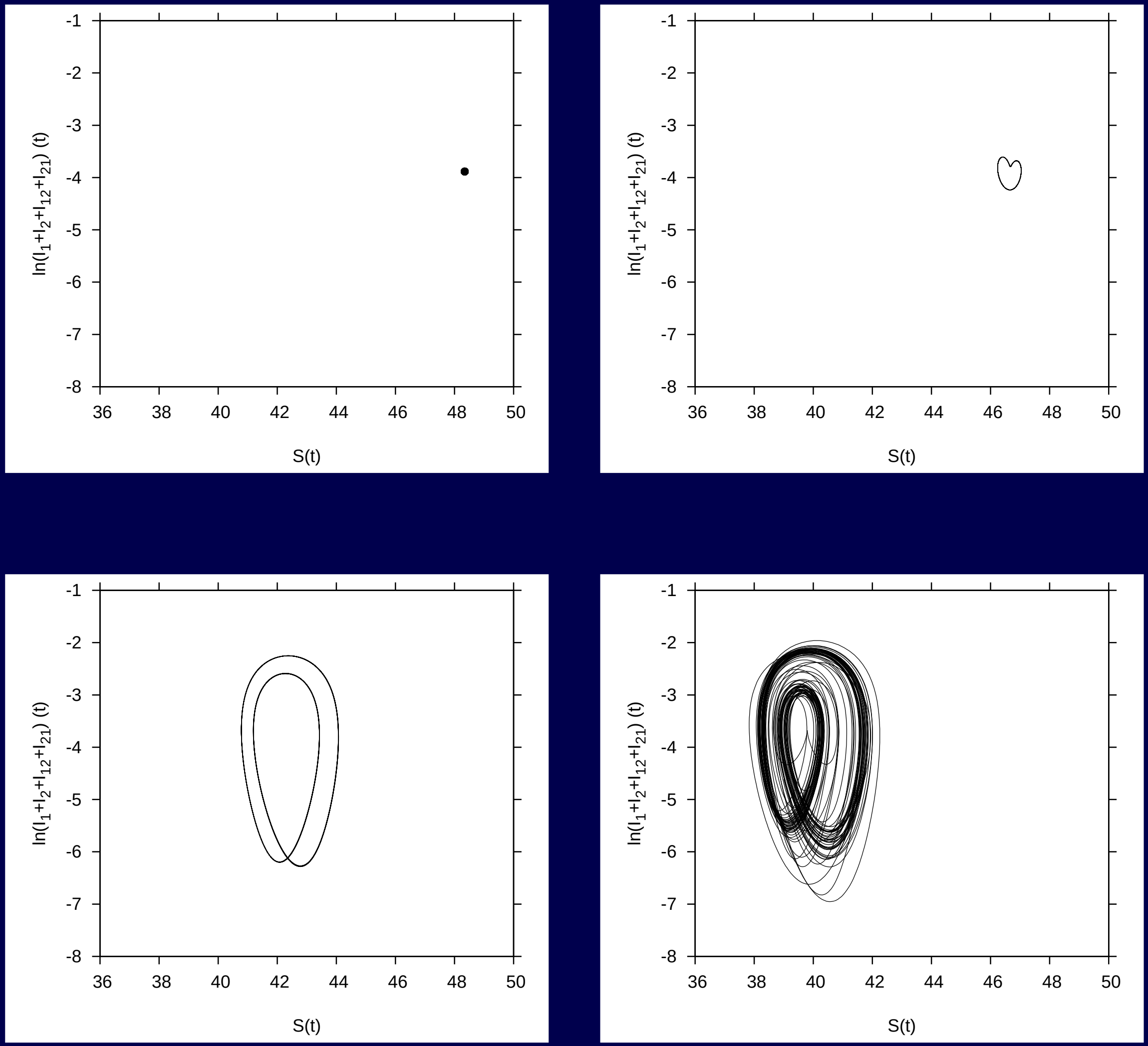

Dengue: Bifurcation diagram

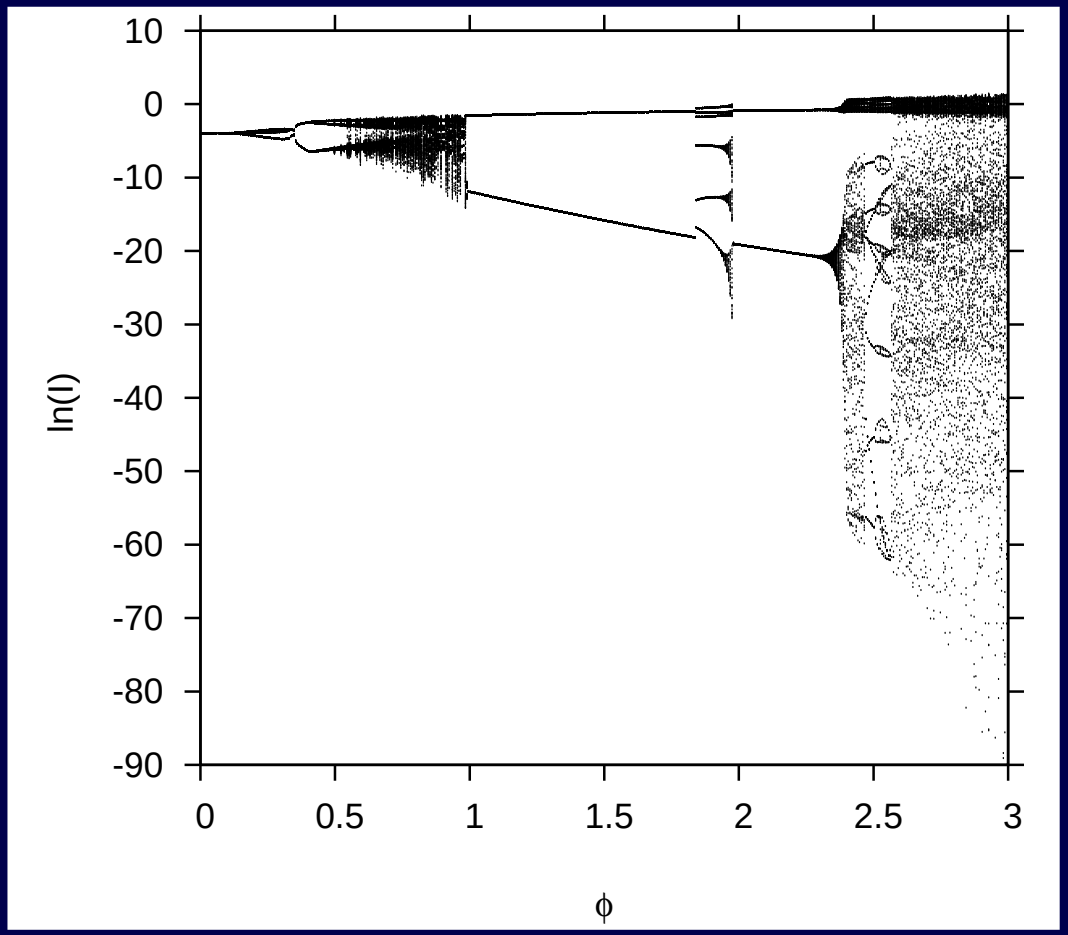

bifurcation diagram for $\alpha = 2$

i.e. $\frac{1}{2}$ year of temporary cross-immunity

Fixed point stability analysis generalized

small deviations $\Delta\underline{x} := \underline{x}(t) - \underline{x}^*$ now from any attractor trajectory $\underline{x}^*(t)$

$$\frac{d}{dt}\underline{x}(t) = \frac{d}{dt}(\underline{x}^* + \Delta\underline{x}) = \frac{d}{dt}\underline{x}^* + \frac{d}{dt}\Delta\underline{x}$$

$$= \underline{f}(\underline{x}) = \underline{f}(\underline{x}^* + \Delta\underline{x})$$

and using Taylor's expansion

$$\underline{f}(\underline{x}^* + \Delta\underline{x}) = \underline{f}(\underline{x}^*) + \left.\frac{d\underline{f}}{d\underline{x}}\right|_{\underline{x}=\underline{x}^*(t)} \cdot \Delta\underline{x} + \mathcal{O}((\Delta\underline{x})^2)$$

gives (with $\frac{d}{dt}\underline{x}^* = f(\underline{x}^*)$) now along the attractor trajectory $\underline{x}^*(t)$

$$\frac{d}{dt}\Delta\underline{x} = \left.\frac{d\underline{f}}{d\underline{x}}\right|_{\underline{x}=\underline{x}^*(t)} \cdot \Delta\underline{x}$$

Stability around a limit cycle

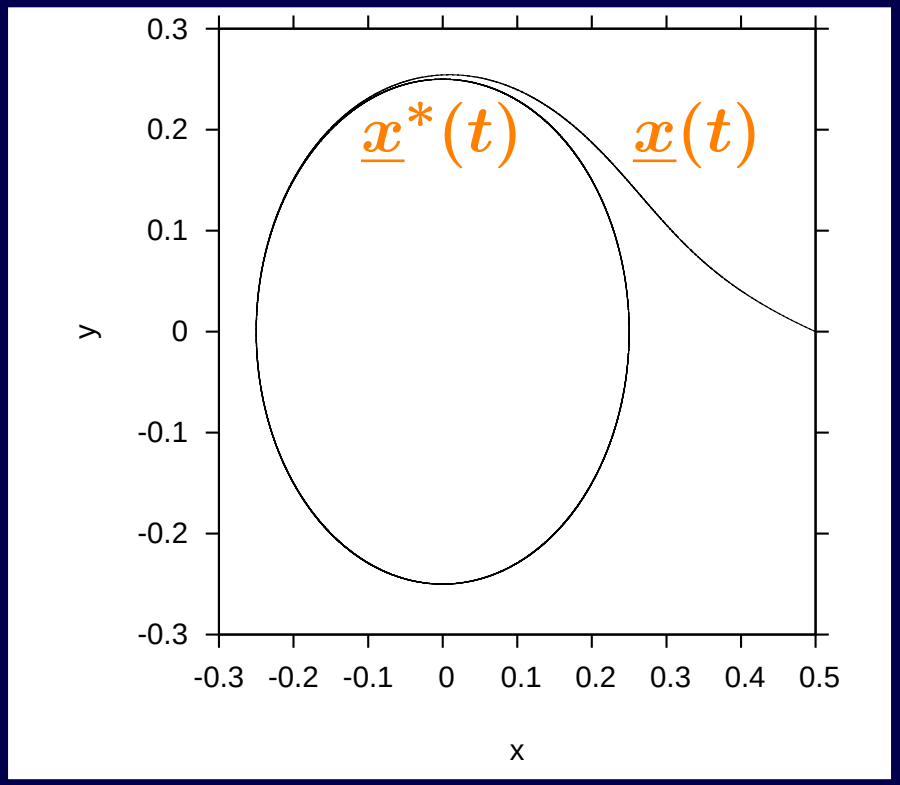

Stability around a limit cycle

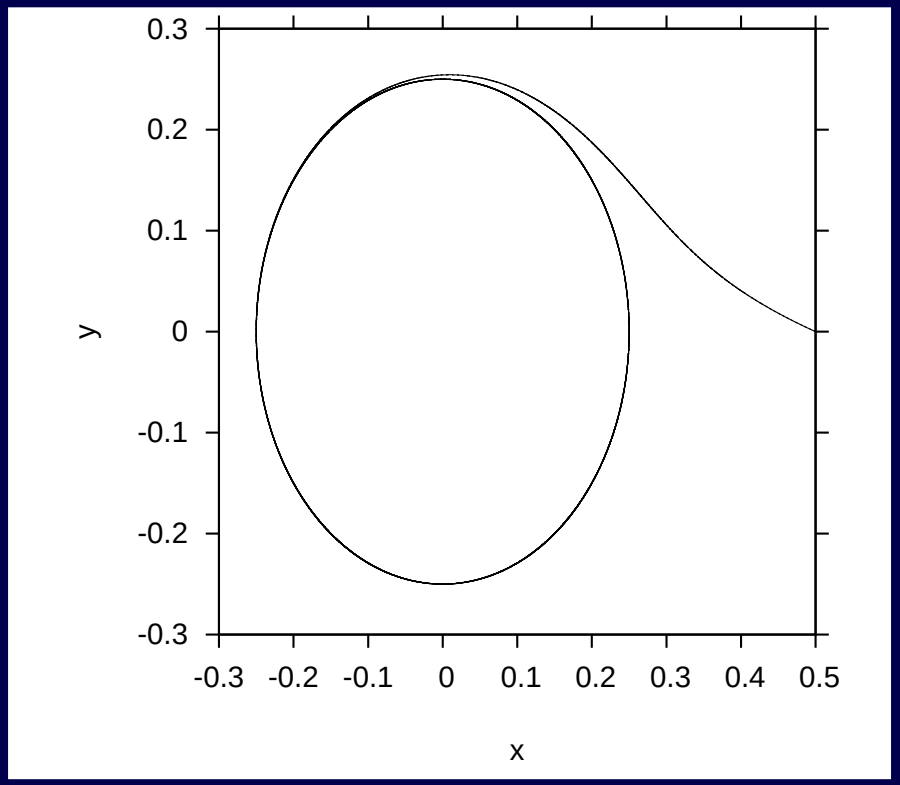

now stability determined around limit cycle $\underline{x}^*(t)$

by Jacobi matrix $A := \left.\frac{df}{d\underline{x}}\right|_{\underline{x}^*}$

Stability around a limit cycle

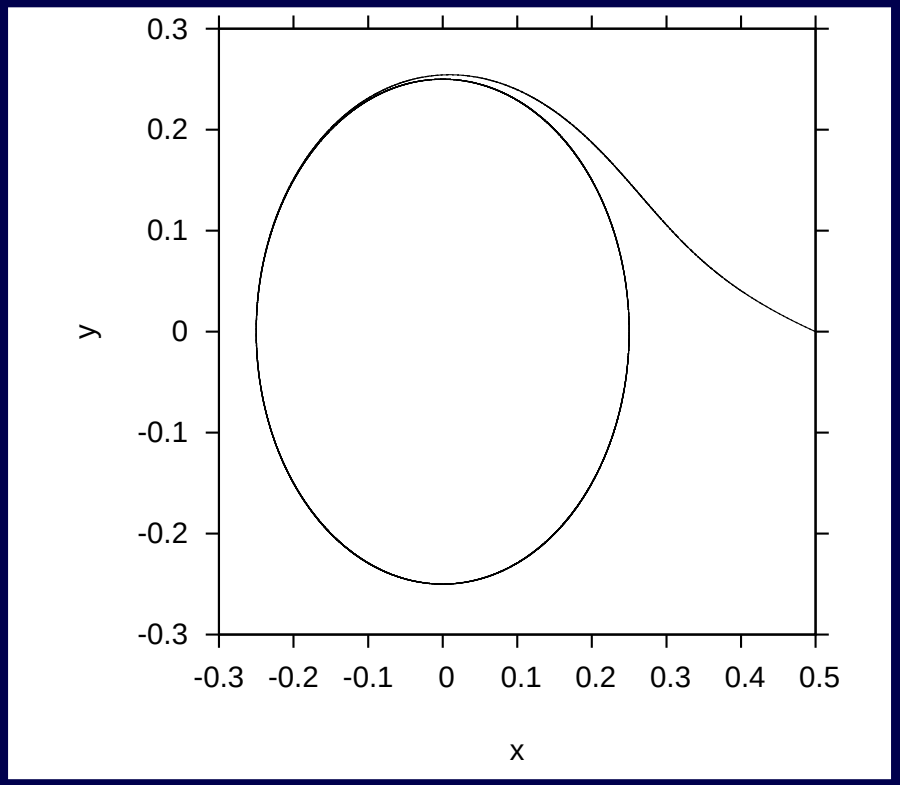

numerically calculate real parts λ_i of eigenvalues of Jacobi matrix along attractor $\underline{x}^*(t)$ via QR-decomposition

λ_i are also called Lyapunov exponents

$$\lambda_i \approx \frac{1}{t-t_0} \, ln \left(\frac{z_i(t)}{z_i(t_0)} \right)$$

Lyapunov exponents characterize deteministic attractors

all Lyapunov exponents smaller zero, $\lambda_i < 0$

$\Rightarrow$ fixed point

largest Lyapunov exponent equal zero, $\lambda_1 = 0$

$\Rightarrow$ limit cycle

largest Lyapunov exponent larger zero, $\lambda_1 > 0$

$\Rightarrow$ chaotic attractor

Quantifying chaos, example Lorenz attractor

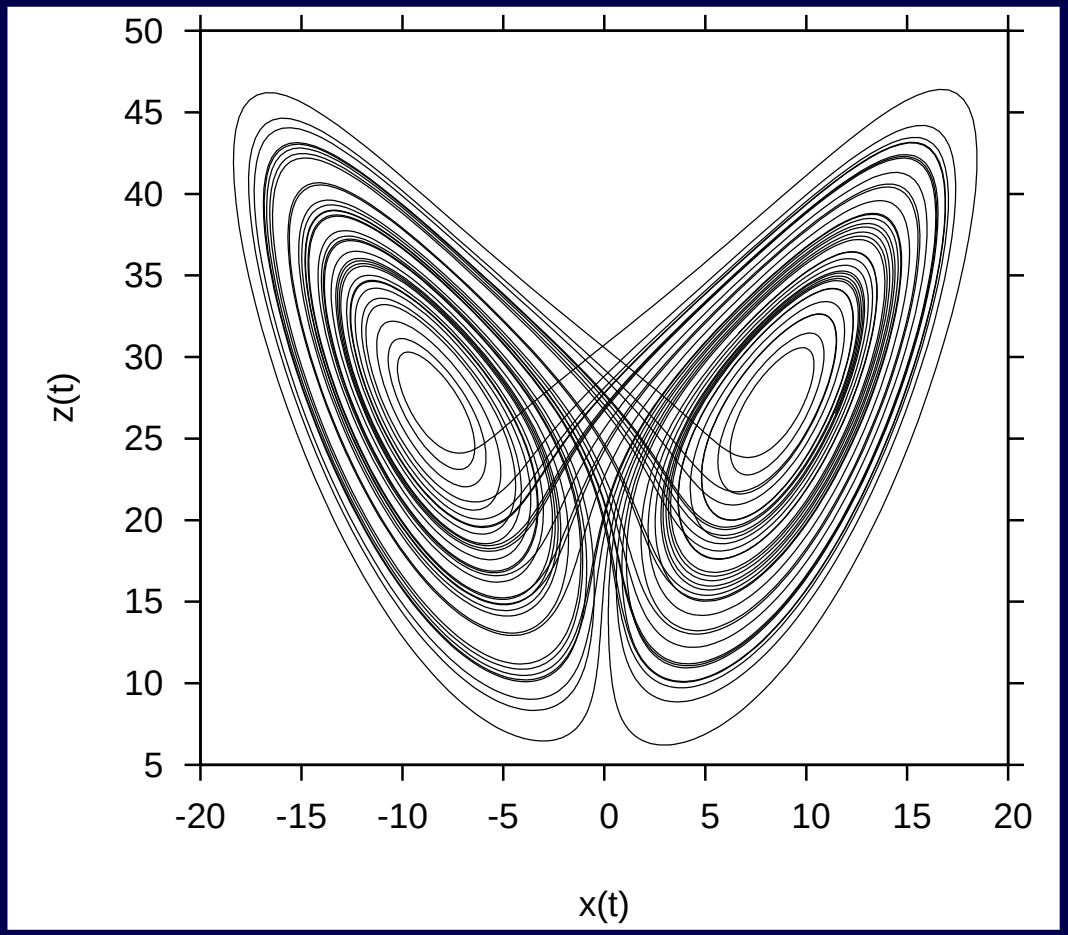

E.N. Lorenz (1963)
Deterministic non-periodic flow, J. Atmos. Sci. 20, 130-141.

Lorenz attractor

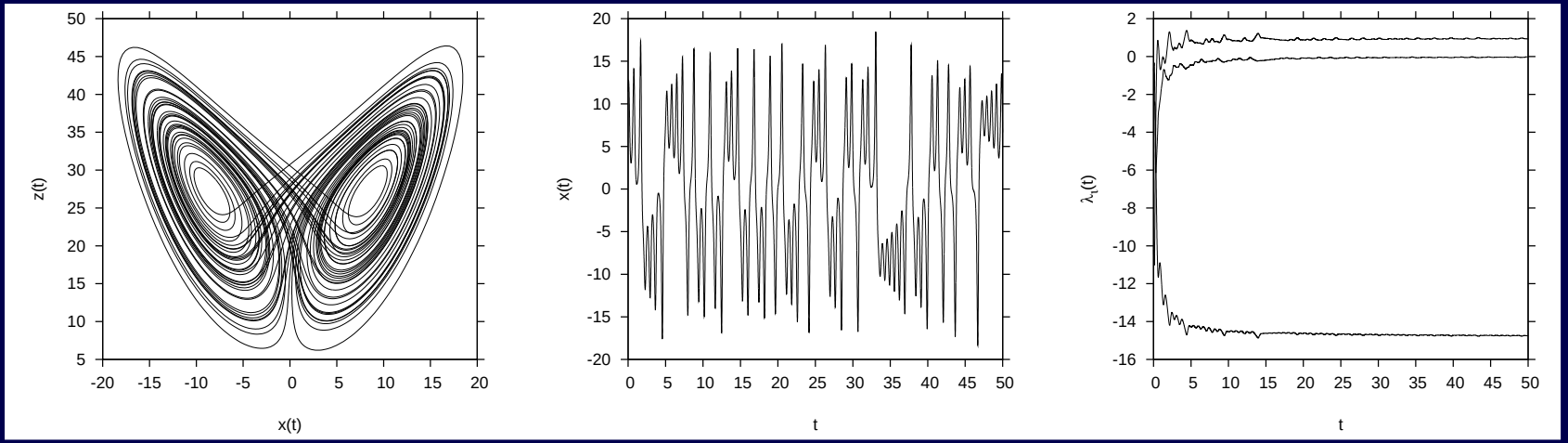

Lyapunov exponents:

$\lambda_1 = 0.9056$

$\lambda_2 = 0$

$\lambda_3 = -14.5723$

measured here (t=50):

$\lambda_1 = 0.93$

$\lambda_2 = -0.028$ (t=200, -0.0029)

$\lambda_3 = -14.74$

Dengue chaos

$$
\begin{aligned}
\frac{dS}{dt} &= -\frac{\beta_1}{N} S(I_1 + \phi_1 I_{21}) - \frac{\beta_2}{N} S(I_2 + \phi_2 I_{12}) + \mu(N - S) \\
\frac{dI_1}{dt} &= \frac{\beta_1}{N} S(I_1 + \phi_1 I_{21}) - (\gamma + \mu) I_1 \\
\frac{dI_2}{dt} &= \frac{\beta_2}{N} S(I_2 + \phi_2 I_{12}) - (\gamma + \mu) I_2 \\
\frac{dR_1}{dt} &= \gamma I_1 - (\alpha + \mu) R_1 \\
\frac{dR_2}{dt} &= \gamma I_2 - (\alpha + \mu) R_2 \\
\frac{dS_1}{dt} &= -\frac{\beta_2}{N} S_1(I_2 + \phi_2 I_{12}) + \alpha R_1 - \mu S_1 \\
\frac{dS_2}{dt} &= -\frac{\beta_1}{N} S_2(I_1 + \phi_1 I_{21}) + \alpha R_2 - \mu S_2 \\
\frac{dI_{12}}{dt} &= \frac{\beta_2}{N} S_1(I_2 + \phi_2 I_{12}) - (\gamma + \mu) I_{12} \\
\frac{dI_{21}}{dt} &= \frac{\beta_1}{N} S_2(I_1 + \phi_1 I_{21}) - (\gamma + \mu) I_{21} \\
\frac{dR}{dt} &= \gamma(I_{12} + I_{21}) - \mu R
\end{aligned}
$$

Jacobi matrix

$$
\begin{pmatrix}
\begin{matrix} -\frac{\beta_1}{N}(I_1+\phi_1 I_{21}) \\ -\frac{\beta_2}{N}(I_2+\phi_2 I_{12}) \\ -\mu \end{matrix} & -\frac{\beta_1}{N}S & -\frac{\beta_2}{N}S & 0 & 0 & 0 & 0 & -\frac{\beta_2}{N}\phi_2 S & -\frac{\beta_1}{N}\phi_1 S \\
\frac{\beta_1}{N}(I_1+\phi_1 I_{21}) & \begin{matrix} \frac{\beta_1}{N}S \\ -(\gamma+\mu) \end{matrix} & 0 & 0 & 0 & 0 & 0 & 0 & \frac{\beta_1}{N}\phi_1 S \\
\frac{\beta_2}{N}(I_2+\phi_2 I_{12}) & 0 & \begin{matrix} \frac{\beta_2}{N}S \\ -(\gamma+\mu) \end{matrix} & 0 & 0 & 0 & 0 & \frac{\beta_2}{N}\phi_2 S & 0 \\
0 & \gamma & 0 & -(\alpha+\mu) & 0 & 0 & 0 & 0 & 0 \\
0 & 0 & \gamma & 0 & -(\alpha+\mu) & 0 & 0 & 0 & 0 \\
0 & 0 & -\frac{\beta_2}{N}S_1 & \alpha & 0 & \begin{matrix} -\frac{\beta_2}{N}I_2 \\ -\frac{\beta_2}{N}\phi_2 I_{12}-\mu \end{matrix} & 0 & -\frac{\beta_2}{N}\phi_2 S_1 & 0 \\
0 & -\frac{\beta_1}{N}S_2 & 0 & 0 & \alpha & 0 & \begin{matrix} -\frac{\beta_1}{N}I_1 \\ -\frac{\beta_1}{N}\phi_1 I_{21}-\mu \end{matrix} & 0 & -\frac{\beta_1}{N}\phi_1 S_2 \\
0 & 0 & \frac{\beta_2}{N}S_1 & 0 & 0 & \frac{\beta_2}{N}(I_2+\phi_2 I_{12}) & 0 & \begin{matrix} \frac{\beta_2}{N}\phi_2 S_1 \\ -(\gamma+\mu) \end{matrix} & 0 \\
0 & \frac{\beta_1}{N}S_2 & 0 & 0 & 0 & 0 & \frac{\beta_1}{N}(I_1+\phi_1 I_{21}) & 0 & \begin{matrix} \frac{\beta_1}{N}\phi_1 S_2 \\ -(\gamma+\mu) \end{matrix}
\end{pmatrix}
$$

Lyapunov exponents along dengue attractor

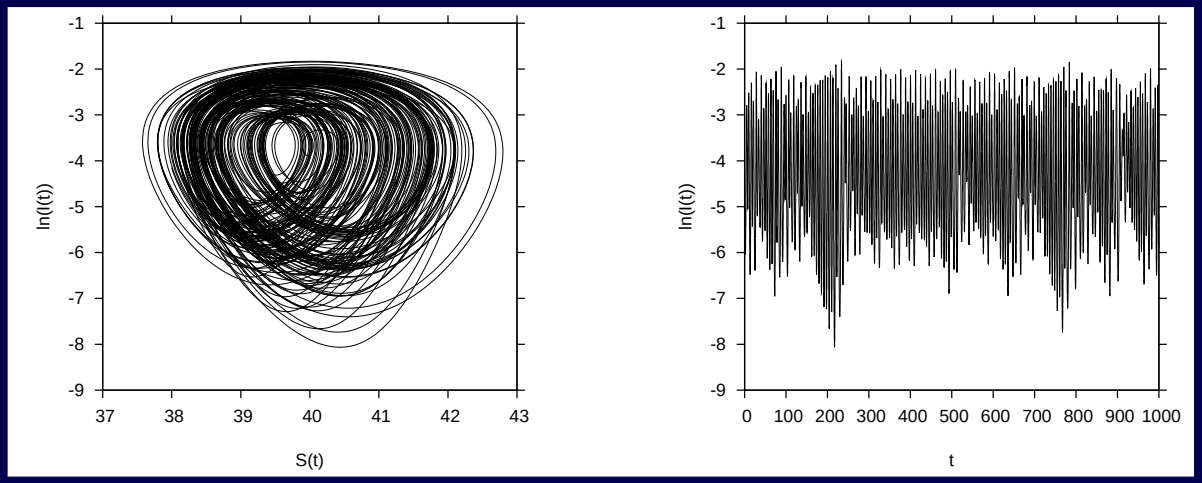

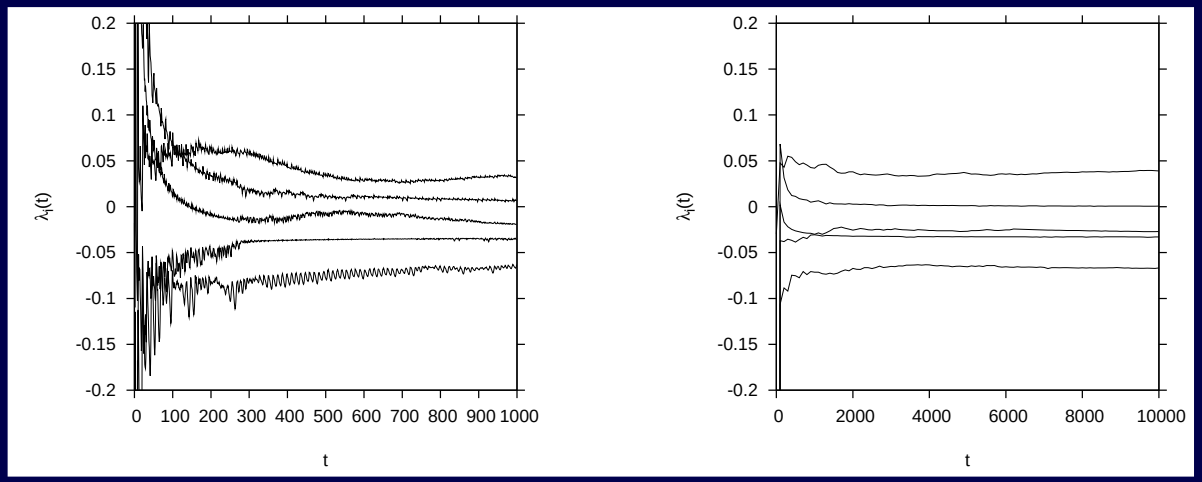

very long trajectories needed
for temporal mean of Lyap. exps. to converge

Dengue: Lyapunov spectrum

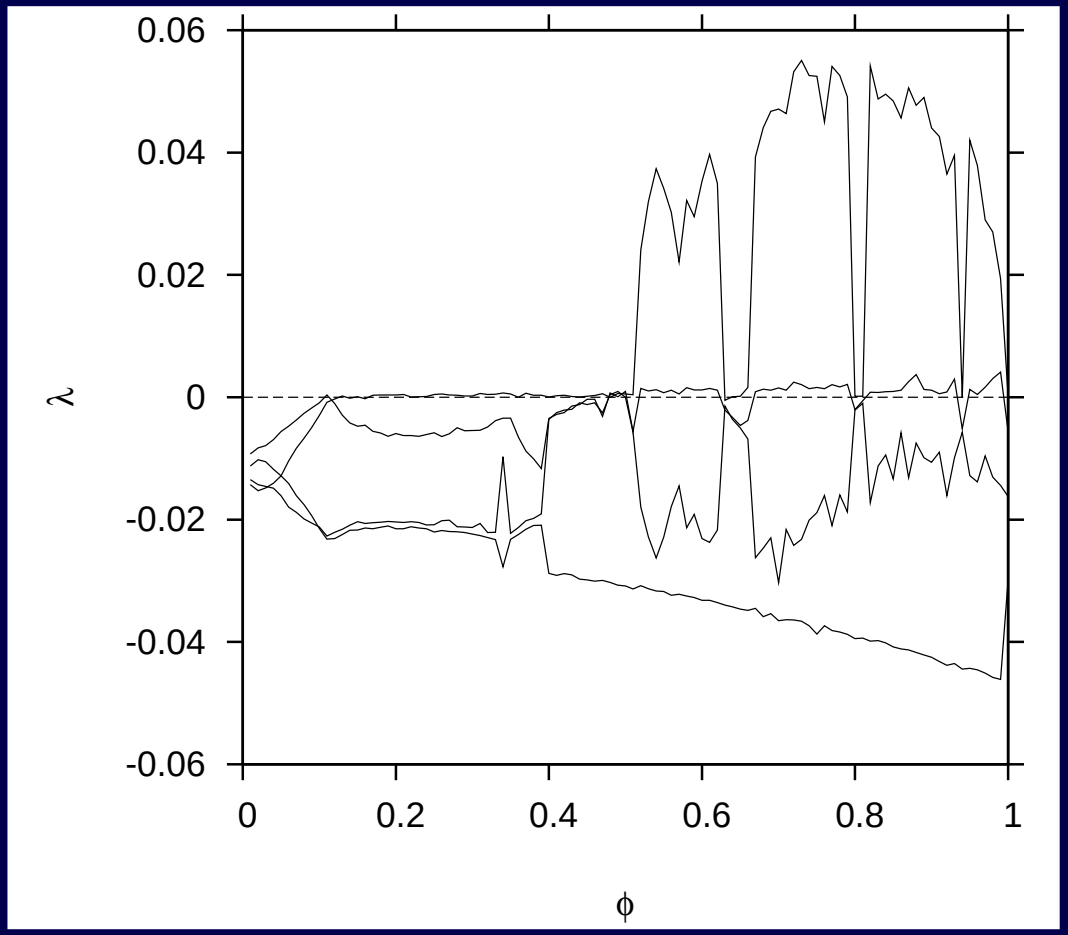

4 largest Lyapunov exponents for $\alpha = 2$ (5000 years trajectory)

Lyapunov spectrum versus bifurcation diagram

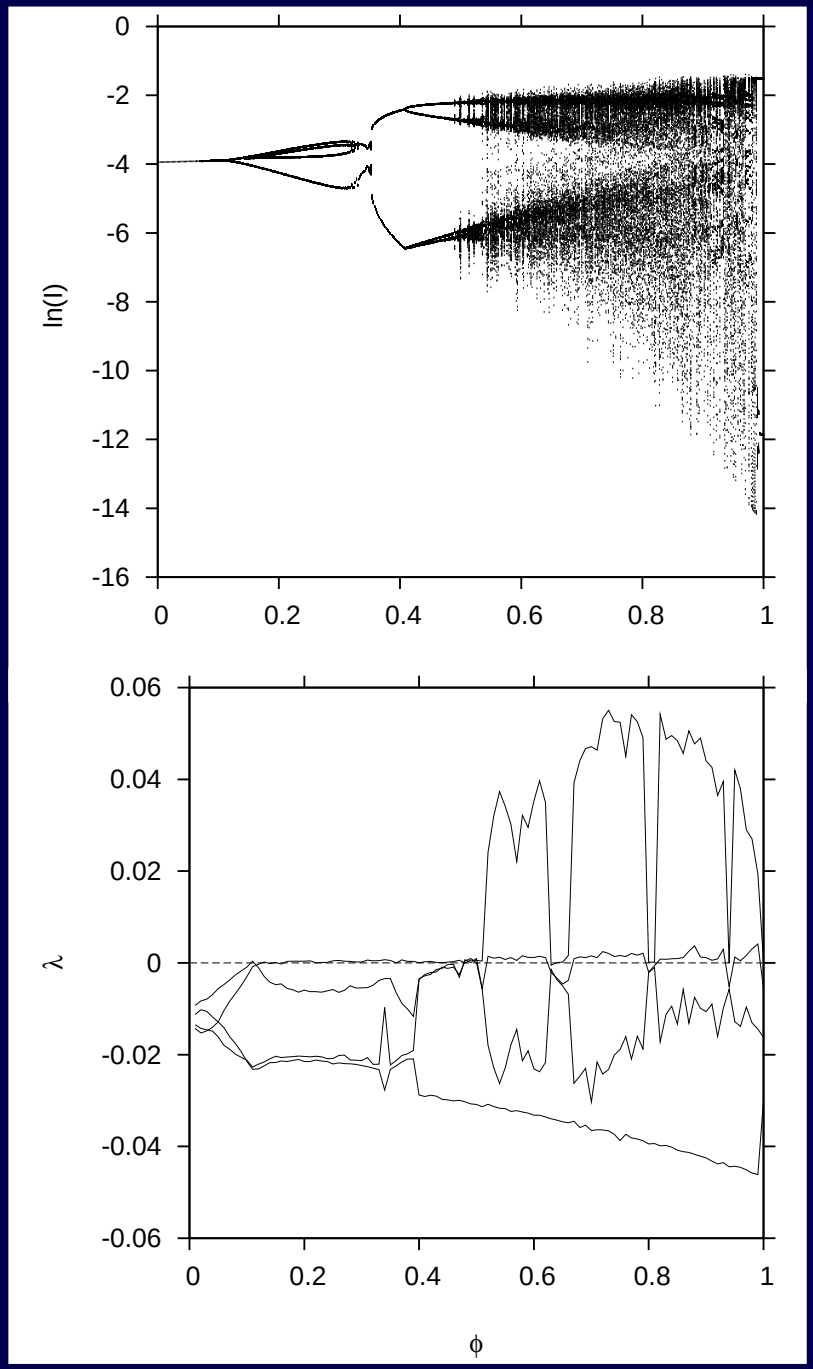

Bifurcation analysis via continuation: AUTO

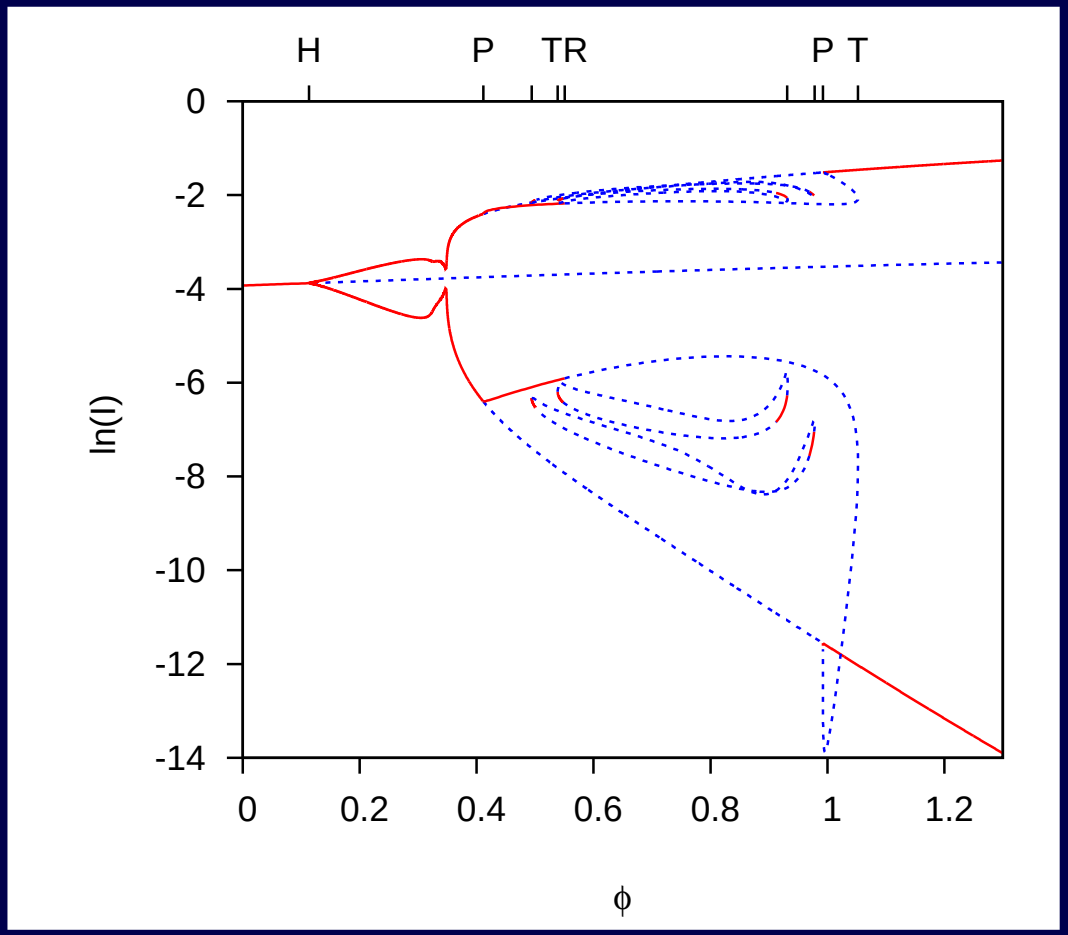

Bifurcation analysis via continuation: AUTO

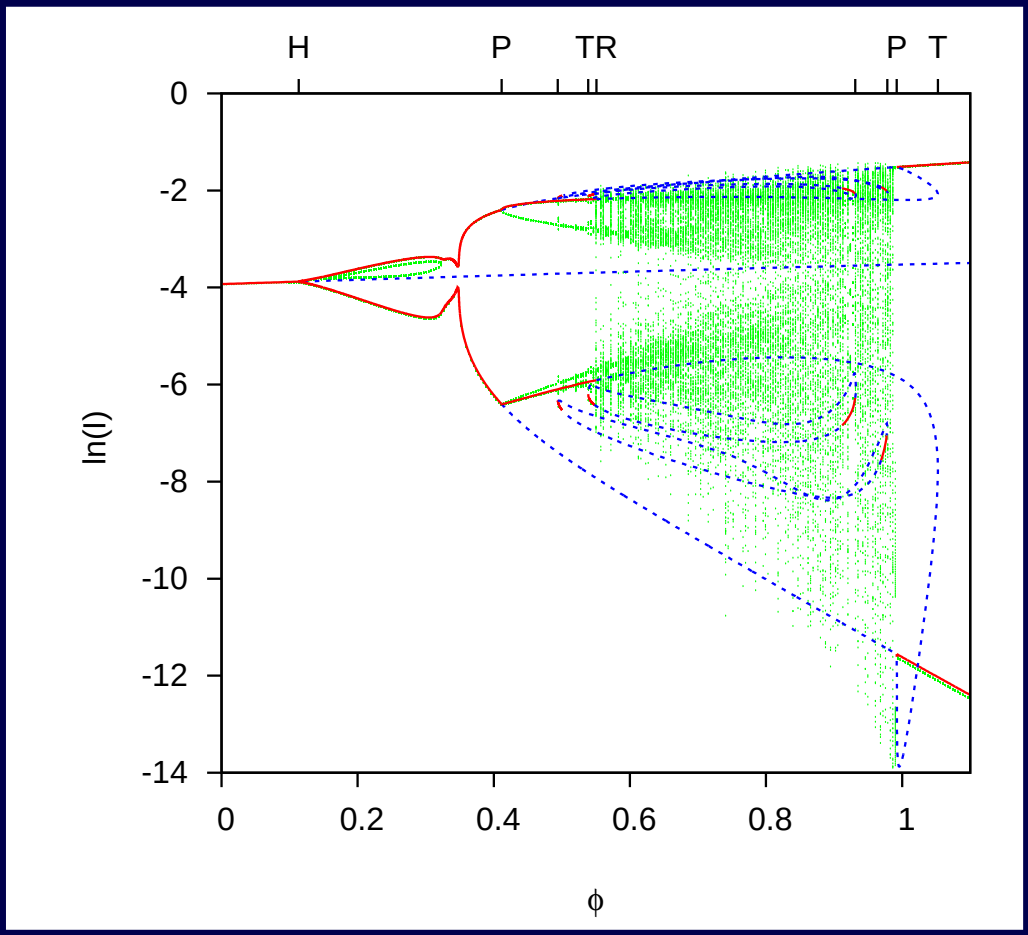

Comparing AUTO, Lyapunov spectra and numerical bifurcation diagrams:

torus bifurcation and soon after deterministic chaos

Dengue data from Thailand, updated till end of 2013

34 years of symptomatic dengue cases for all 77 provinces

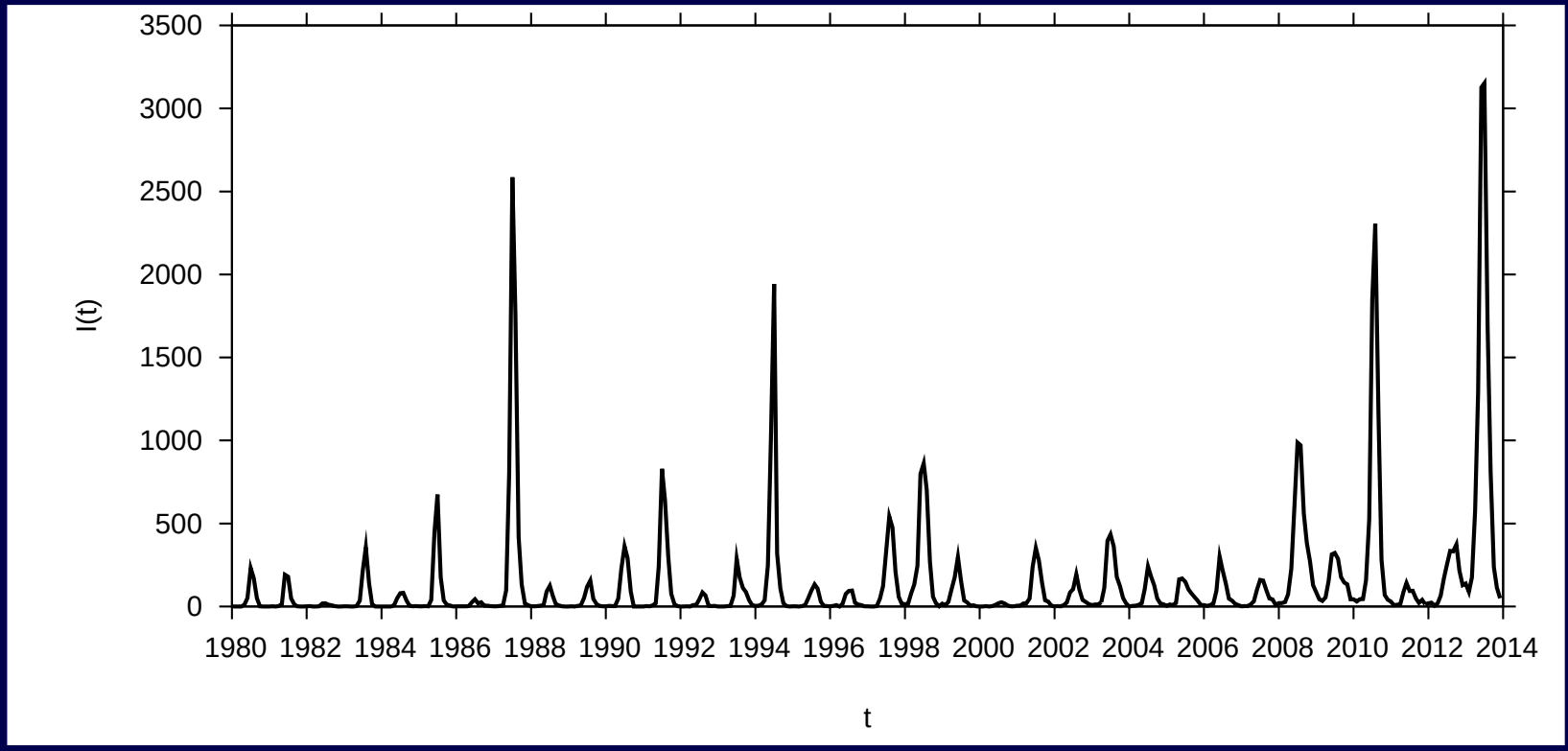

monthly symptomatic dengue cases
in Chiang Mai 1980-2014

Dengue data from Thailand, updated till end of 2013

34 years of symptomatic dengue cases for all 77 provinces

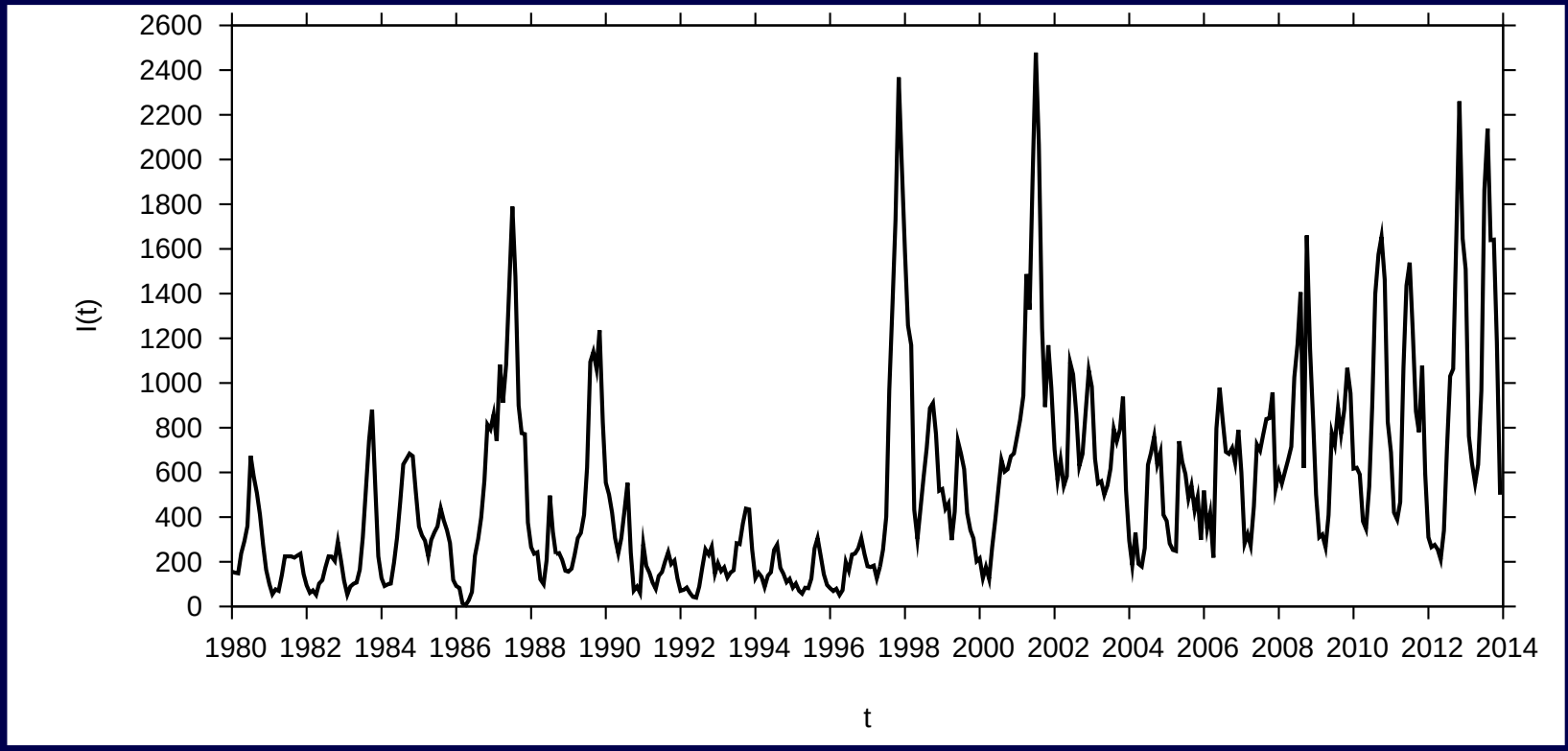

monthly symptomatic dengue cases
in Bangkok 1980-2014

Dengue data from Thailand, updated till end of 2013

34 years of symptomatic dengue cases for all 77 provinces

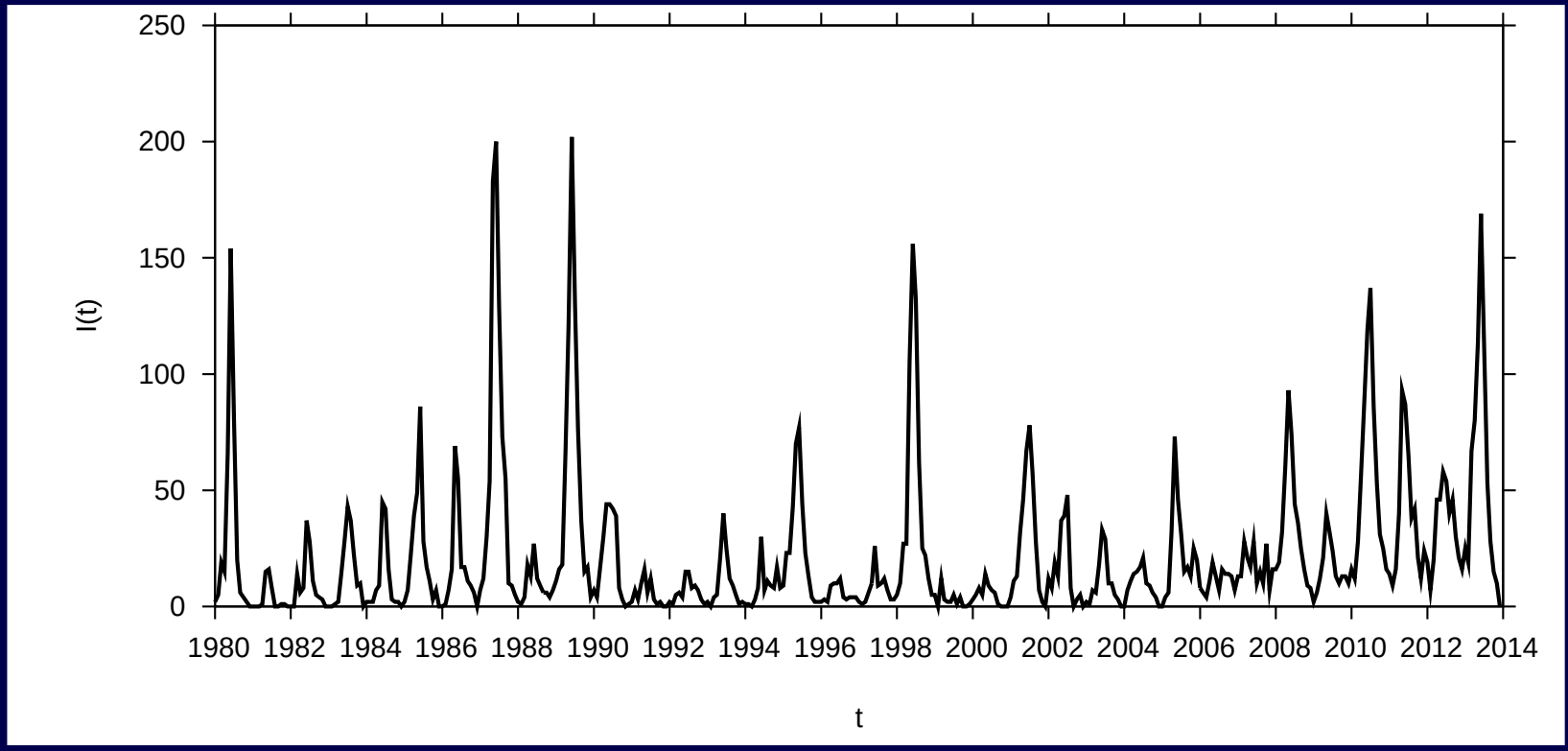

monthly symptomatic dengue cases
in Trat 1980-2014

Modelling multi-strain dynamics gives time series comparable to data

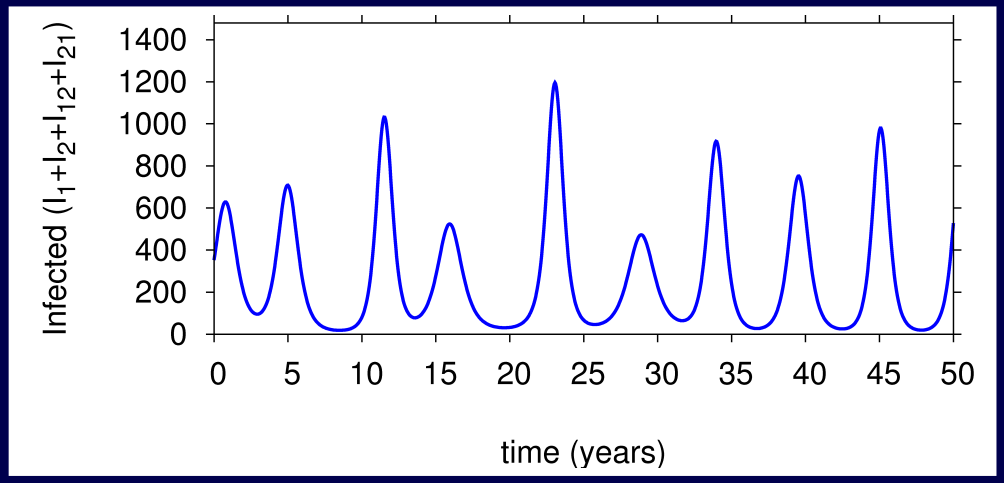

non-seasonal model in chaotic region

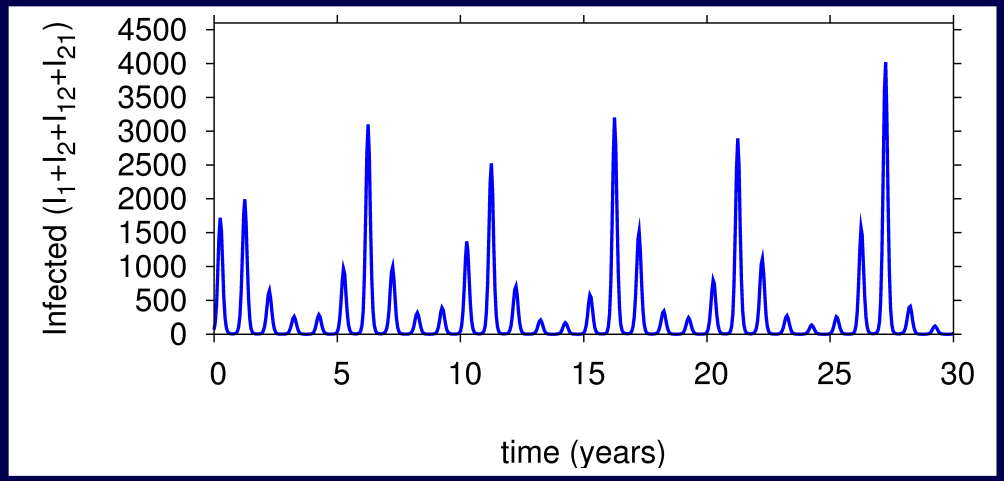

seasonality preserves chaotic pattern

Data matching:
compare simulations with data

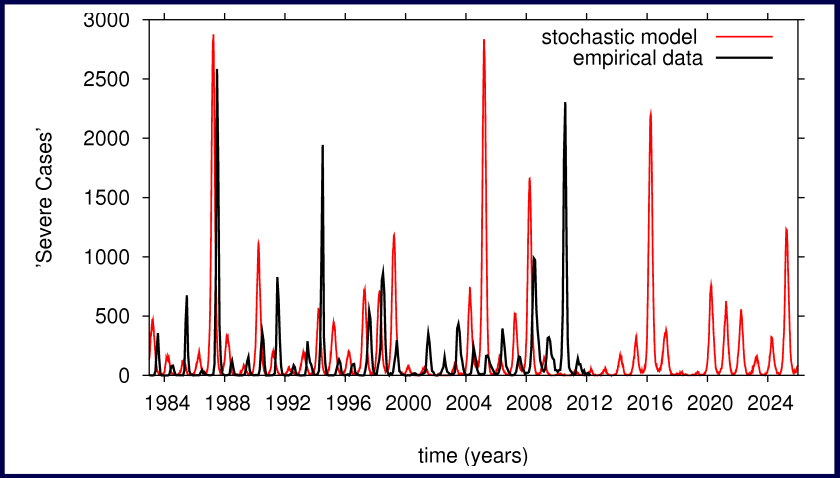

Chiang Mai

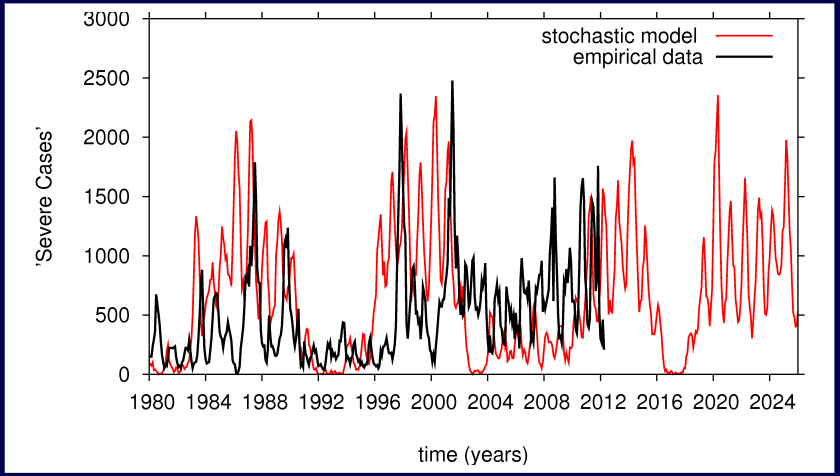

Krung Tep ("Bangkok")

Iterated Filtering

algorithmic description after Bretó et al. 2009:

MODEL INPUT: $f(\cdot)$, $g(\cdot|\cdot)$, $y_1, ..., y_N$, $t_0, ..., t_N$

ALGORITHMIC PARAMETERS: integers J, L, M; scalars $0 < a < 1$, $b > 0$; vectors $X_I^{(1)}$, $\theta^{(1)}$; positive definite symmetric matrices Σ_I ,Σ_θ.

1. FOR $m = 1$ to M
2. $X_I(t_0, j) \sim N[X_I^{(m)}, a^{m-1}\Sigma_I], \quad j = 1, ..., J$
3. $X_F(t_0, j) = X_I(t_0, j)$
4. $\theta(t_0, j) \sim N[\theta^{(m)}, ba^{m-1}\Sigma_\theta]$
5. $\bar{\theta}(t_0) = \theta^{(m)}$
6. FOR $n = 1$ to N
7. $X_P(t_n, j) = f(X_F(t_{n-1}, j), t_{n-1}, t_n, \theta(t_{n-1}, j), W)$
8. $w(n, j) = g(y_n|X_P(t_n, j), t_n, \theta(t_{n-1}, j))$
9. draw $k_1, ..., k_J$ such that $\text{Prob}(k_j = i) = w(n, i)/\sum_\ell w(n, \ell)$
10. $X_F(t_n, j) = X_P(t_n, k_j)$
11. $X_I(t_n, j) = X_I(t_{n-1}, k_j)$
12. $\theta(t_n, j) \sim N[\theta(t_{n-1}, k_j), a^{m-1}(t_n - t_{n-1})\Sigma_\theta]$
13. Set $\bar{\theta}_i(t_n)$ to be the sample mean of $\{\theta_i(t_{n-1}, k_j), \quad j = 1, ..., J\}$
14. Set $V_i(t_n)$ to be the sample variance of $\{\theta_i(t_n, j), \quad j = 1, ..., J\}$
15. END FOR
16. $\theta_i^{(m+1)} = \theta_i^{(m)} + V_i(t_1) \sum_{n=1}^{N} V_i^{-1}(t_n)(\bar{\theta}_i(t_n) - \bar{\theta}_i(t_{n-1}))$
17. Set $X_I^{(m+1)}$ to be the sample mean of $\{X_I(t_L, j), \quad j = 1, ..., J\}$
18. END FOR

RETURN
maximum likelihood estimate for parameters, $\hat{\theta} = \theta^{(M+1)}$
maximum likelihood estimate for initial values, $\hat{X}(t_0) = X_I^{(M+1)}$
maximized conditional log likelihood estimates, $\ell_n(\hat{\theta}) = log(\sum_j w(n, j)/J)$
maximized log likelihood estimate, $\ell(\hat{\theta}) = \sum_n \ell_n(\hat{\theta})$

Short term predictability, long term unpredictability

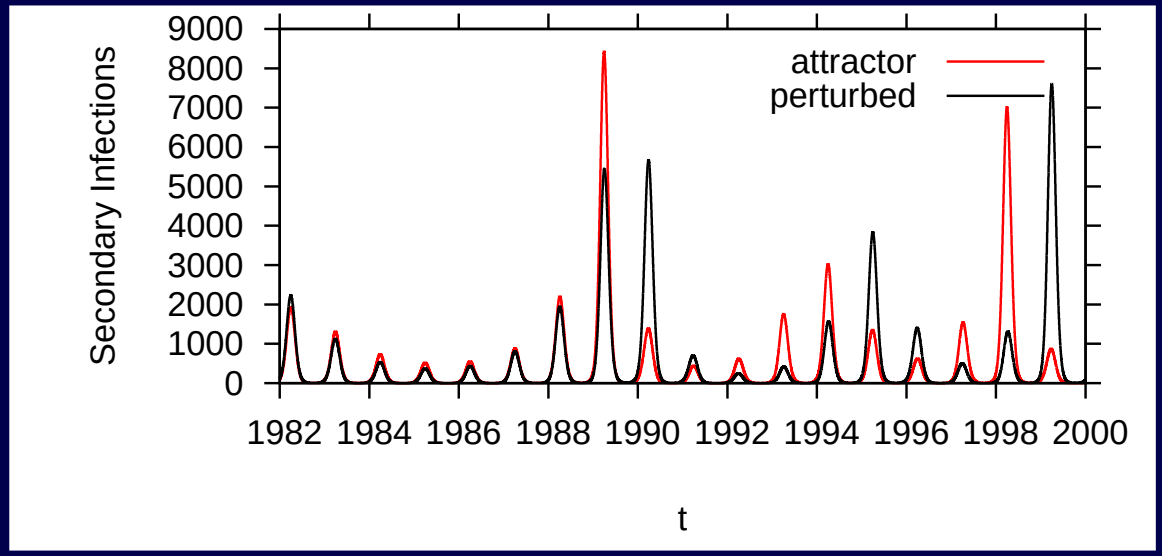

simulations with different initial conditions

implications for data analysis: Maximum Likelihood Iterated Filtering (MIF) is choice for such systems (Ionides et al 2006/ Bretó et al. 2009)

So what is needed?

toy models

with torus bifurcation

stochastic version

chaos after torus bifurcation

Rinaldi, Muratori, Kuznetsov 1993

regions. When this curve is crossed from below, the forced stable cycle of period 1 smoothly bifurcates into a stable quasi-periodic solution. While continuing curve $h^{(1)}$ from the left to the right the multipliers $\mu_{1,2}^{(1)} = e^{\pm i\alpha}$ of the Poincaré map vary and become equal to -1 when the terminal point A is reached.

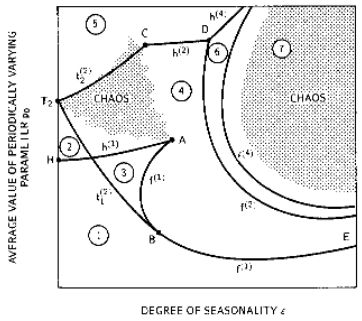

Figure 3. A general qualitative bifurcation diagram for systems (1), (2). Curves $h^{(1)}$, $h^{(2)}$, $h^{(4)}$, $f^{(1)}$, $f^{(2)}$, $f^{(4)}$, $t^{(2)}$ are bifurcation curves. Points A, B, C, D are codimension two bifurcation points.

Point A is a codimension two bifurcation point, called *strong resonance* 1 : 2, studied in Arnold (1982) by means of the normal form approach. The two coefficients of the normal form are of opposite sign and this suffices to say that only two bifurcation curves, namely, a Hopf $h^{(1)}$ and a flip $f^{(1)}$, are rooted at point A (as already said, the branch of $f^{(1)}$ not involving attractors is not shown in the figure). Curve $f^{(1)}$ can be generated by the continuation technique starting from point A. Along curve $f^{(1)}$ the normal form coefficient (computed as in Kuznetsov and Rinaldi, 1991) varies and becomes equal to 0 at point B, which is therefore a codimension two bifurcation point. Thus, curve $f^{(1)}$ is divided into two segments (AB and BE) and the period doubling takes place in opposite directions on these two segments, namely from region 4 on segment AB and from region 1 on segment BE. More precisely, when curve $f^{(1)}$ is crossed from region 1 to region 4 the forced cycle of period 1 loses stability and smoothly bifurcates into a stable period 2 cycle. On the contrary, if $f^{(1)}$ is crossed from region 3 to region 4, the stable cycle of period 1 collides with a saddle cycle of period 2 and becomes a saddle cycle of period 1.

The codimension two bifurcation point B is the terminal point of one of the

Rosenzweig-MacArthur model with Holling type II response function

preys X and predators Y governed by ODE-system

$$\dot{X} = \varrho X \left(1 - \frac{X}{\kappa}\right) - k \frac{X}{\frac{k}{b} N + X} Y$$

$$\dot{Y} = \nu \frac{X}{\frac{k}{b} N + X} Y - \mu Y$$

with Holling type II response function

$$\varphi(X) := \frac{X}{\frac{k}{b} N + X}$$

instead of $\varphi(X) = X$ as in Lotka-Volterra systems

Extended system with searching and handling predators and time scale separation => RM-H

preys X, searching predators Y_s and handling predators Y_h

$$
\begin{aligned}
S + X &\xrightarrow{\beta} X + X \\
X &\xrightarrow{\alpha} S \\
X + Y_s &\xrightarrow{b} S + Y_h \\
Y_h &\xrightarrow{k} Y_s \\
Y_h &\xrightarrow{\nu} Y_h + Y_s \\
Y_s &\xrightarrow{\mu} \emptyset \\
Y_h &\xrightarrow{\mu} \emptyset
\end{aligned}
$$

with predators X occupying space (or resources) S with birth rate β and giving space (resources) free with death rate α, hence growth rate $\varrho := \beta - \alpha$ and carrying capacity $\kappa := N(1 - \alpha/\beta)$

Extended system with searching and handling predators and time scale separation => RM-H

preys X, searching predators Y_s and handling predators Y_h

$$
\begin{aligned}
S + X &\xrightarrow{\beta} X + X \\
X &\xrightarrow{\alpha} S \\
X + Y_s &\xrightarrow{b} S + Y_h \\
Y_h &\xrightarrow{k} Y_s \\
Y_h &\xrightarrow{\nu} Y_h + Y_s \\
Y_s &\xrightarrow{\mu} \emptyset \\
Y_h &\xrightarrow{\mu} \emptyset
\end{aligned}
$$

with predators X occupying space (or resources) S with birth rate β and giving space (resources) free with death rate α, hence growth rate $\varrho := \beta - \alpha$ and carrying capacity $\kappa := N(1 - \alpha/\beta)$

gives stochastic version of RM-H

Mean field approximation of extended system

preys X, handling predators Y_h and searching predators Y_s

$$\begin{aligned}
\dot{X} &= \frac{\beta}{N} X(N - X) - \alpha X - \frac{b}{N} X Y_s \\
\dot{Y}_h &= \frac{b}{N} X Y_s - k Y_h - \mu Y_h \\
\dot{Y}_s &= -\frac{b}{N} X Y_s + k Y_h - \mu Y_s + \nu Y_h
\end{aligned}$$

and time scale separation via rescaled variables

$$\hat{k} := \varepsilon k \quad \text{and} \quad \hat{b} := \varepsilon b$$

gives sub-system of handlers and searchers in stationarity

$$\begin{aligned}
0 &= \frac{\hat{b}}{N} X Y_s - \hat{k} Y_h \\
0 &= -\frac{\hat{b}}{N} X Y_s + \hat{k} Y_h
\end{aligned}$$

Mean field approximation of extended system

subsystem in equlibrium gives with total predators $Y = Y_h + Y_s$, hence $Y_h = Y - Y_s$ etc. the solutions

$$Y_s = \frac{\hat{k}Y}{\hat{k} + \frac{\hat{b}}{N}X} = \frac{\varepsilon k Y}{\varepsilon k + \frac{\varepsilon b}{N}X} = \frac{kY}{k + \frac{b}{N}X}$$

$$Y_h = X\frac{Y}{\frac{\hat{k}}{\hat{b}}N + X} = X\frac{Y}{\frac{\varepsilon k}{\varepsilon b}N + X} = X\frac{Y}{\frac{k}{b}N + X}$$

and with

$$\frac{d}{dt}Y = \frac{d}{dt}(Y_s + Y_h) = -\mu(Y_s + Y_h) + \nu Y_h = -\mu Y + \nu X\frac{Y}{\frac{k}{b}N + X}$$

the Rosenzweig-MacArthur type model with Holling type II response function back

$$\dot{X} = \varrho X\left(1 - \frac{X}{\kappa}\right) - k\frac{X}{\frac{k}{b}N + X}Y$$

$$\dot{Y} = -\mu Y + \nu\frac{X}{\frac{k}{b}N + X}Y$$

Limit cycle with trajectory from initial condition spiraling into it

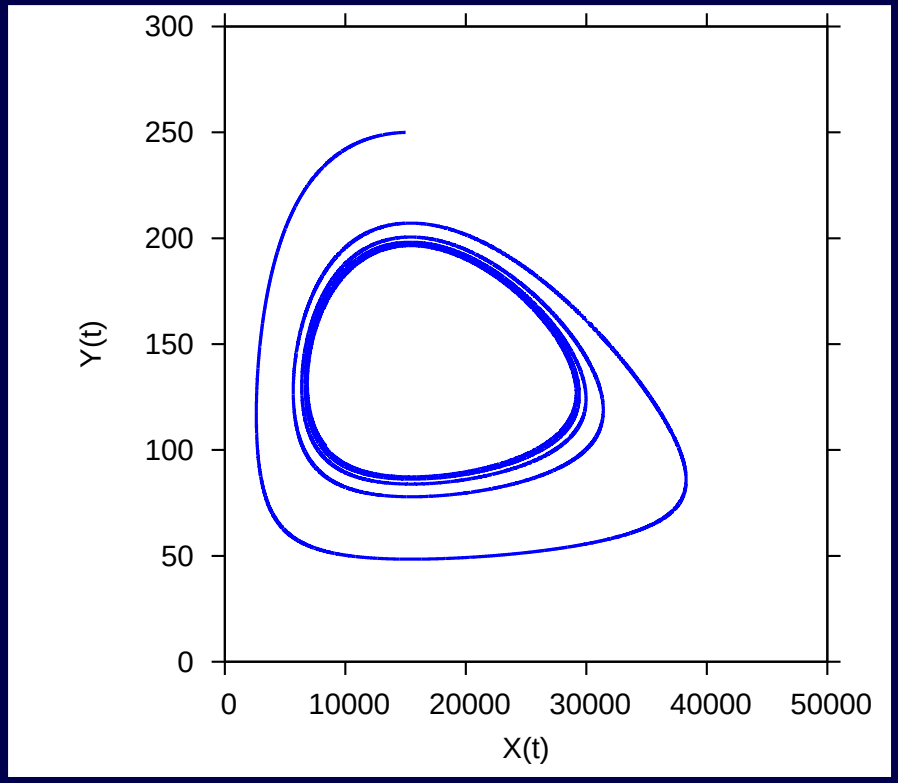

deterministic mean field ODE system (blue) with Hopf bif. point $b_H = k\frac{N}{\kappa}\frac{\nu+\mu}{\nu-\mu}$

Corresponding stochastic process of extended system

with variables X, $Y := Y_h + Y_s$ and $Z := Y_s$ we have

$$
\begin{aligned}
\frac{d}{dt}p(X,Y,Z,t) \;=\; & \frac{\beta}{N}(N-(X-1))(X-1)\; p(X-1,Y,Z,t) \\
& +\alpha(X+1)\; p(X+1),Y,Z,t) \\
& +\frac{b}{N}(X+1)(Z+1)\; p(X+1,Y,Z+1,t) \\
& +k(Y-Z+1)\; p(X,Y,Z-1,t) \\
& +\nu(Y-Z)\; p(X,Y-1,Z-1,t) \\
& +\mu(Z+1)\; p(X,Y+1,Z+1,t) \\
& +\mu(Y-Z+1)\; p(X,Y+1,Z,t) \\
& -\left(\frac{\beta}{N}(N-X)X+\alpha X+\frac{b}{N}XZ+k(Y-Z)\right. \\
& \left. +\,\nu(Y-Z)+\mu Z+\mu(Y-Z)\right)\; p(X,Y,Z,t)
\end{aligned}
$$

Comparison of deterministic and stochastic systems both with spiraling into Hopf limit cycle

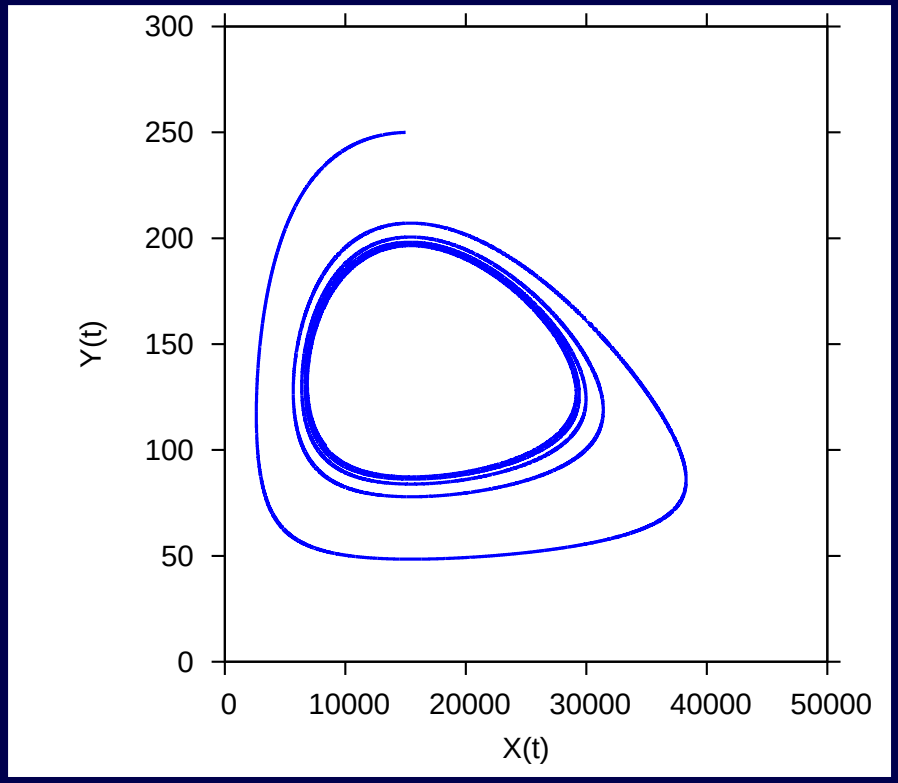

deterministic mean field ODE system (blue)

Comparison of deterministic and stochastic systems both with spiraling into Hopf limit cycle

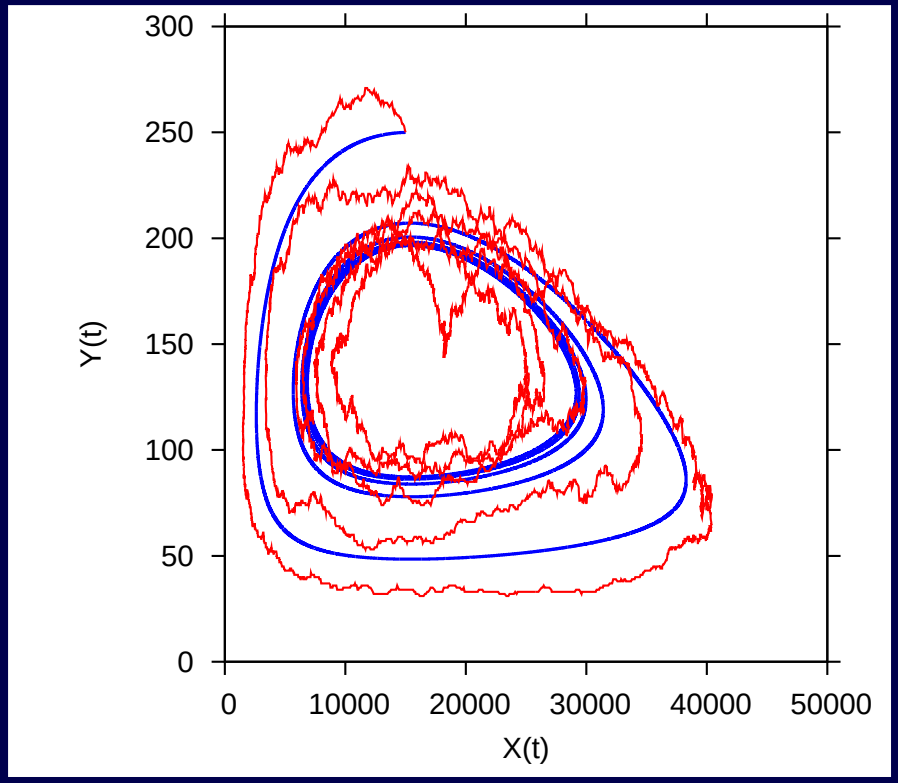

deterministic mean field ODE system (blue)
and stochastic system, master equation realization (red)

Stochastic simulations for varying population sizes N

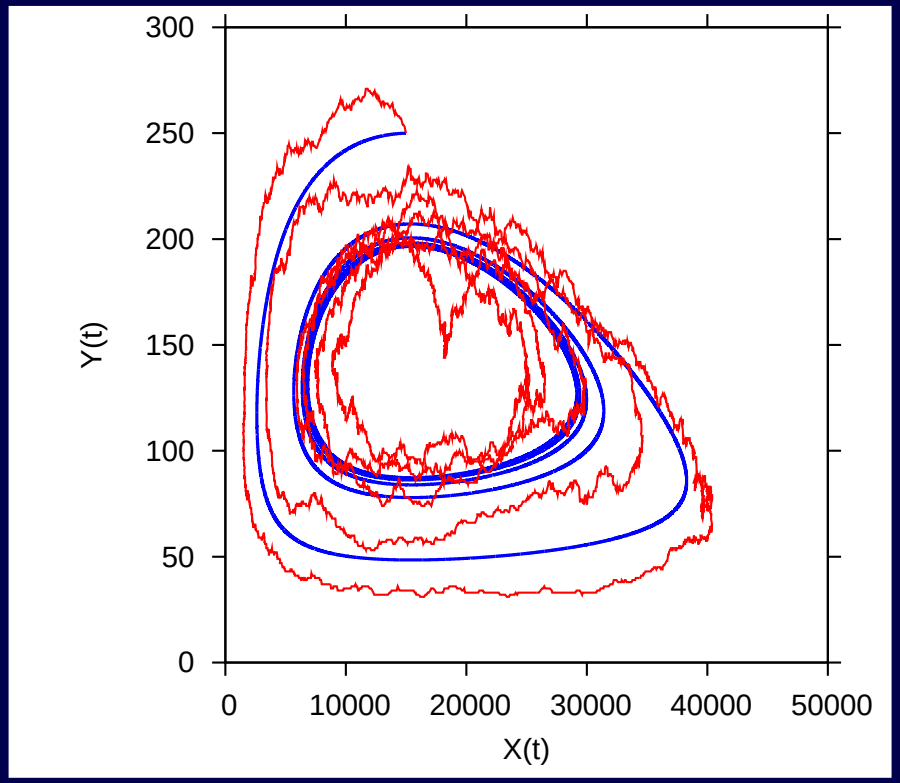

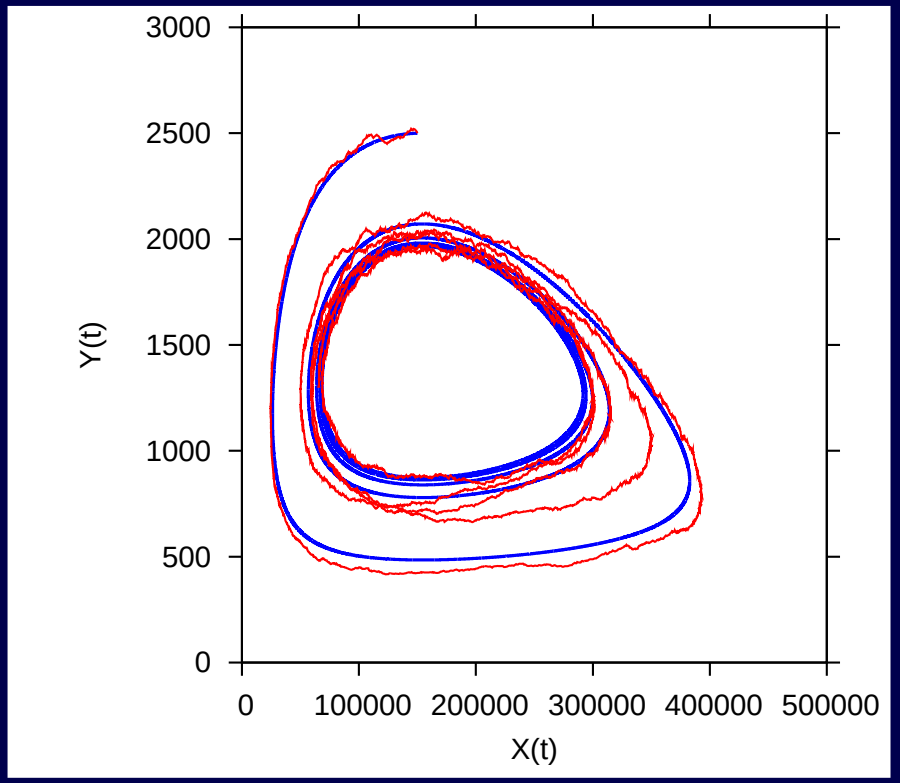

population sizes of $N = 100\,000$ and $N = 10^6$

From master equation to Fokker-Planck equation via Kramers-Moyal expansion

with densities $x := X/N$, $y := Y/N$ and $z := Z/N$ we have the master equation

$$\frac{d}{dt}\, p(x,y,z,t) \;=\; N\beta \left(x - \frac{1}{N}\right)\left(1 - \left(x - \frac{1}{N}\right)\right)\; p\left(x - \frac{1}{N}, y, z, t\right)$$
$$+ N\alpha \left(x + \frac{1}{N}\right)\; p\left(x + \frac{1}{N}, y, z, t\right) ...$$
$$- \left(N\beta x(1-x) + N\alpha x + ...\right)\; p(x,y,z,t)$$

and with $\underline{x} := (x,y,z)^{tr}$ as state vector and for the $n = 7$ transitions $w_j(\underline{x})$ and vectors of small changes $\Delta\underline{x}_j := \frac{1}{N} \cdot \underline{r}_j$, here with $\underline{r}_1 = (-1,0,0)^{tr}$, $\underline{r}_2 = (1,0,0)^{tr}$ ... we have the general form

$$\frac{d}{dt}\, p(\underline{x},t) \;=\; \sum_{j=1}^{n} \left(N w_j(\underline{x} + \Delta\underline{x}_j) \cdot p(\underline{x} + \Delta\underline{x}_j, t) \;- N w_j(\underline{x}) \cdot p(\underline{x},t) \right)$$

in Taylor's expansion

$$w_j(\underline{x} + \Delta\underline{x}_j) \cdot p(\underline{x} + \Delta\underline{x}_j, t) = \sum_{\nu=0}^{\infty} \frac{1}{\nu!} \left(\Delta\underline{x}_j \cdot \nabla_{\underline{x}} \right)^{\nu} w_j(\underline{x})\; p(\underline{x},t)$$

From master equation to Fokker-Planck equation via Kramers-Moyal expansion

giving to second order in $1/N$ a Fokker-Planck equation

$$\frac{\partial}{\partial t}\, p(\underline{x},t) \;=\; -\nabla_{\underline{x}} \left(\sum_{j=1}^{n} (-\underline{r}_j \cdot w_j(\underline{x}))\; p(\underline{x},t) \right) + \frac{\sigma^2}{2} \sum_{j=1}^{n} (\underline{r}_j \cdot \nabla_{\underline{x}})^2 w_j(\underline{x})\; p(\underline{x},t)$$

with

$$\nabla_{\underline{x}} = \begin{pmatrix} \frac{\partial}{\partial x} \\ \frac{\partial}{\partial y} \\ \frac{\partial}{\partial z} \end{pmatrix} = \partial_{\underline{x}}$$

or in different notation

$$\frac{\partial}{\partial t}\, p(\underline{x},t) = -\partial_{\underline{x}} \left(\underline{f}(\underline{x})\; p(\underline{x},t) \right) + \frac{\sigma^2}{2}\, \vec{\partial}_{\underline{x}} \left(G^2(\underline{x})\; p(\underline{x},t) \right) \overleftarrow{\partial}_{\underline{x}}$$

From master equation to Fokker-Planck equation via Kramers-Moyal expansion

in new notation

$$\frac{\partial}{\partial t}\, p(\underline{x},t) = -\partial_{\underline{x}} \left(\underline{f}(\underline{x})\; p(\underline{x},t) \right) + \frac{\sigma^2}{2}\, \overrightarrow{\partial}_{\underline{x}} \left(G^2(\underline{x})\; p(\underline{x},t) \right) \overleftarrow{\partial}_{\underline{x}}$$

using simply a quadratic form $\overrightarrow{\partial_{\underline{x}}}\; (G^2(\underline{x})\; p(\underline{x},t))\; \overleftarrow{\partial_{\underline{x}}}$ here with

$$\overrightarrow{\partial}_{\underline{x}}\; (G^2\; p)\; \overleftarrow{\partial}_{\underline{x}} = \left(\frac{\partial}{\partial x}, \frac{\partial}{\partial y}, \frac{\partial}{\partial z} \right) \cdot \begin{pmatrix} g_{11} & g_{12} & g_{13} \\ g_{21} & g_{22} & g_{23} \\ g_{31} & g_{32} & g_{33} \end{pmatrix}^2 \; p(\underline{x},t) \; \cdot \begin{pmatrix} \overleftarrow{\frac{\partial}{\partial x}} \\ \overleftarrow{\frac{\partial}{\partial y}} \\ \overleftarrow{\frac{\partial}{\partial z}} \end{pmatrix}$$

and

$$\underline{f}(\underline{x}) \;=\; \sum_{j=1}^{n} \underline{f}_j(\underline{x}) = \sum_{j=1}^{n} (-\underline{r}_j \cdot w_j(\underline{x}))$$

$$G^2(\underline{x}) \;=\; \sum_{j=1}^{n} G_j^2(\underline{x}) = \sum_{j=1}^{n} \underline{r}_j \cdot \underline{r}_j^{tr}\; w_j(\underline{x})$$

From master equation to Fokker-Planck equation via Kramers-Moyal expansion

Fokker-Planck equation

$$\frac{\partial}{\partial t}\, p(\underline{x},t) = -\partial_{\underline{x}} \left(\underline{f}(\underline{x})\, p(\underline{x},t) \right) + \frac{\sigma^2}{2}\, \overrightarrow{\partial}_{\underline{x}} \left(G^2(\underline{x})\, p(\underline{x},t) \right) \overleftarrow{\partial}_{\underline{x}}$$

gives stochastic differential equation system with $\sigma = 1/\sqrt{N}$ and in the XYZ case the three dimensional Gaussian normal noise vector $\underline{\varepsilon}(t) = (\varepsilon_x(t), \varepsilon_y(t), \varepsilon_z(t))^{tr}$ as

$$\frac{d}{dt}\underline{x} = \underline{f}(\underline{x}) + \sigma G(\underline{x}) \cdot \underline{\varepsilon}(t)$$

and using matrix square root from eigenvalue-eigenvector decomposition $G^2(\underline{x}) = T \Lambda T^{-1}$ as

$$G(\underline{x}) = T \sqrt{\Lambda} T^{tr}$$

to be numerically implemented easily

Comparison of master equation and Fokker-Planck approx.

spiraling into fixed point

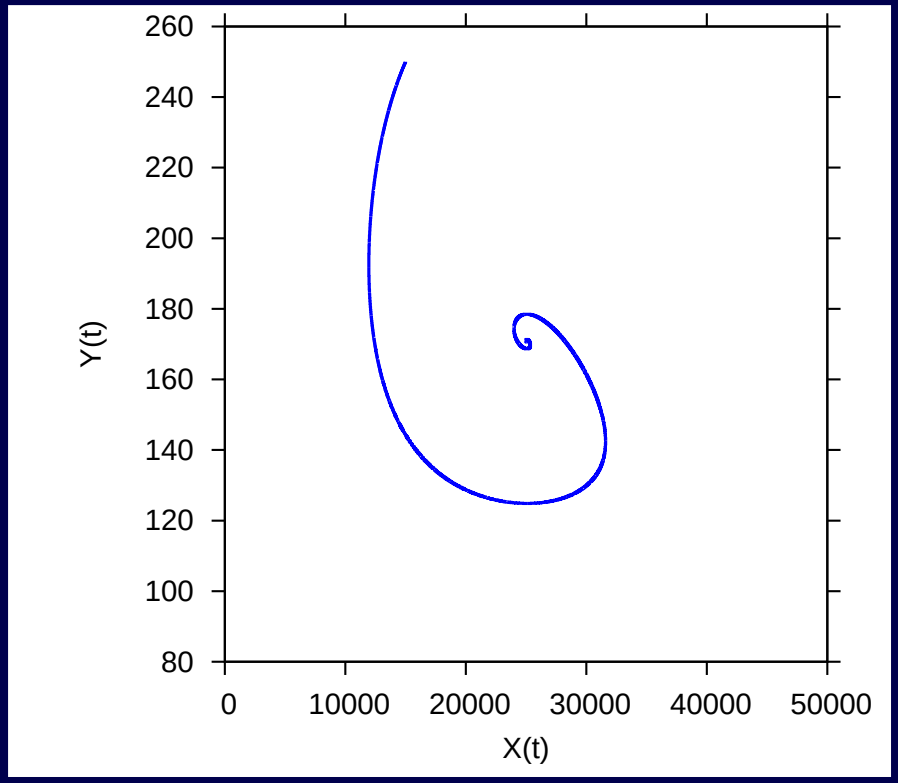

mean field ODE system (blue)

Comparison of master equation and Fokker-Planck approx.

spiraling into fixed point

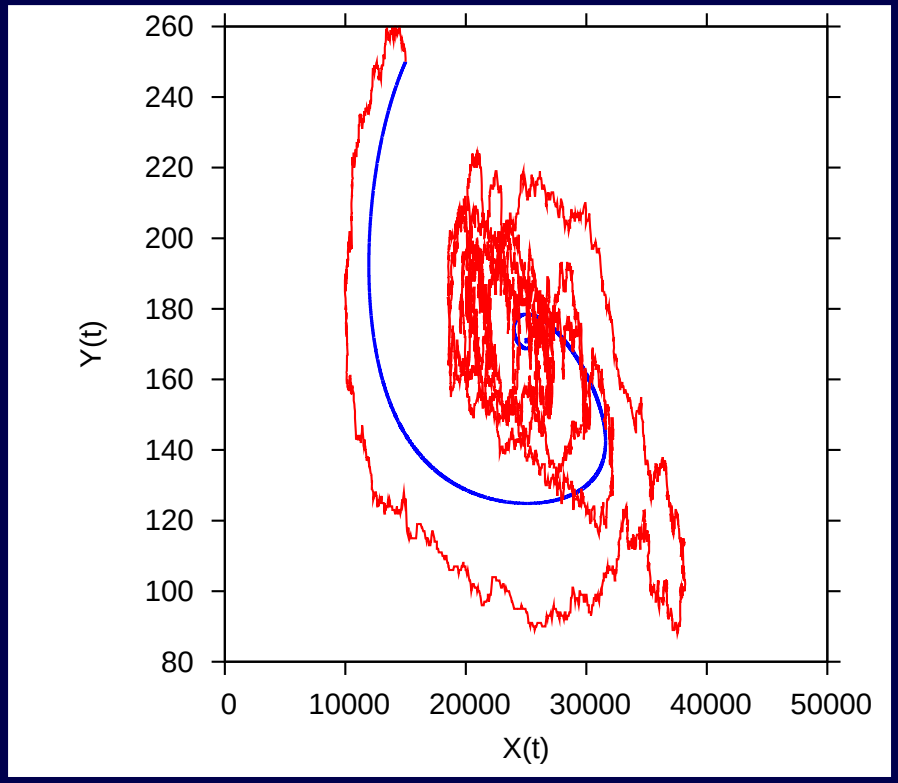

mean field ODE system (blue)

master equation realization (red)

Comparison of master equation and Fokker-Planck approx.
spiraling into fixed point

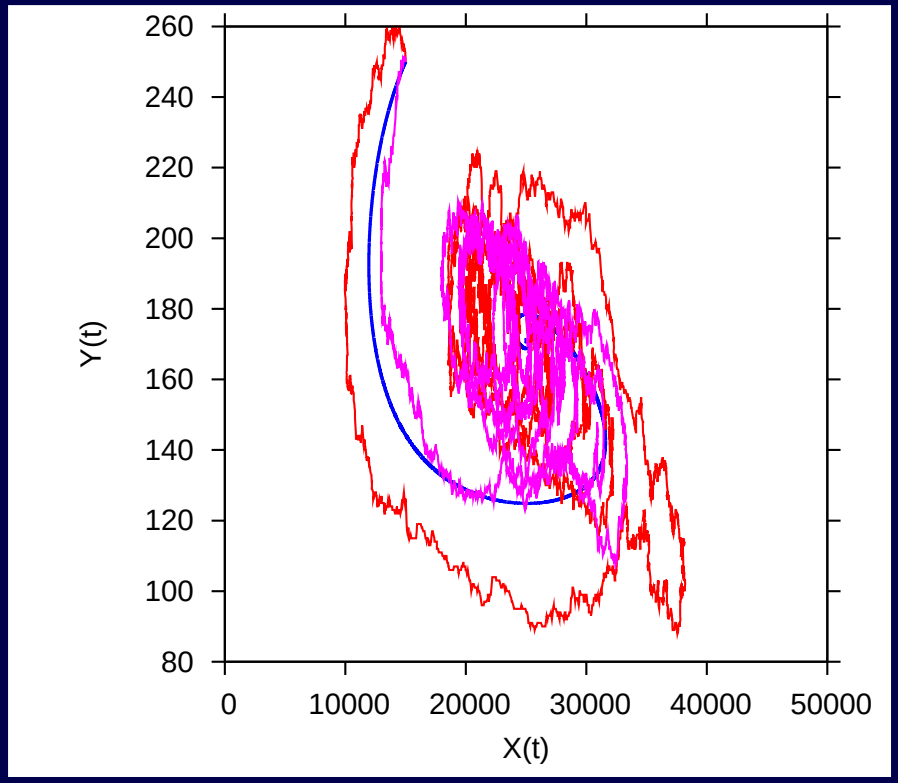

mean field ODE system (blue)
master equation realization (red)
SDE system from Fokker-Planck approx. (pink)

Time series keep oscillating

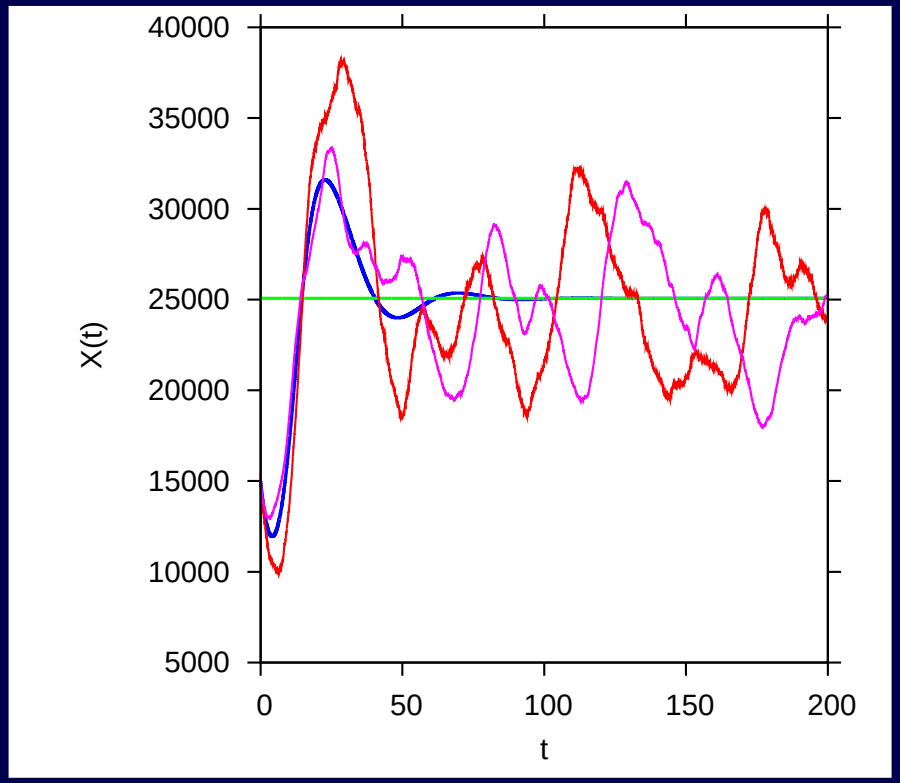

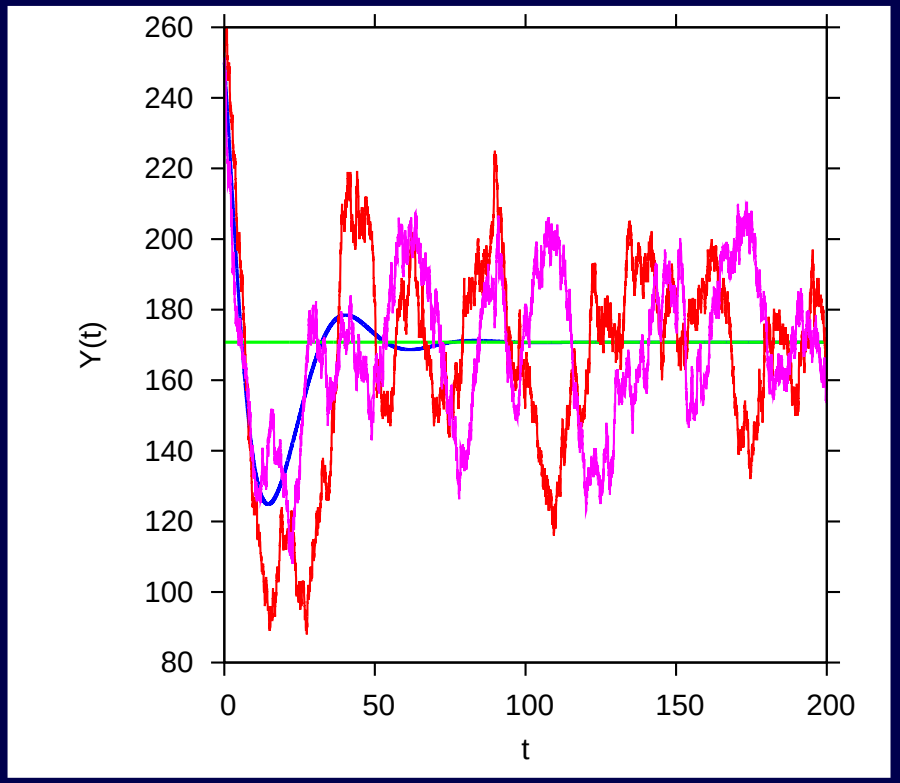

time series of $X(t)$ and $Y(t)$

Including seasonal forcing makes the non-forced Hopf to a torus bifurcation

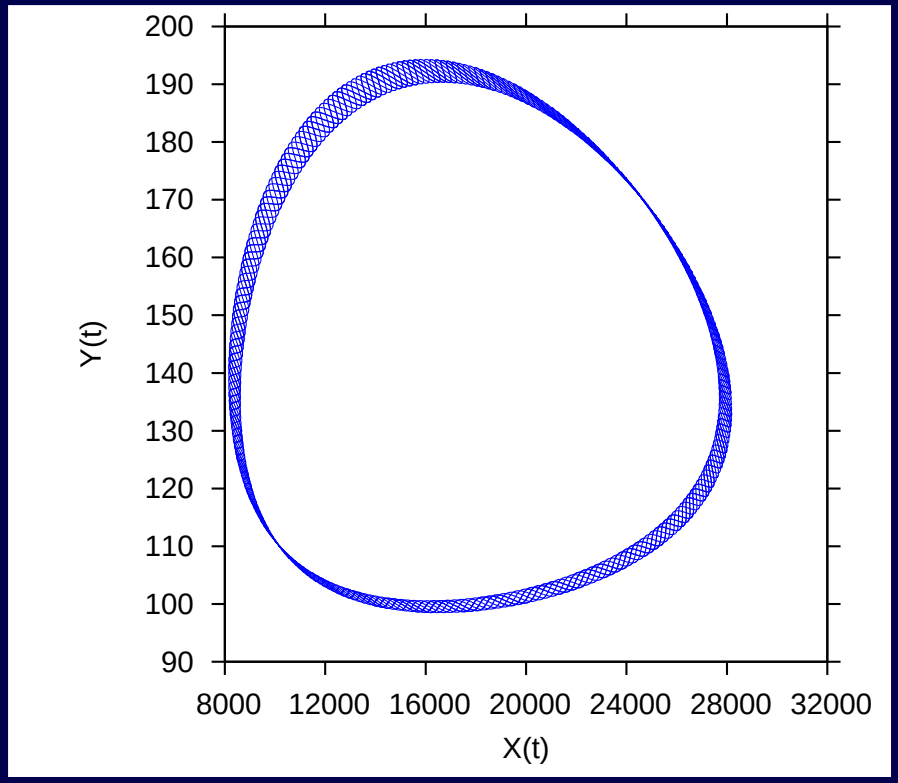

torus in seasonally forced model

Rinaldi, Muratori, Kuznetsov 1993

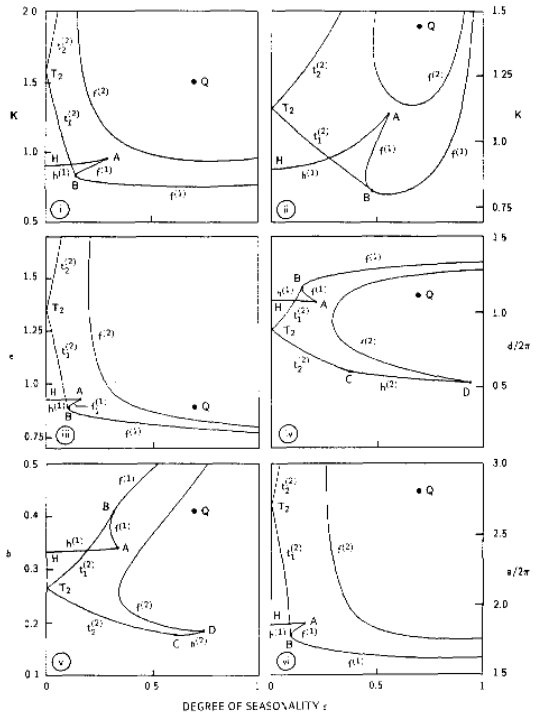

Figure 2. Bifurcation diagrams for system (1), (2). Each case (i), . . . , (vi) refers to the corresponding seasonality mechanism identified in Section 2. Curves $h^{(k)}$, $t^{(2)}$ and $f^{(k)}$, $k = 1, 2$ are Hopf, tangent and flip bifurcation curves, respectively. Points A, B, C, D are codimension two bifurcation points.

Rinaldi, Muratori, Kuznetsov 1993

regions. When this curve is crossed from below, the forced stable cycle of period 1 smoothly bifurcates into a stable quasi-periodic solution. While continuing curve $h^{(1)}$ from the left to the right the multipliers $\mu_{1,2}^{(1)} = e^{\pm i\alpha}$ of the Poincaré map vary and become equal to -1 when the terminal point A is reached.

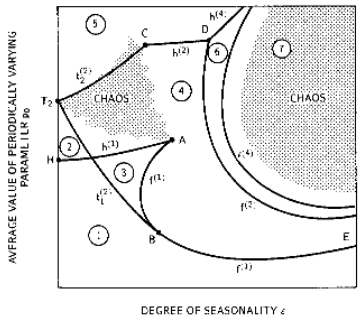

Figure 3. A general qualitative bifurcation diagram for systems (1), (2). Curves $h^{(1)}$, $h^{(2)}$, $h^{(4)}$, $f^{(1)}$, $f^{(2)}$, $f^{(4)}$, $t^{(2)}$ are bifurcation curves. Points A, B, C, D are codimension two bifurcation points.

Point A is a codimension two bifurcation point, called *strong resonance* 1 : 2, studied in Arnold (1982) by means of the normal form approach. The two coefficients of the normal form are of opposite sign and this suffices to say that only two bifurcation curves, namely, a Hopf $h^{(1)}$ and a flip $f^{(1)}$, are rooted at point A (as already said, the branch of $f^{(1)}$ not involving attractors is not shown in the figure). Curve $f^{(1)}$ can be generated by the continuation technique starting from point A. Along curve $f^{(1)}$ the normal form coefficient (computed as in Kuznetsov and Rinaldi, 1991) varies and becomes equal to 0 at point B, which is therefore a codimension two bifurcation point. Thus, curve $f^{(1)}$ is divided into two segments (AB and BE) and the period doubling takes place in opposite directions on these two segments, namely from region 4 on segment AB and from region 1 on segment BE. More precisely, when curve $f^{(1)}$ is crossed from region 1 to region 4 the forced cycle of period 1 loses stability and smoothly bifurcates into a stable period 2 cycle. On the contrary, if $f^{(1)}$ is crossed from region 3 to region 4, the stable cycle of period 1 collides with a saddle cycle of period 2 and becomes a saddle cycle of period 1.

The codimension two bifurcation point B is the terminal point of one of the

Lyapunov spectrum for unforced system

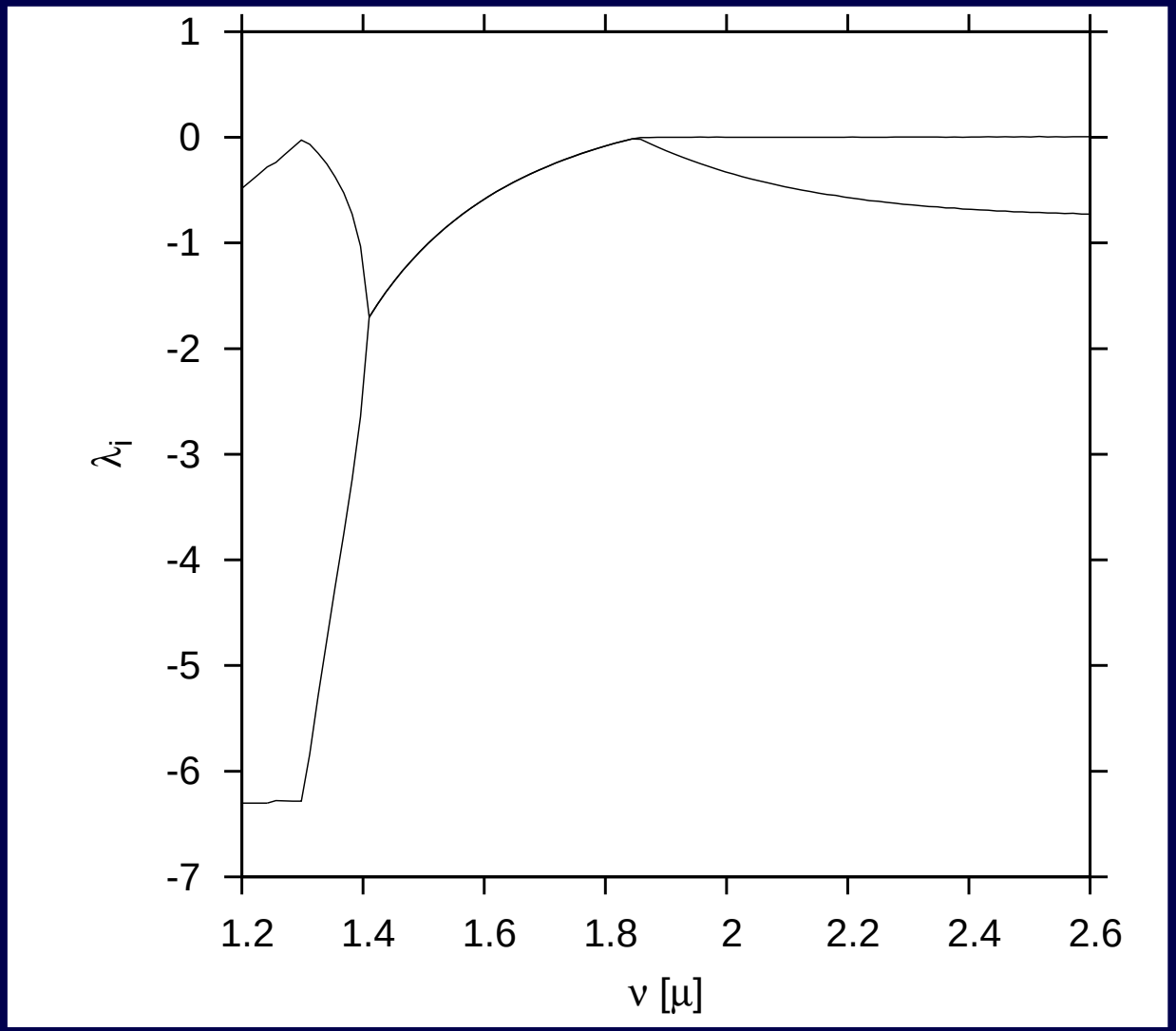

Rosenzweig-MacA. unforced, Lyaps. reveal bifs.

Seasonally forced Rosenzweig-MacArthur system: forced predator birth system

Rosenzweig-MacArthur system with $\nu(t)$

$$\begin{aligned} \dot{X} &= \varrho X\left(1-\frac{X}{\kappa}\right) - k\cdot\varphi(X)Y \\ \dot{Y} &= -\mu Y + \nu(t)\cdot\varphi(X)Y \end{aligned} \tag{1}$$

being

$$\nu(t) = \nu_0\cdot(1+\eta\cdot cos(\omega t))$$

gives 2-dim Jacobian matrix around trajectory for Lyapunov exponent calculation

$$A = \begin{pmatrix} \varrho\left(1-2\frac{X}{\kappa}\right) - k\varphi'(X)Y & -k\varphi(X) \\ \nu(t)\varphi'(X)Y & -\mu+\nu(t)\varphi(X) \end{pmatrix} \tag{2}$$

Seasonally forced Rosenzweig-MacArthur system: autonomous system via Hopf oscillator

Rosenzweig-MacArthur system with $\nu(t)$

$$\begin{aligned}
\dot{X} &= \varrho X\left(1-\frac{X}{\kappa}\right) - k\cdot\varphi(X)Y \\
\dot{Y} &= -\mu Y + \nu_0(1+x)\cdot\varphi(X)Y \\
\dot{x} &= -\omega y + c\cdot x(\eta^2-(x^2+y^2)) \\
\dot{y} &= \omega x + c\cdot y(\eta^2-(x^2+y^2))
\end{aligned} \tag{3}$$

with solution of the Hopf oscillator to force R-MacA system

$$x(t) = \eta\cdot cos(\omega\cdot t)$$

gives 4-dim Jacobian matrix around trajectory for Lyapunov exponent calculation

$$B = \begin{pmatrix}
\varrho\left(1-2\frac{X}{\kappa}\right) - k\varphi'(X)Y & -k\varphi(X) & 0 & 0 \\
\nu_0(1+x)\cdot\varphi'(X)Y & -\mu+\nu_0(1+x)\cdot\varphi(X) & \nu_0\varphi(X)Y & 0 \\
0 & 0 & c(\eta^2-(x^2+y^2))-2cx^2 & -\omega-2cxy \\
0 & 0 & \omega-2cxy & c(\eta^2-(x^2+y^2))-2cy^2
\end{pmatrix} \tag{4}$$

Lyapunov spectrum for forced system

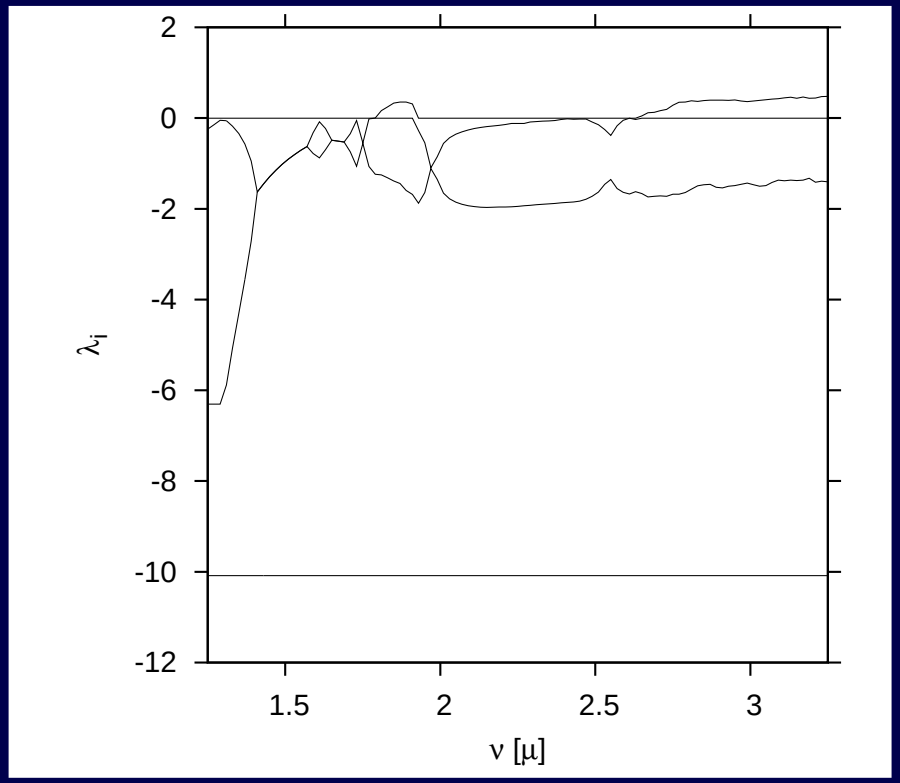

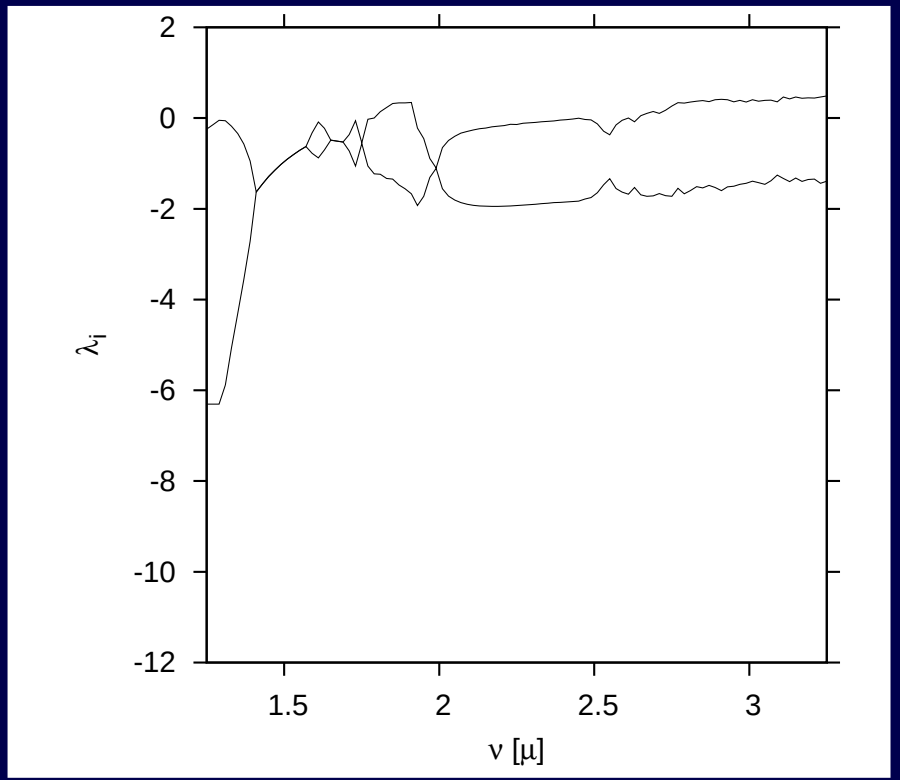

forcing via coupled Hopf-oscillator versus direct forcing

Rinaldi, Muratori, Kuznetsov 1993

regions. When this curve is crossed from below, the forced stable cycle of period 1 smoothly bifurcates into a stable quasi-periodic solution. While continuing curve $h^{(1)}$ from the left to the right the multipliers $\mu_{1,2}^{(1)} = e^{\pm i\alpha}$ of the Poincaré map vary and become equal to -1 when the terminal point A is reached.

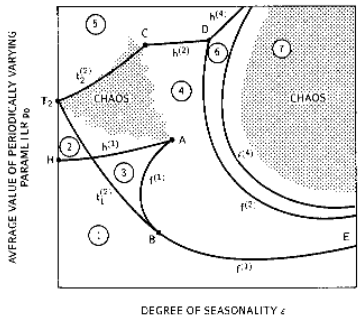

Figure 3. A general qualitative bifurcation diagram for systems (1), (2). Curves $h^{(1)}$, $h^{(2)}$, $h^{(4)}$, $f^{(1)}$, $f^{(2)}$, $f^{(4)}$, $t^{(2)}$ are bifurcation curves. Points A, B, C, D are codimension two bifurcation points.

Point A is a codimension two bifurcation point, called *strong resonance* 1 : 2, studied in Arnold (1982) by means of the normal form approach. The two coefficients of the normal form are of opposite sign and this suffices to say that only two bifurcation curves, namely, a Hopf $h^{(1)}$ and a flip $f^{(1)}$, are rooted at point A (as already said, the branch of $f^{(1)}$ not involving attractors is not shown in the figure). Curve $f^{(1)}$ can be generated by the continuation technique starting from point A. Along curve $f^{(1)}$ the normal form coefficient (computed as in Kuznetsov and Rinaldi, 1991) varies and becomes equal to 0 at point B, which is therefore a codimension two bifurcation point. Thus, curve $f^{(1)}$ is divided into two segments (AB and BE) and the period doubling takes place in opposite directions on these two segments, namely from region 4 on segment AB and from region 1 on segment BE. More precisely, when curve $f^{(1)}$ is crossed from region 1 to region 4 the forced cycle of period 1 loses stability and smoothly bifurcates into a stable period 2 cycle. On the contrary, if $f^{(1)}$ is crossed from region 3 to region 4, the stable cycle of period 1 collides with a saddle cycle of period 2 and becomes a saddle cycle of period 1.

The codimension two bifurcation point B is the terminal point of one of the

Stollenwerk et al. 2016

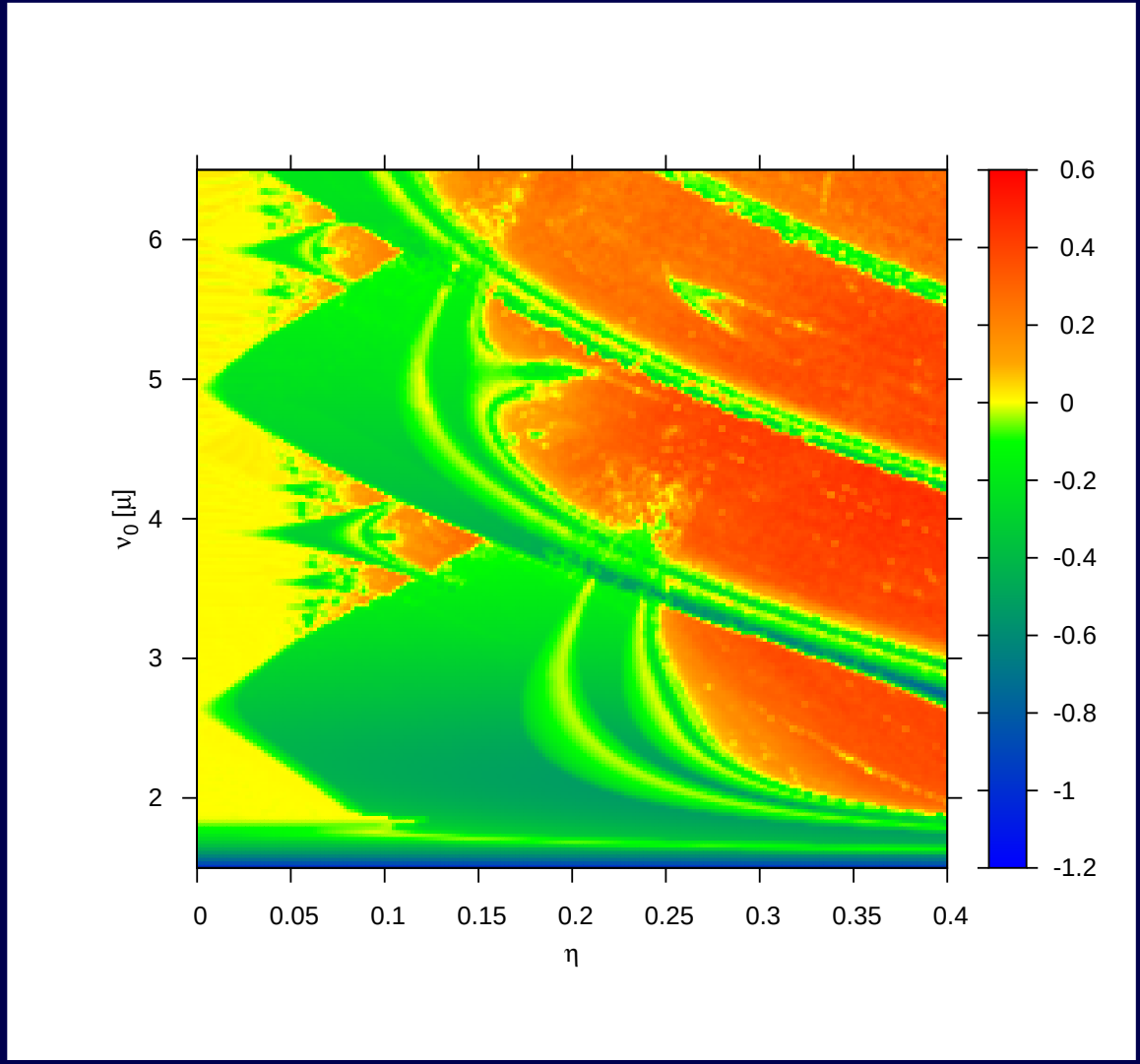

Lyapunov dominant exponents, Yuri's param.

Stollenwerk et al. 2016

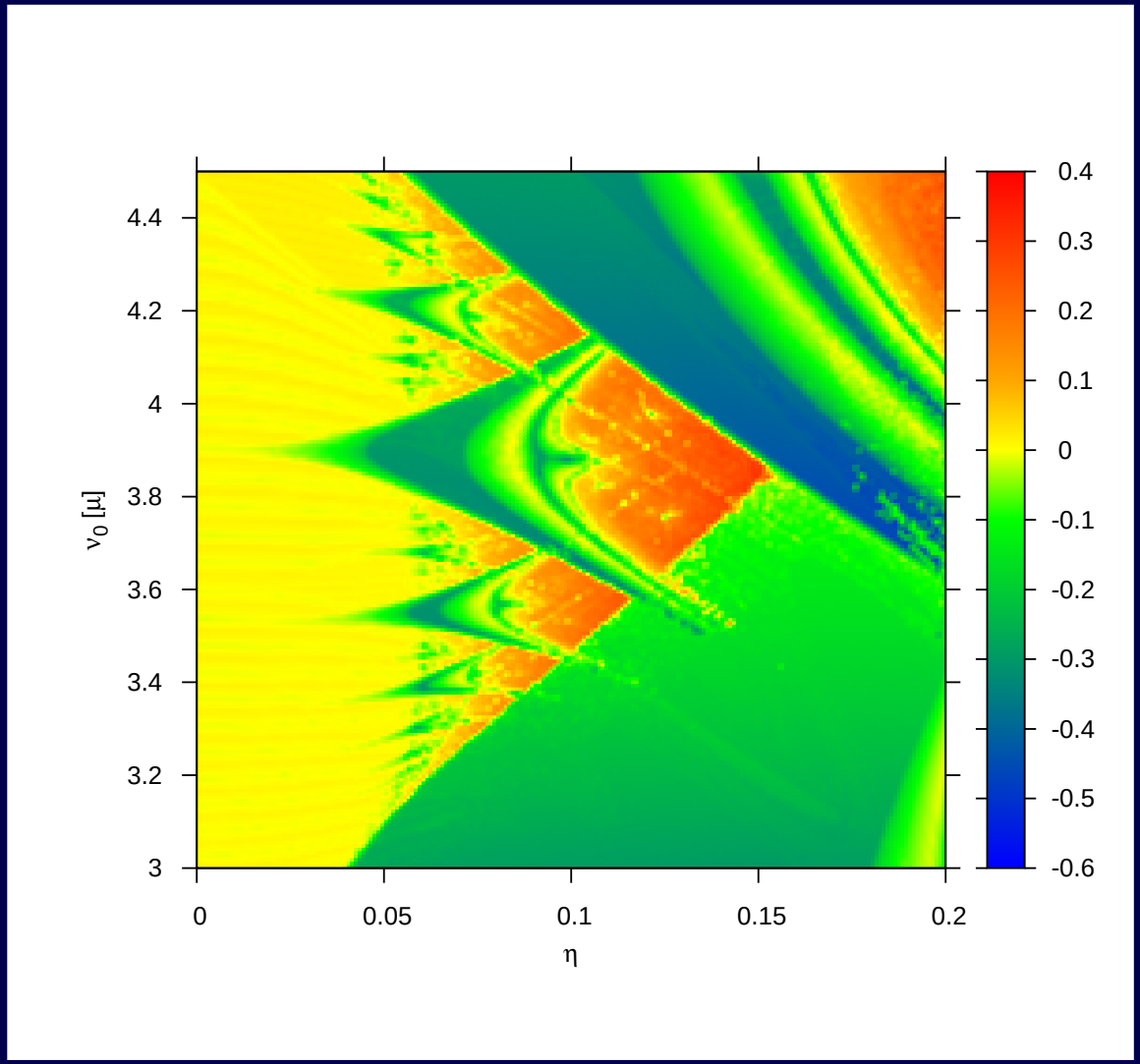

zooming in reveals Arnol'd tongues, Yuri's param.

First results with AUTO

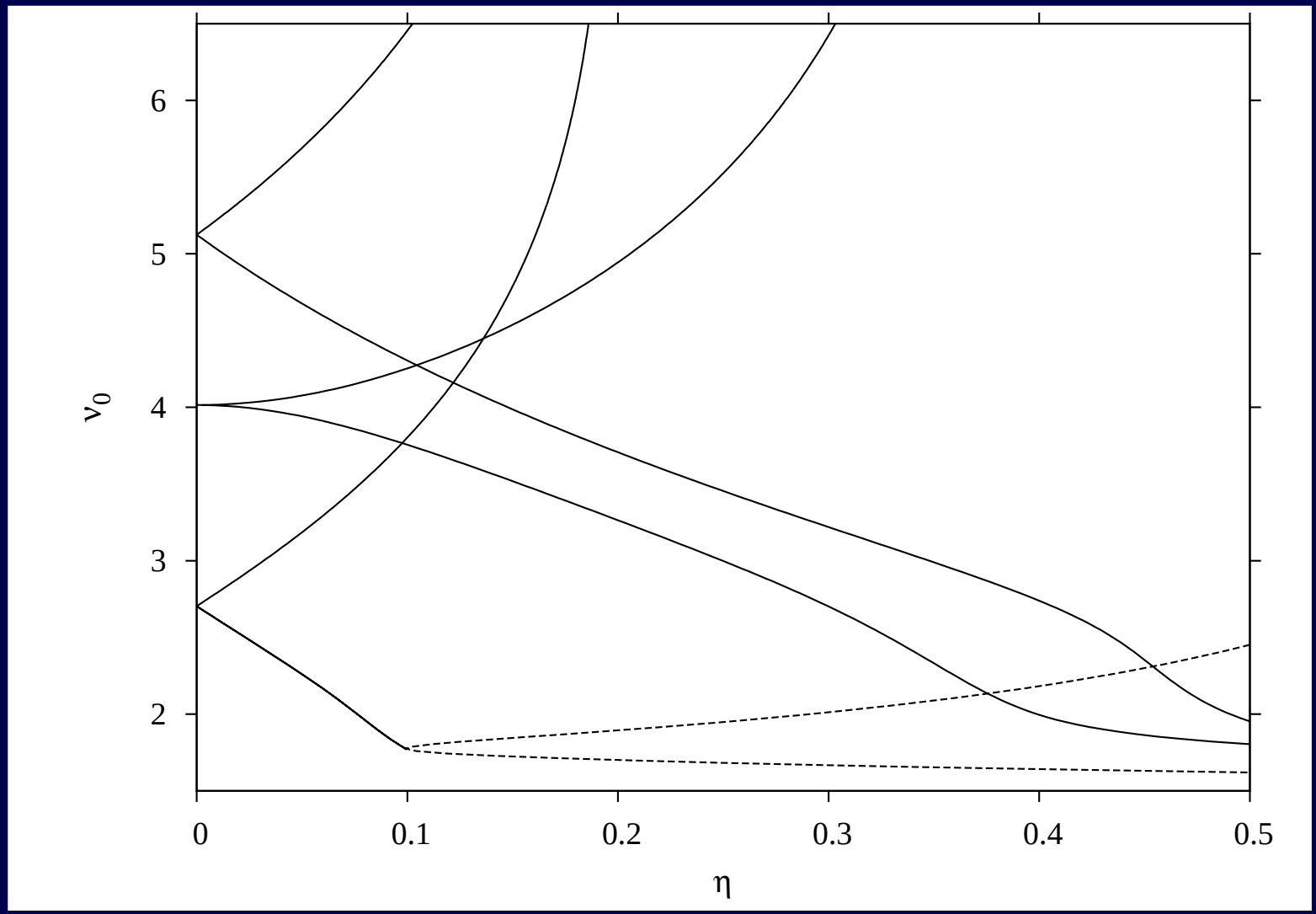

bifurcation continuation compares well
with Lyapunov analysis

Stollenwerk et al. 2016

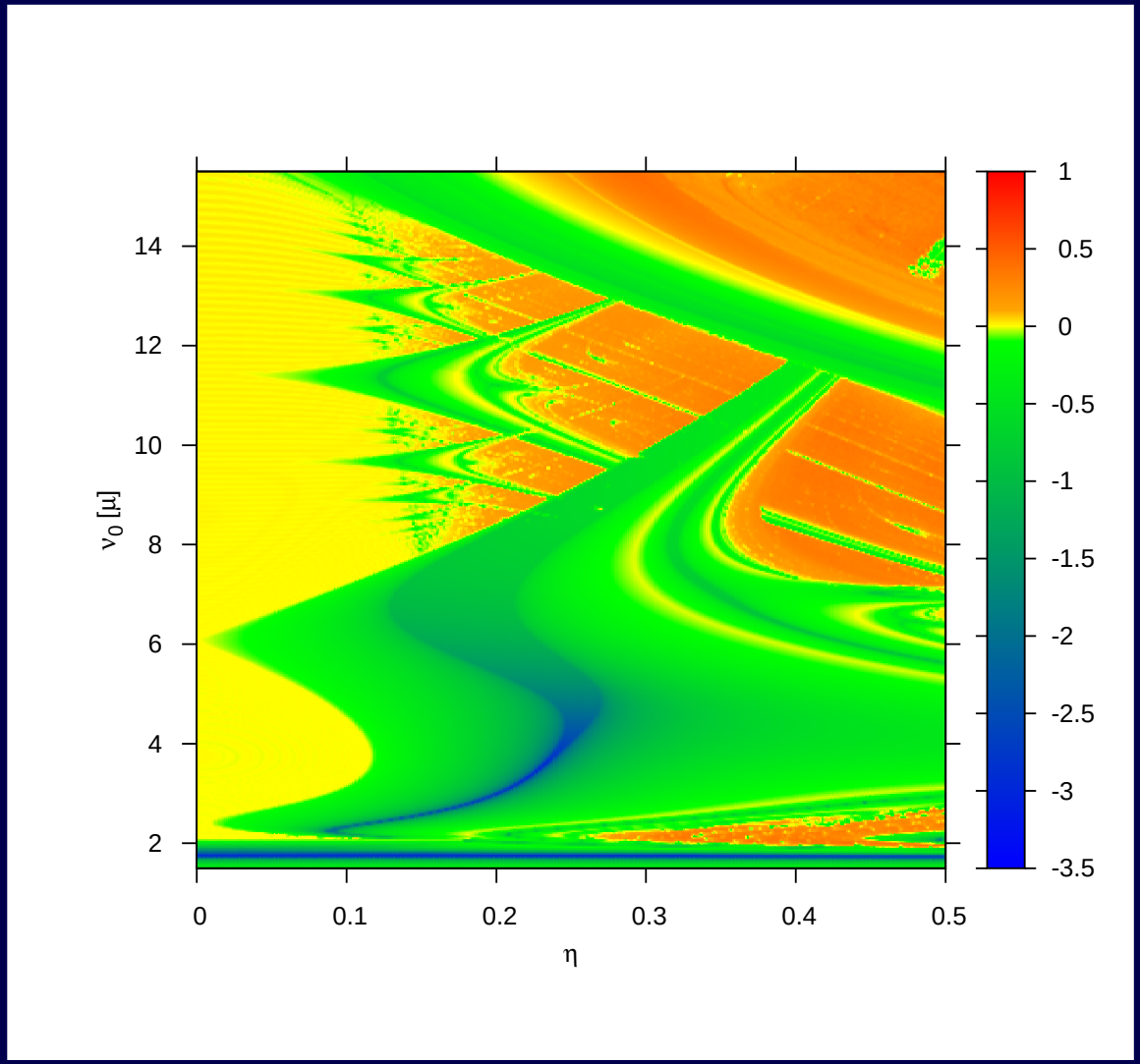

works also with time scale separable param. (stoch. version)

Further discussions and future work

discussion: Is the prey dynamics really just logistic growth?

Does it matter in understanding ecological systems? Data!

ecological data classically: Hudson Bay Company data on hares and lynx

problems in understanding the data: "Do hares eat lynx?"

Further discussions and future work

problems in understanding the Hudson Bay data: "Do hares eat lynx?"

Are super-predators (with predator preference) important?

... more important than time scales in preys?

Data from the Hudson Bay Company on on furs of hares and lynx

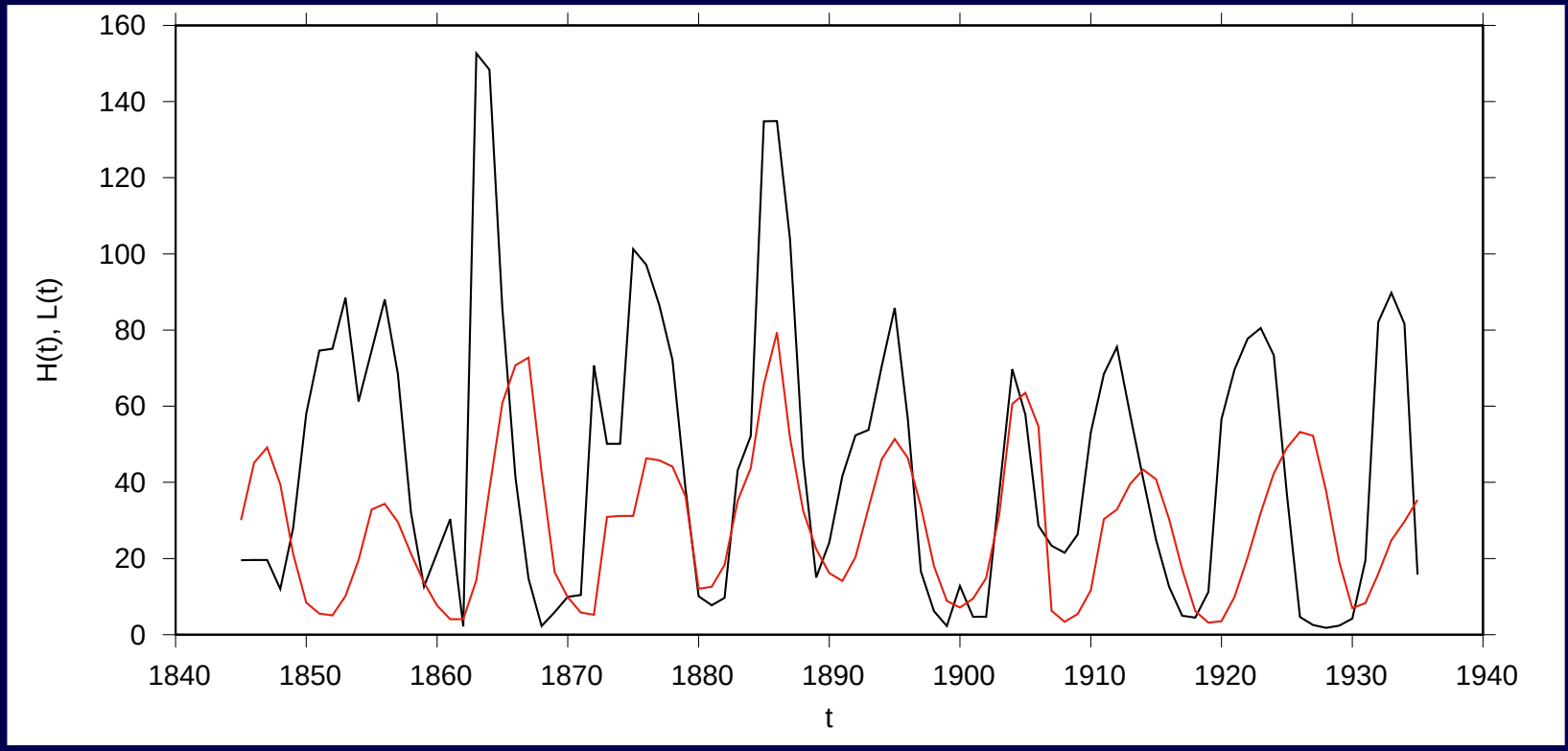

data on hares (black) and lynx (red) in thousands from 1845 to 1935 yearly

Model Comparison

Consider, for a given data set $\underline{I}$, two models: M_1 with parameter β and M_2 with parameter λ

$$\frac{p(M_1|\underline{I})}{p(M_2|\underline{I})} = \frac{\frac{p(\underline{I}|M_1)}{p(\underline{I})} \cdot p(M_1)}{\frac{p(\underline{I}|M_2)}{p(\underline{I})} \cdot p(M_2)} = \frac{p(\underline{I}|M_1)}{p(\underline{I}|M_2)} \cdot \frac{p(M_1)}{p(M_2)}$$

Model Comparison

Consider, for a given data set $\underline{I}$, two models: M_1 with parameter β and M_2 with parameter λ

$$\frac{p(M_1|\underline{I})}{p(M_2|\underline{I})} = \frac{\frac{p(\underline{I}|M_1)}{p(\underline{I})} \cdot p(M_1)}{\frac{p(\underline{I}|M_2)}{p(\underline{I})} \cdot p(M_2)} = \frac{p(\underline{I}|M_1)}{p(\underline{I}|M_2)} \cdot \frac{p(M_1)}{p(M_2)}$$

Assuming $p(M_1) = p(M_2) = \frac{1}{2}$ we obtain the Bayes factor k via

$$\frac{p(M_1|\underline{I})}{p(M_2|\underline{I})} = \frac{p(\underline{I}|M_1)}{p(\underline{I}|M_2)} := k$$

Model Comparison

Consider, for a given data set $\underline{I}$, two models: M_1 with parameter β and M_2 with parameter λ

$$\frac{p(M_1|\underline{I})}{p(M_2|\underline{I})} = \frac{\frac{p(\underline{I}|M_1)}{p(\underline{I})} \cdot p(M_1)}{\frac{p(\underline{I}|M_2)}{p(\underline{I})} \cdot p(M_2)} = \frac{p(\underline{I}|M_1)}{p(\underline{I}|M_2)} \cdot \frac{p(M_1)}{p(M_2)}$$

Assuming $p(M_1) = p(M_2) = \frac{1}{2}$ we obtain the Bayes factor k via

$$\frac{p(M_1|\underline{I})}{p(M_2|\underline{I})} = \frac{p(\underline{I}|M_1)}{p(\underline{I}|M_2)} := k$$

and with $p(\underline{I}|M_1) := \int p(\underline{I}|\beta, M_1)p(\beta, M_1)\, d\beta$

$$p(\underline{I}|M_1) = k_1 \cdot \frac{\Gamma(a_1 + b_1)}{\Gamma(a_1)\Gamma(a_2)} \cdot \frac{\Gamma(a_1 + k_2)\Gamma(b_1 + k_3)}{\Gamma(a_1 + k_2 + b_1 + k_3)}$$

and $p(\underline{I}|M_2) := \int p(\underline{I}|\lambda, M_2)p(\lambda, M_2)\, d\lambda$

$$p(\underline{I}|M_2) = k_5 \cdot \frac{b_2^{a_2}}{\Gamma(a_2)} \cdot \frac{\Gamma(a_2 + k_2)}{(b_2 + n)^{a_2 + k_2}}$$

Model Comparison

we get for Bayes factor k

$$k = \frac{k_1 \cdot \Gamma(a_1 + b_1) \cdot \Gamma(a_1 + k_2) \cdot \Gamma(b_1 + k_3) \cdot \Gamma(a_2) \cdot (b_2 + n)^{a_2 + k_2}}{k_5 \cdot \Gamma(a_1) \cdot \Gamma(b_1) \cdot \Gamma(a_1 + k_2 + b_1 + k_3) \cdot \Gamma(a_2 + k_2) \cdot b_2^{a_2}}$$

where

$$k_1 := \left(\prod_{\nu=0}^{n-1} \binom{N - I_\nu}{I_{\nu+1} - I_\nu} \right) \qquad k_2 := \sum_{\nu=0}^{n-1} (I_{\nu+1} - I_\nu)$$

$$k_3 := \sum_{\nu=0}^{n-1} (N - I_{\nu+1}) \qquad k_5 := \prod_{\nu=0}^{n-1} \frac{1}{(I_{\nu+1} - I_\nu)!}$$

Numerical examples

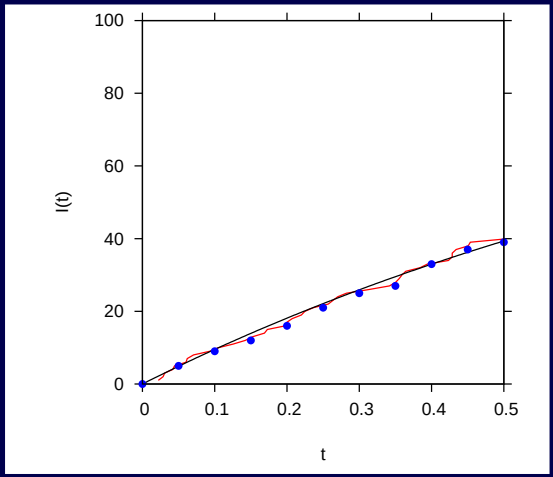

$\beta = 1.0$

$k = 0.957514$

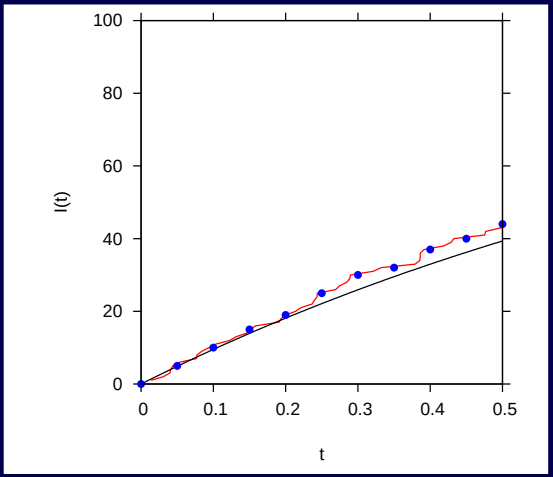

$\beta = 1.0$

$k = 1.394059$

Numerical examples

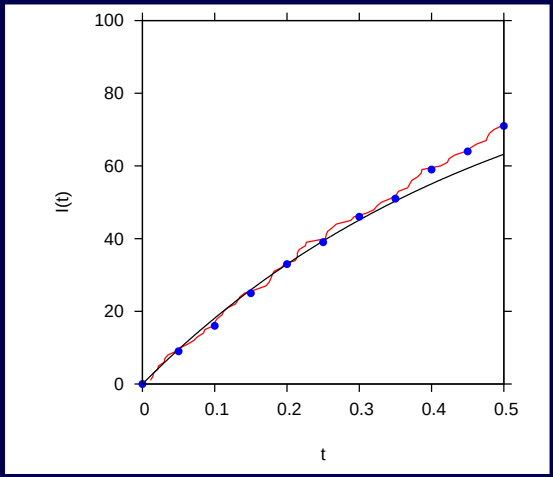

$\beta = 2.0$

$k = 0.650476$

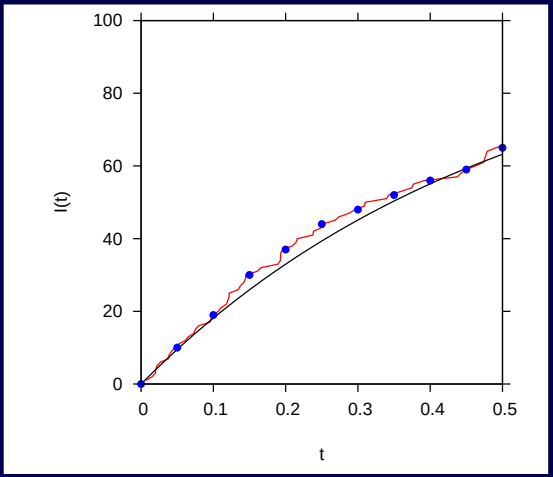

$\beta = 2.0$

$k = 83.234998$

Numerical examples

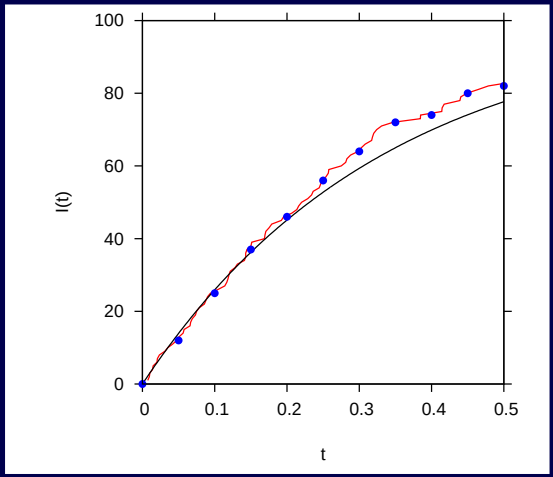

$\beta = 3.0$

$k = 3343.696$

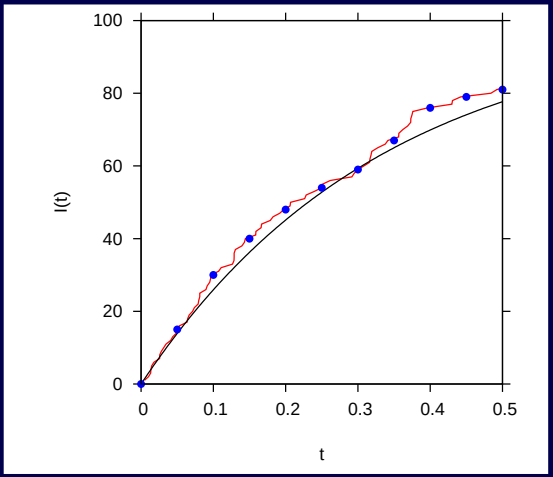

$\beta = 3.0$

$k = 10941.218$

Bayes factor for many realizations over changing parameter

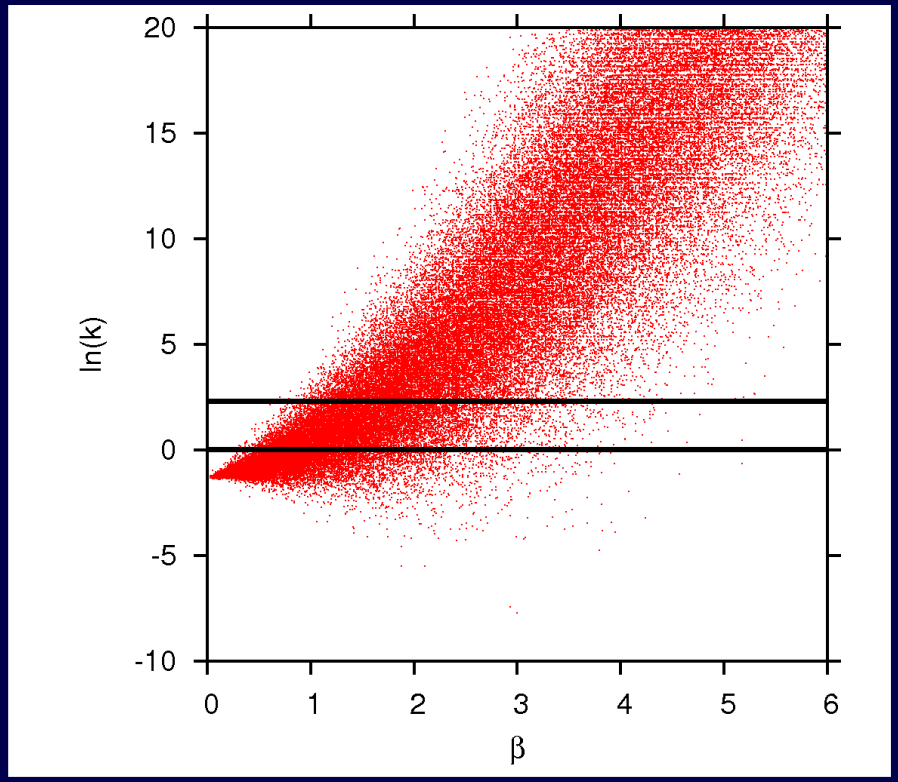

many realizations show more evidence for simplistic model than for the underlying model

(lines for ln(1), no evidence, and ln(10), "strong evidence" for more complex model)

Application to systems without anlytic solutions: Comparison of data with simulations

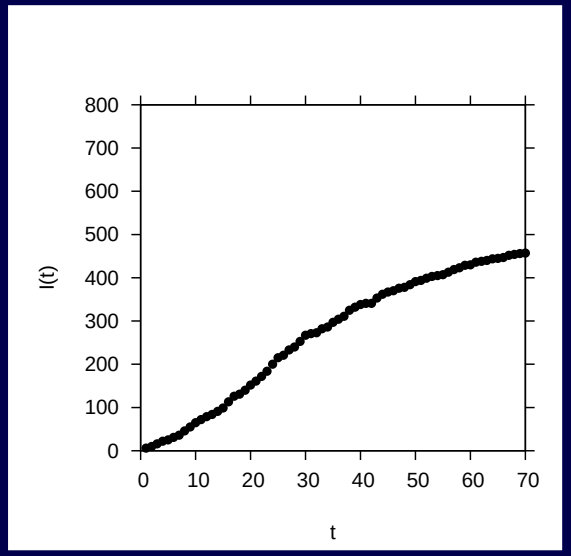

flu data cumulative

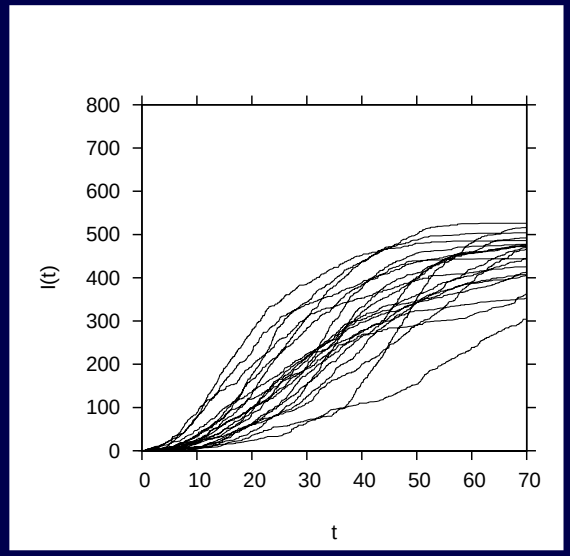

simulations of SIR-system

number of simulations in η-ball vicinity to data set gives likelihood of data under this model parameter set

=> estimate of likelihood function (Stollenwerk, Briggs 2000)

Comparison of data with simulations

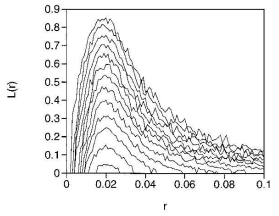

Fig. 4. Empirical likelihood curves for the one parameter r for various values of η-neighbourhoods. The maximum does not change much with varying η, showing that the estimate for the parameter is rather robust.

mates of the parameters used for our likelihood sections are obtained with this method.

From the Padé approximation in Section 6 instead of likelihood sections we could also easily generate likelihood profiles as described for example in Ref. [12]. These profiles are calculated by varying one parameter and maximizing the likelihood in respect to all other model parameters, which is rather cumbersome for the Empirical Likelihood Method due to the fluctuations around the empirical likelihood maximum (see Fig. 4). In biological systems one often has information about some of the model parameters from other experiments and searches for an otherwise difficult obtainable parameter like the contact rate, which is r in our case. In such situations the Empirical Likelihood Method is easiest and best applicable. However, we have also investigated empirical likelihoods with variation of two parameters [11].

8. Summary and prospect

We have solved the Master equation for a plant disease model analytically and also obtained numerically stable solutions over the whole range of states, which was previously not possible using the matrix exponential.

The solution is used for constructing likelihood sections from empirical microcosm data. The Master equation approach can be easily generalized to more complex models, allowing for likelihood estimations on the basis of simulated trajectories. Further research on this Empirical Likelihood Method is in progress.

The form of the Master equation we use here gives exponential waiting times between events and in the Gillespie algorithm this property is used explicitly to construct stochastic realizations of the process. However, the exponential waiting time is not a principal restriction, but arbitrary waiting time distributions can be included in a Master equation with time-convolution [13,14]. It would be an interesting extension of the present work to combine numerically this time-convolved Master equation with our Empirical Likelihood Method.

Also the Master equation approach opens naturally the way to a Fock space formulation of stochastic processes [15] which is easily generalizable to the field theoretic treatment of spatial epidemic systems see Ref. [16], and related Refs. [17–21]). Such a field theory is needed to describe the underlying experimental system more appropriately, as first experiments by Bailey et al. indicate [22]). The time decaying susceptibility drives the system through a threshold region between a simple spreading regime and a non-spreading regime.

Acknowledgements

We gratefully acknowledge discussions and provision of experimental data by Gavin Gibson, Adam Kleczkowski and Doug Bailey, and financial support of the BBSRC obtained by Chris Gilligan. We also thank the referees for some helpful references.

References

[1] N.G. van Kampen, Stochastic Processes in Physics and Chemistry, North-Holland, Amsterdam, 1992.
[2] N.S. Goel, N. Richter-Dyn, Stochastic models in Biology, Academic Press, New York, 1974.
[3] A. Kleczkowski, D.J. Bailey, C.A. Gilligan, Proc. R. Soc. (London) B 263 (1996) 777.
[4] C.W. Gardiner, Handbook of Stochastic Methods, Springer, Berlin, 1985;

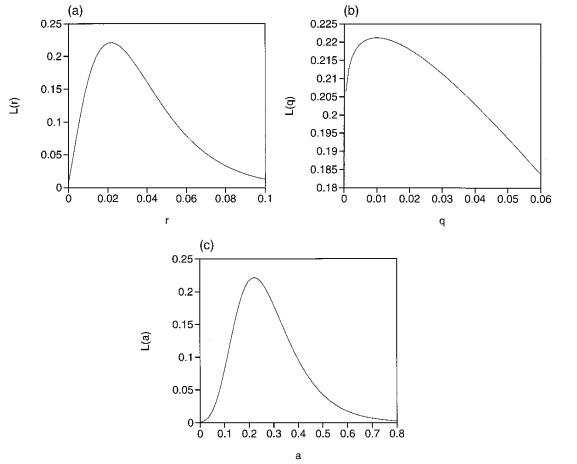

Fig. 3. Likelihood sections for all three parameters, i.e. variation of one parameter, keeping the others fixed at their maximal values, as obtained from the likelihood maximization. The estimates are: $r = 0.022$, $q = 0.0099$ and $a = 0.22$.

using the β-recursion, i.e. using Eq. (14). We obtained in this way the same value for L from both methods. Only the machine precision prevented using the β-recursion for higher values of k_i.

7. Empirical likelihood

The above mentioned solution cannot be carried through to more general Master equations, which have different time-dependent transition rates for different transitions as likely in multicompartmental models, for example models with an additional exposed class (SEI models) between susceptible and infected classes (as in the SI models we consider here). Still, the single trajectory simulation method holds for time-dependent multicompartment models and even can be used for constructing empirically obtained likelihoods. We experiment with such a method by estimating the joint probability of the data, that is, Eq. (12), directly from simulated stochastic trajectories. In the space of dimensionality of the number of data points the estimate is given by using balls around the measured data with radius η (η-balls) and counting the number of simulated trajectories inside these neighborhoods (for details see a forthcoming article by Stollenwerk [11]). The esti-

estimate of likelihood function (Stollenwerk, Briggs 2000)

η-ball method:
estimation of $p(I_1, I_2, ...|\beta)$

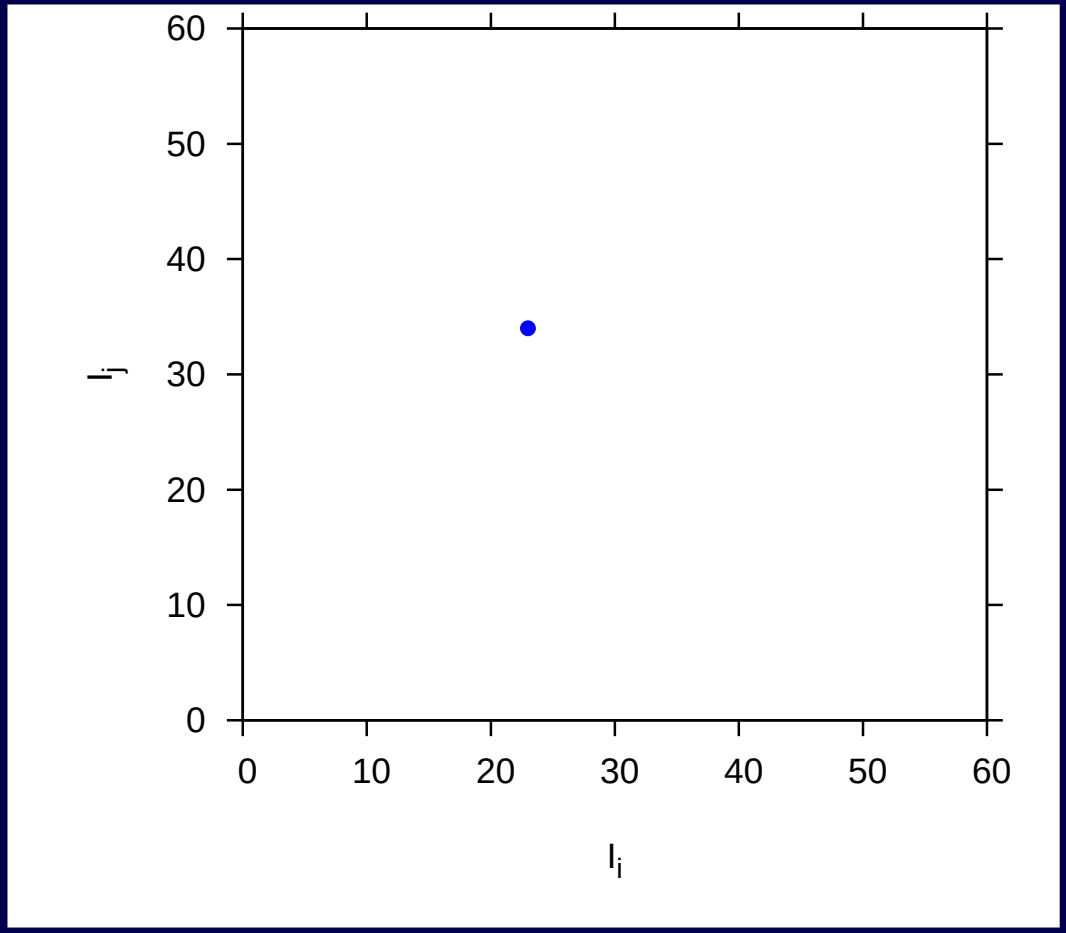

data vector $\underline{I} := (I_1, I_2, ...)$

η-ball method:
estimation of $p(I_1, I_2, ...|\beta)$

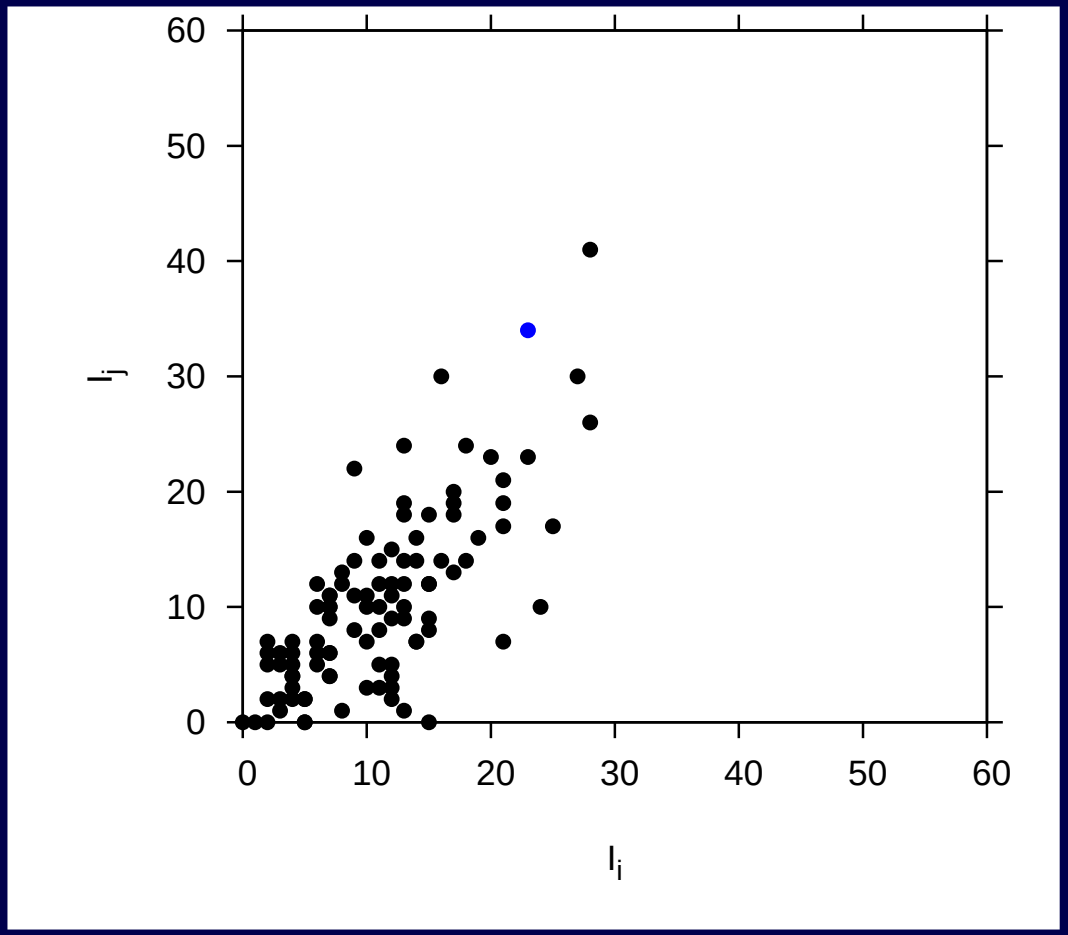

data vector $\underline{I} := (I_1, I_2, ...)$
compared with simulations $\underline{I}$ for one β-value

η-ball method:
estimation of $p(I_1, I_2, ...|\beta)$

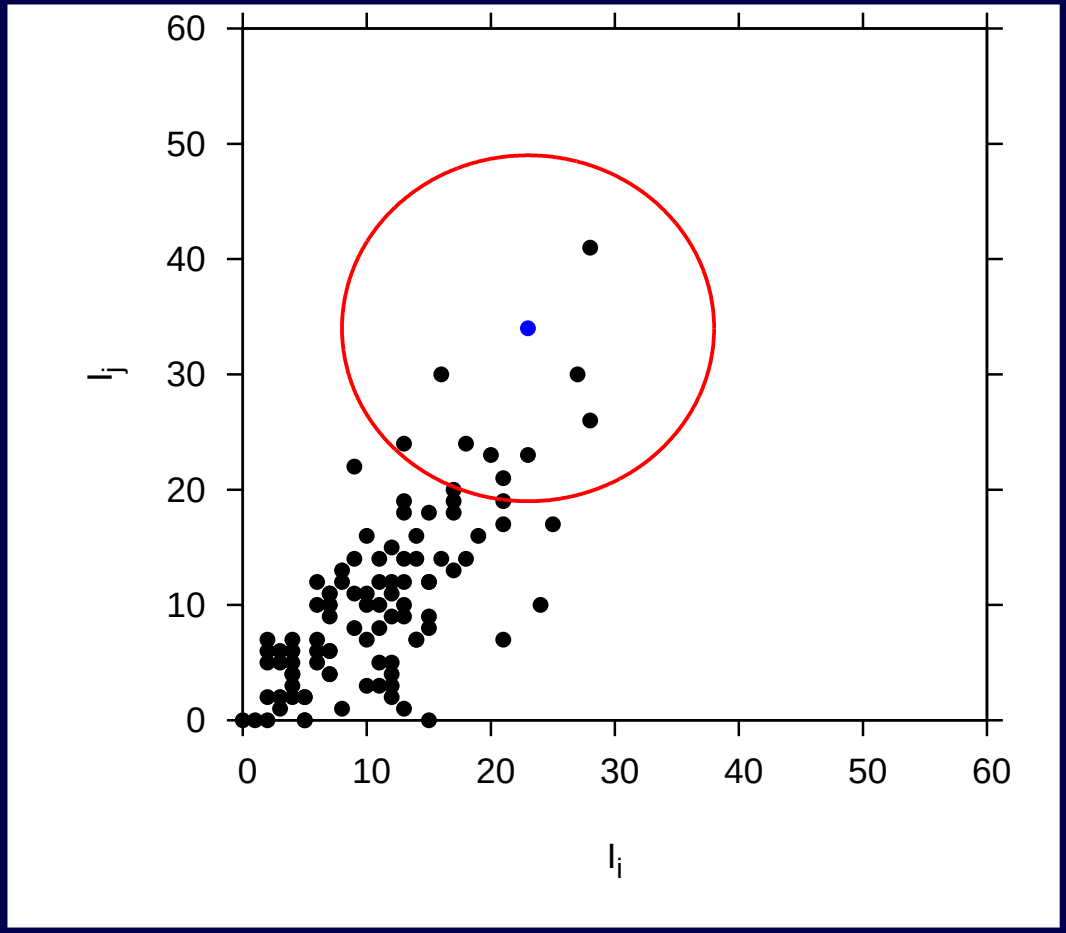

data vector $\underline{I} := (I_1, I_2, ...)$
compared with simulations $\underline{I}$ for one β-value in η-distance

η-ball method:
estimation of $p(I_1, I_2, ...|\beta)$

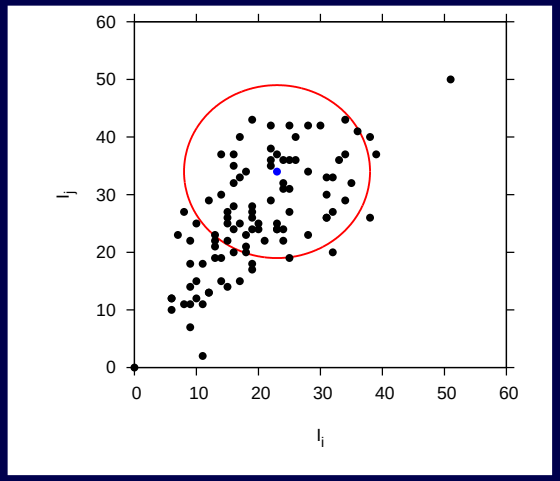

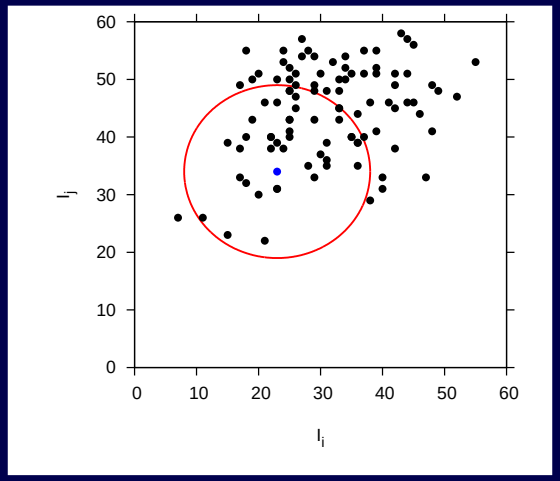

varying β gives estimated likelihood function

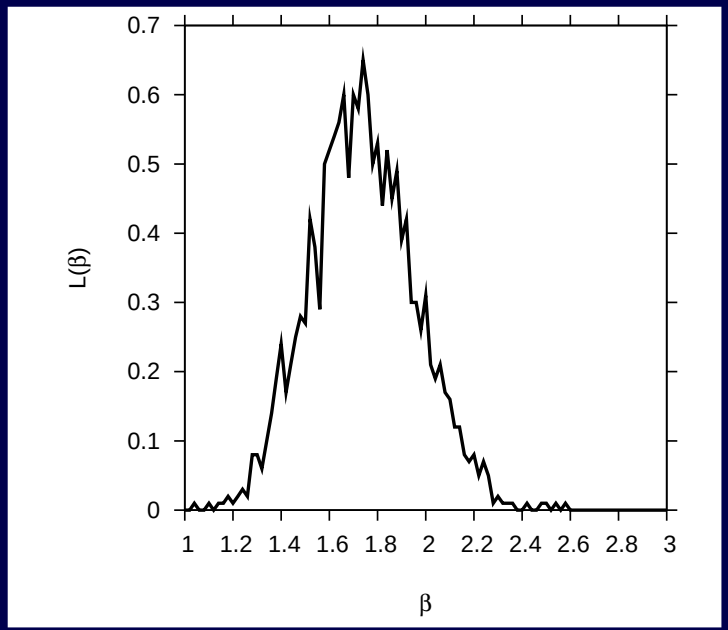

η-ball method:
estimation of $p(I_1, I_2, ...|\beta)$

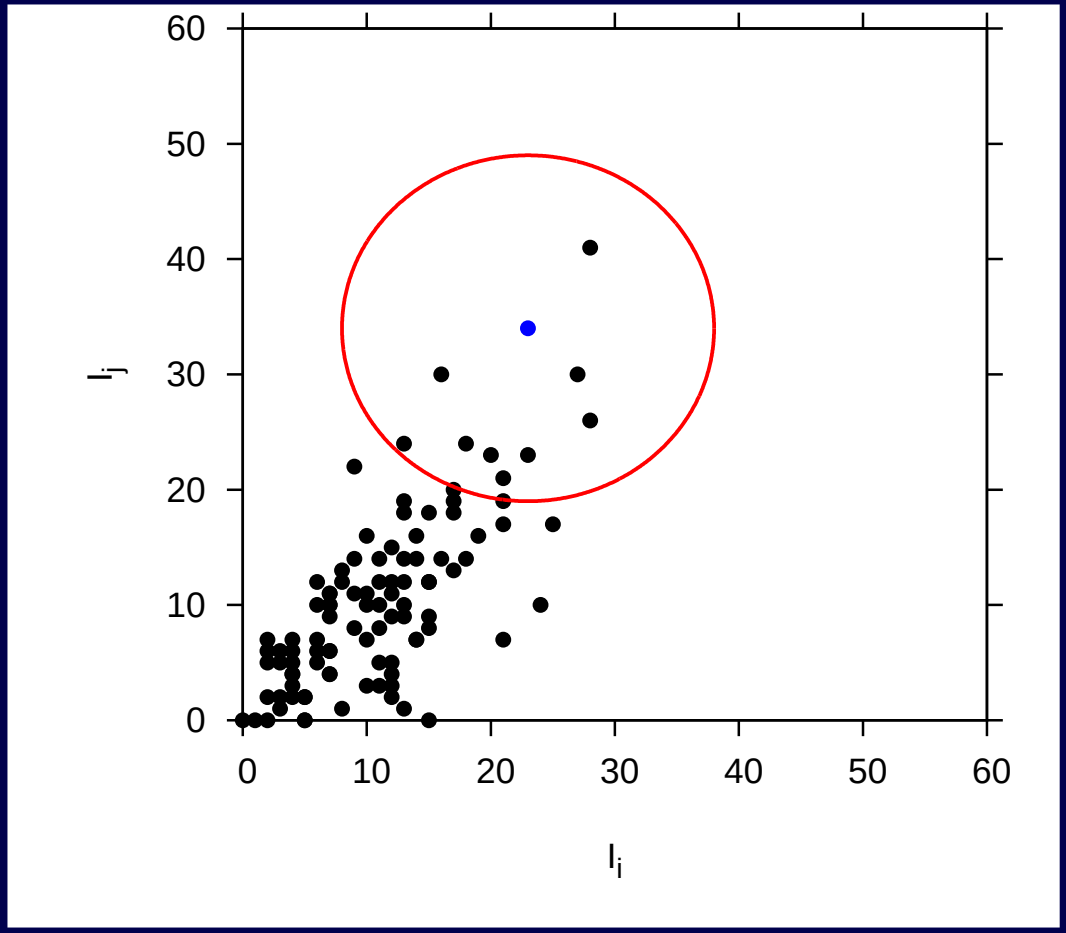

data vector $\underline{I} := (I_1, I_2, ...)$
compared with simulations $\underline{I}$ for β-values in $\eta \longrightarrow 0$

η-ball method:
estimation of $p(I_1, I_2, ...|\beta)$

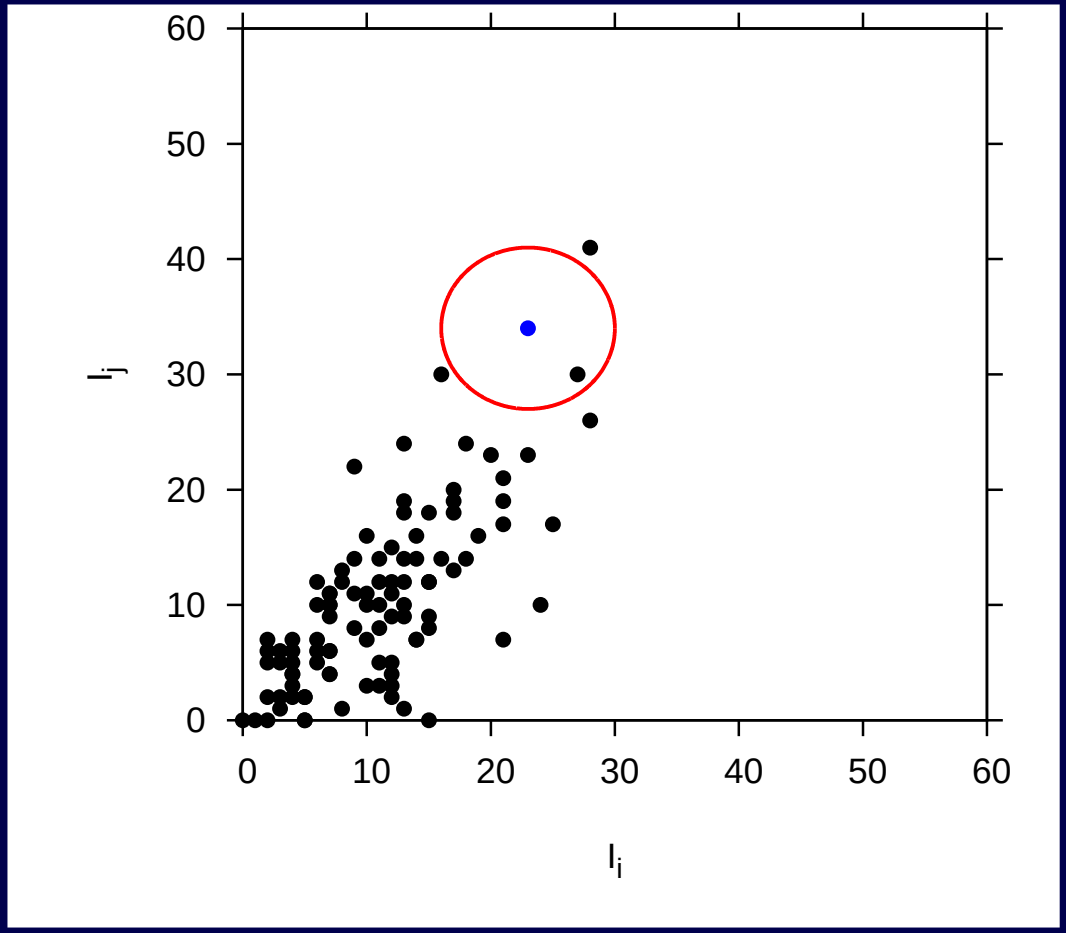

data vector $\underline{I} := (I_1, I_2, ...)$
compared with simulations $\underline{I}$ for β-values in $\eta \longrightarrow 0$

Computer practical in Biomaths-Lecture 2014: data from SIS system in η-ball method

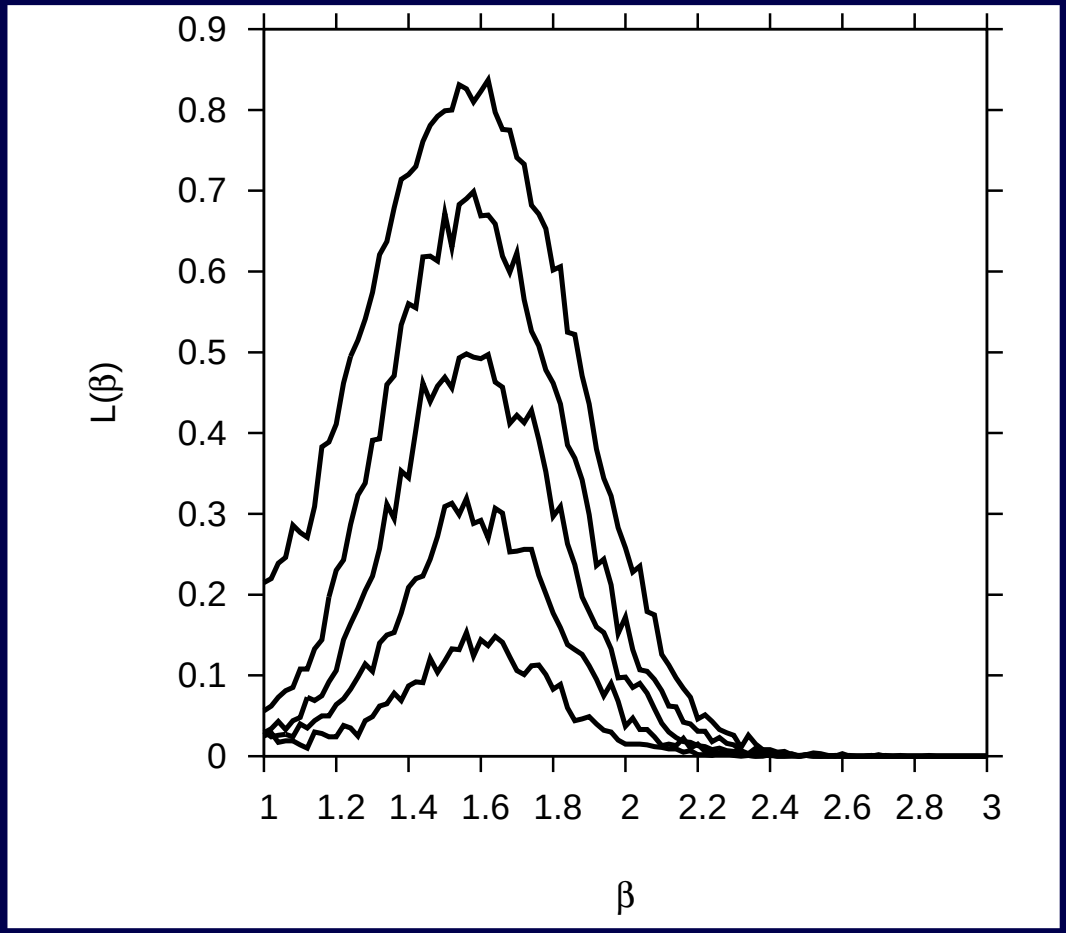

histogram of $p(||\underline{I}_{sim,k} - \underline{I}_{data}|| < \eta|\beta)$ for various η-values

η-ball method for Dutch influenza data

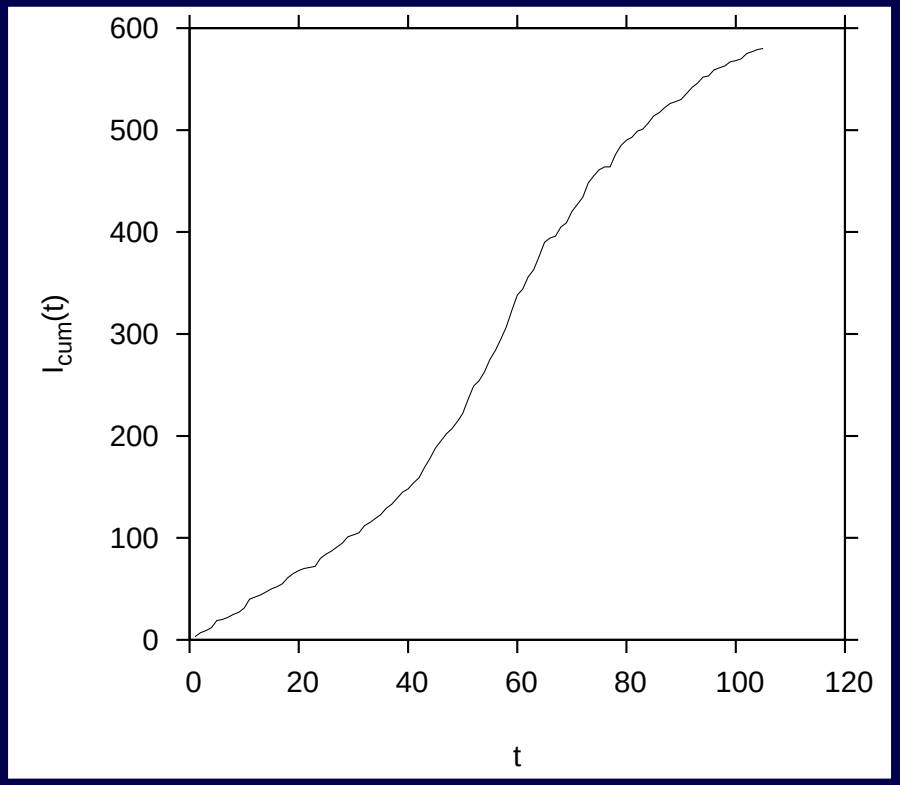

daily influenza data between 1st of January and 15th of April 2007 for the Netherlands (from InfluenzaNet, EPIWORK project)

... to be compared with SIR stochastic simulations for various parameter values

Estimated likelihood function

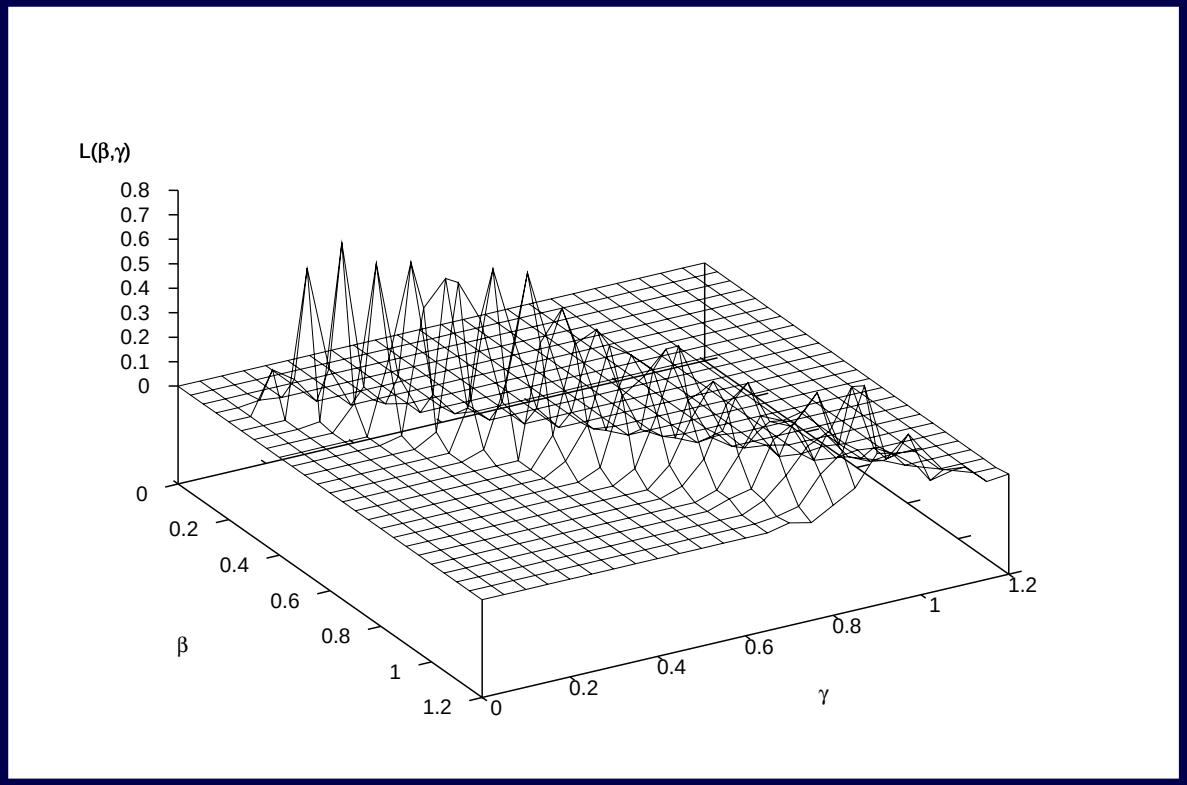

Likelihood per data point

Estimated likelihood function

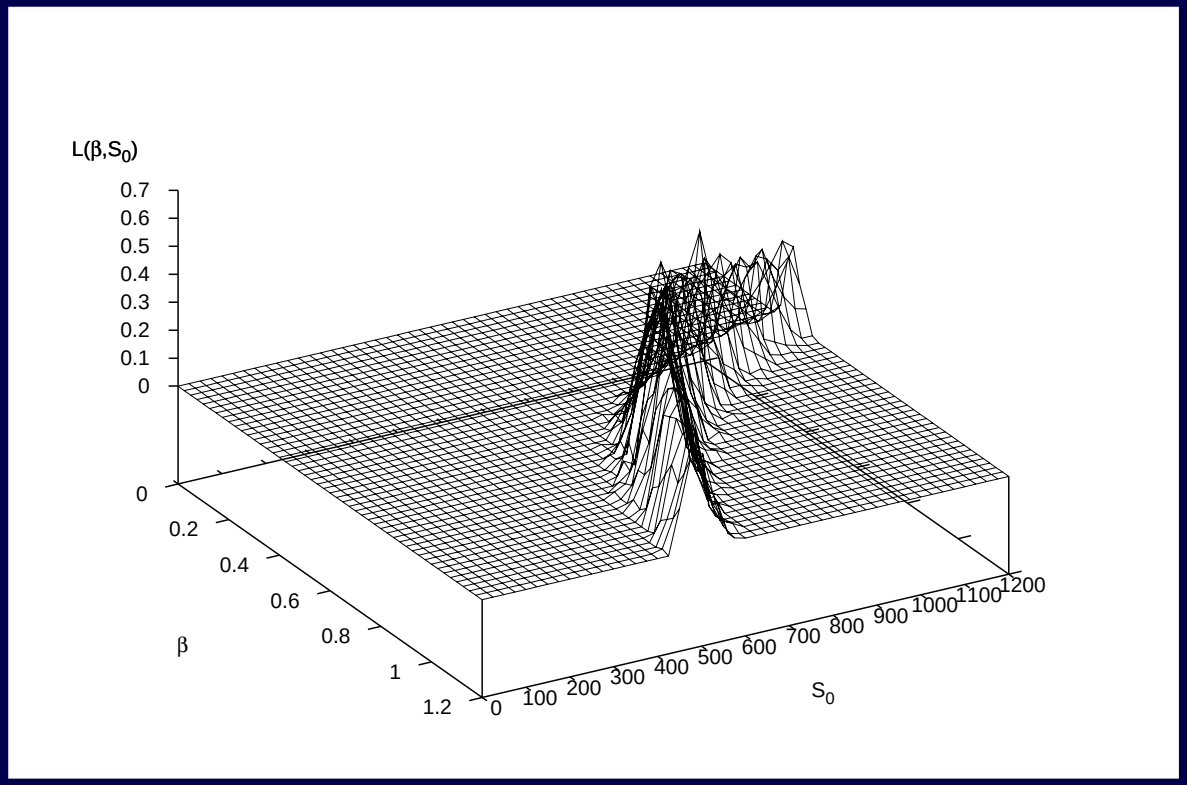

Likelihood profiles versus likelihood sections

Can we obtain Bayes factor from η-ball method ???

Test example:
Linear infection model versus Poisson model

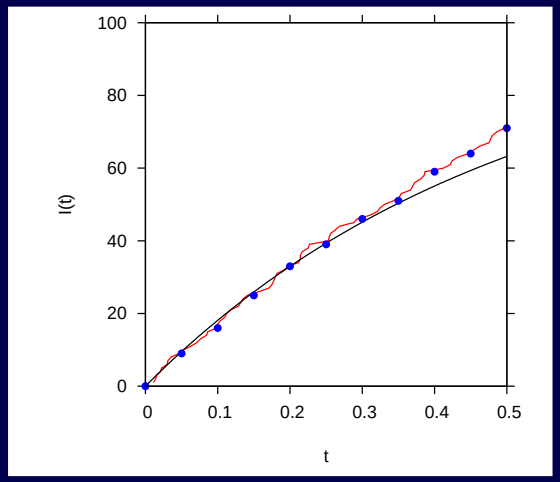

$\beta = 2.0$

$k = 0.650476$

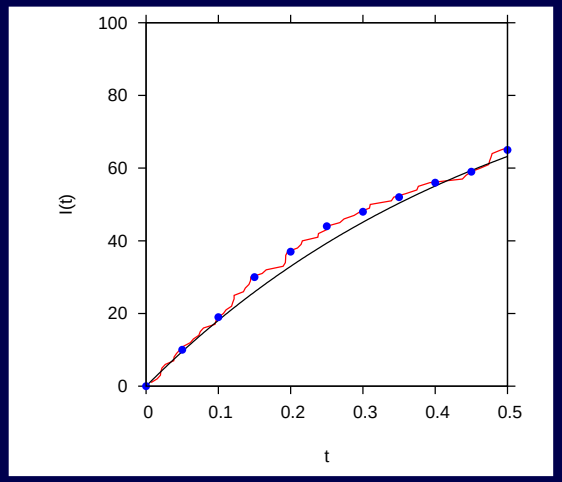

$\beta = 2.0$

$k = 83.234998$

For Bayes factor k we need

1)

$$p(M_1|\underline{I}) = \int p(M_1, \beta|\underline{I})\ d\beta$$

hence simulate κ trajectories with β-values drawn from a prior $p(\beta)$ (can be just the uniform distribution between a β_{min} and a β_{max})

and count the number of times the simulations are at the data $\underline{I}$ (or η-near) irrespectively which β-value is used gives

$$\frac{\#\underline{I}|M_1}{\#M_1} =: \hat{p}(\underline{I}|M_1) \longrightarrow p(\underline{I}|M_1) = \int p(\underline{I}|\beta, M_1)p(\beta)\ d\beta$$

using the intuitive notation of $\#M_1 = \kappa$ as the number of simulations of model M_1 and for the number of hits of the data (or η-near) from runs of M_1 as $\#\underline{I}|M_1$

2) respectively

$$p(M_2|\underline{I}) = \int p(M_2, \lambda|\underline{I})\ d\lambda$$

For Bayes factor k we need

3)

$$k = \frac{p(M_1|\underline{I})}{p(M_2|\underline{I})} = \frac{p(\underline{I}|M_1)}{p(\underline{I}|M_2)} \cdot \underbrace{\frac{p(M_1)}{p(M_2)}}_{=1}$$

hence from the simulations we obtain

$$k = \frac{p(\underline{I}|M_1)}{p(\underline{I}|M_2)} \longleftarrow \frac{\left(\frac{\#\underline{I}|M_1}{\#M_1}\right)}{\left(\frac{\#\underline{I}|M_2}{\#M_2}\right)} = \frac{\#\underline{I}|M_1}{\#\underline{I}|M_2}$$

using the the same number of realizations from model M_1 and model M_2 with parameters each drawn from suitable priors counting the hits of the data $\underline{I}$ (or η-near) resulting simply in

$$\hat{k} = \frac{\#\underline{I}|M_1}{\#\underline{I}|M_2}$$

Numerical results

data (from linear infection model M_1 and $\beta = 2.0$) and model simulations from M_1 and M_2. the Poisson model

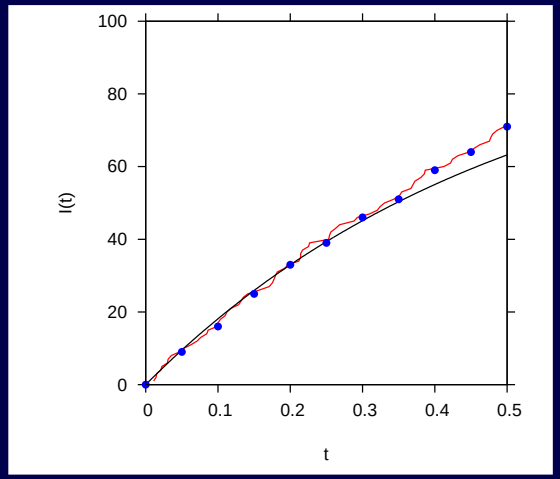

η-ball method internal parameters

$$\eta = 15 \quad , \quad \kappa = 10\,000$$

with $\kappa = \#M_1 = \#M_2$ as the number of simulations of model M_1 respectively M_2 gives Bayes factor

$$\hat{k} = \frac{\#\underline{I}|M_1}{\#\underline{I}|M_2} = \frac{1327}{1504} = 0.8823$$

compared to analytical value of $k = 0.650476$

Reduce $\eta \longrightarrow 0$ to improve

with η-ball method internal parameters

$$\eta = 15 \quad , \quad \kappa = 10\ 000$$

we had Bayes factor

$$\hat{k} = \frac{\#\underline{I}|M_1}{\#\underline{I}|M_2} = \frac{1327}{1504} = 0.8823$$

compared to analytical value of $k = 0.650476$

now with reduced η-ball size

$$\eta = 5 \quad , \quad \kappa = 10\ 000$$

we obtain Bayes factor

$$\hat{k} = \frac{\#\underline{I}|M_1}{\#\underline{I}|M_2} = \frac{101}{202} = 0.5$$

in better agreement with the analytical $k = 0.650476$

Prediction into future based on data $(I_0, I_1, ...I_n)$

Prediction into future based on data $(I_0, I_1, ...I_n)$

joint probability of data points gives likelihood e.g. for the linear infection model $L(\beta)$

$$p(I_n, t_n, I_{n-1}, t_{n-1}, ..., I_1, t_1, I_0, t_0|\beta) = \prod_{\nu=0}^{n-1} p(I_{\nu+1}, t_{\nu+1}|I_\nu, t_\nu, \beta) \cdot p(I_0, t_0)$$

$$= L(\beta)$$

and transition probability now into the future $t > t_n = t_{max}$ knowing I_n at t_n was already calculated previously :-)

$$p(I, t|I_n, t_n, \beta) = \begin{pmatrix} N - I_n \\ I - I_n \end{pmatrix} \left(e^{-\beta(t-t_n)}\right)^{N-I} \left(1 - e^{-\beta(t-t_n)}\right)^{I-I_n}$$

is a function of the estimated model parameter β

$$p(I, t|I_n, t_n, \beta) = p(I, t|I_n, t_n, \hat{\beta})$$

with maximum likelihood estimate $\hat{\beta}$ or any best value from the Bayesian posterior $p(\beta|\underline{I})$, maximum, median etc., inserted

Prediction into future based on data $(I_0, I_1, ...I_n)$

then best prediction $\hat{I}_{n+1}$ for next time step t_{n+1} given by maximum of $p(I_{n+1}, t_{n+1}|I_n, t_n, \hat{\beta})$

$$\frac{\partial}{\partial I_{n+1}} ln\ p(I_{n+1}, t_{n+1}|I_n, t_n, \hat{\beta})\Big|_{\hat{I}_{n+1}} = 0$$

using $x! = \Gamma(x+1)$ or for large values Stirling's formula $x! \approx e^{x\ ln(x)}$ and for quantifying the insecurity of this prediction use

$$p(I_{n+1}, t_{n+1}|I_n, t_n, \hat{\beta})$$

but:

Where is the insecurity

of the underlying previous data $(I_0, I_1, ...I_n)$???

Prediction into future based on data $(I_0, I_1, ...I_n)$

from the prediction probability $p(I_{n+1}, t_{n+1}|I_n, t_n, \hat{\beta})$ and the Bayesian posterior $p(\beta|\underline{I})$

$$p(\beta|\underline{I}) = p(\beta|I_1, I_2, ..., I_n)$$

we can construct a joint probability as the product

$$p(I_{n+1}, t_{n+1}|I_n, t_n, \beta) \cdot p(\beta|\underline{I}) = p(I_{n+1}, t_{n+1}, \beta|\underline{I})$$

and integrate over the model parameter β to obtain the prediction based on the underlying data only (and including the parameter insecurity naturally)

$$p(I_{n+1}, t_{n+1}|\underline{I}) = \int_0^\infty p(I_{n+1}, t_{n+1}|I_n, t_n, \beta) \cdot p(\beta|\underline{I})\, d\beta$$

and only in the limiting case of exactly known parameter $p(\beta|\underline{I}) := \delta(\beta - \hat{\beta})$ we obtain the previous result $p(I_{n+1}, t_{n+1}|\underline{I}, \hat{\beta})$.

Prediction into future based on data $(I_0, I_1, ...I_n)$

prediction probability $p(I_{n+1}, t_{n+1}|\underline{I})$ for the linear infection model (including parameter insecurity)

$$p(I_{n+1}, |\underline{I}) = \int_0^\infty p(I_{n+1}, t_{n+1}|I_n, t_n, \beta) \cdot p(\beta|\underline{I})\, d\beta$$

$$= \begin{pmatrix} N - I_n \\ I_{n+1} - I_n \end{pmatrix} \frac{B(a + I_{n+1} - I_n + k_2, b + N - I_{n+1} + k_3)}{B(a + k_2, b + k_3)}$$

again in terms of the beta-function, still depending on prior parameters but not explicitly on model parameter β, with $k_2 := \sum_{\nu=0}^{n-1}(I_{\nu+1} - I_\nu)$ and $k_3 := \sum_{\nu=0}^{n-1}(N - I_{\nu+1})$ only being data dependent

expected to have wide distribution in case of few data

Prediction into future based on data $(I_0, I_1, ...I_n)$

prediction probability $p(I_{n+1}, t_{n+1}|\underline{I})$ for the linear infection model (including parameter insecurity)

$$p(I_{n+1}, |\underline{I}) = \int_0^\infty p(I_{n+1}, t_{n+1}|I_n, t_n, \beta) \cdot p(\beta|\underline{I})\, d\beta$$

$$= \begin{pmatrix} N - I_n \\ I_{n+1} - I_n \end{pmatrix} \frac{B(a + I_{n+1} - I_n + k_2, b + N - I_{n+1} + k_3)}{B(a + k_2, b + k_3)}$$

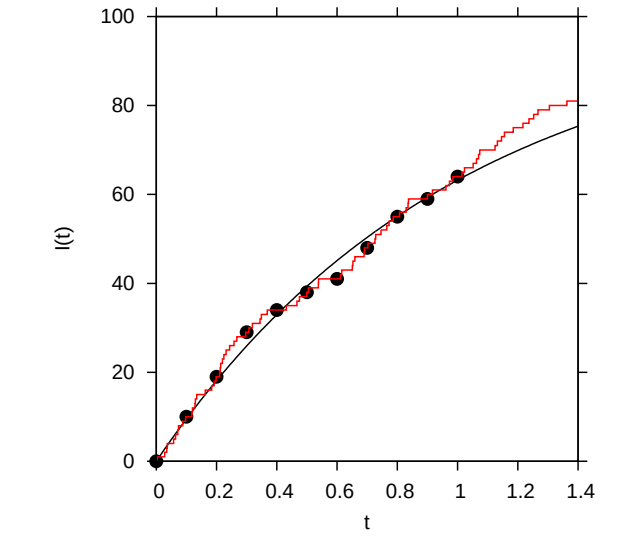

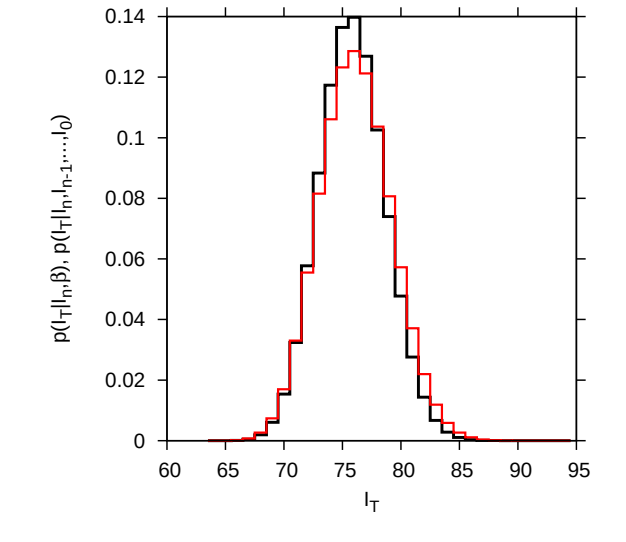

dynamics after data

prediction

Difference between $p(I_{n+1}|\hat{\beta})$ and $p(I_{n+1}|\underline{I})$ more pronounced in non-analytical models (e.g. SIS)

Computer practical in Biomaths-Lecture 2014: data from SIS system in η-ball method

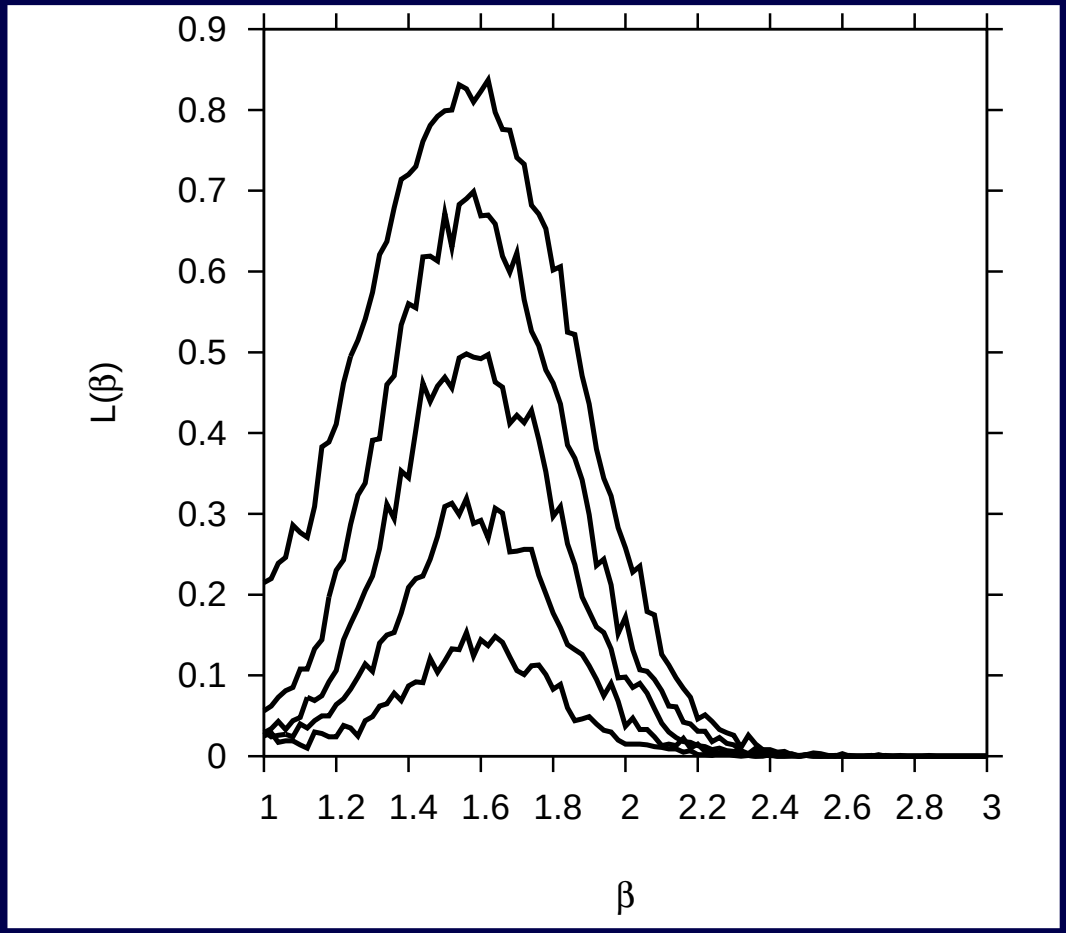

histogram of $p(||\underline{I}_{sim,k} - \underline{I}_{data}|| < \eta|\beta)$ for various η-values

Parameter estimation with SIS under η-ball: extended to prediction for I_{n+1} at time t_{n+1}

Parameter estimation with SIS under η-ball: extended to prediction for I_{n+1} at time t_{n+1}

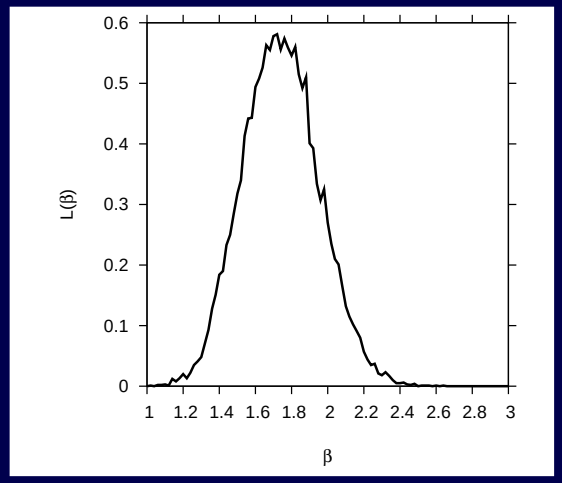

varying β

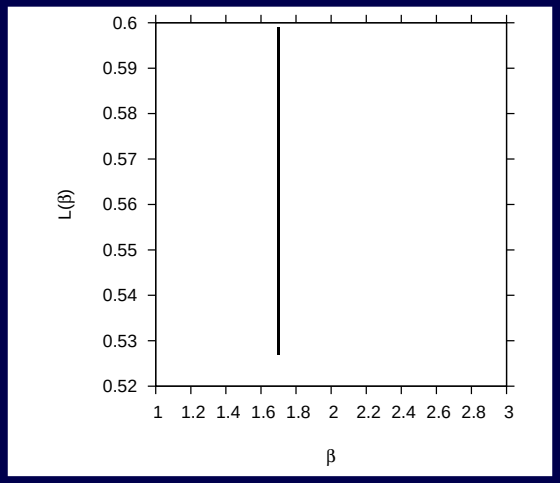

estimate $\hat{\beta}$

Parameter estimation with SIS under η-ball: extended to prediction for I_{n+1} at time t_{n+1}

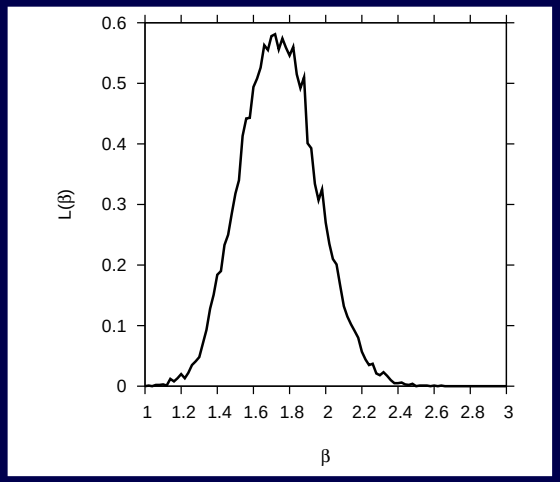

varying β

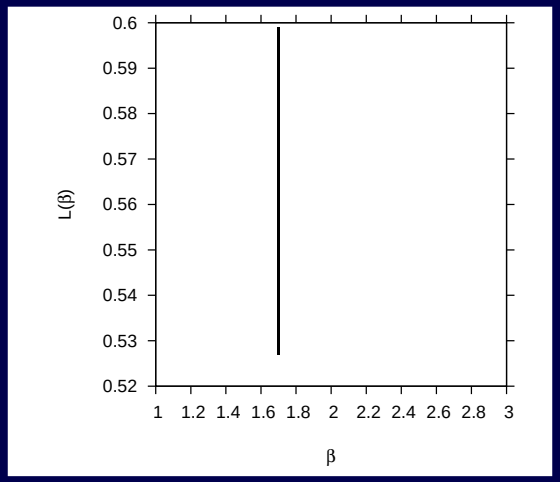

estimate $\hat{\beta}$

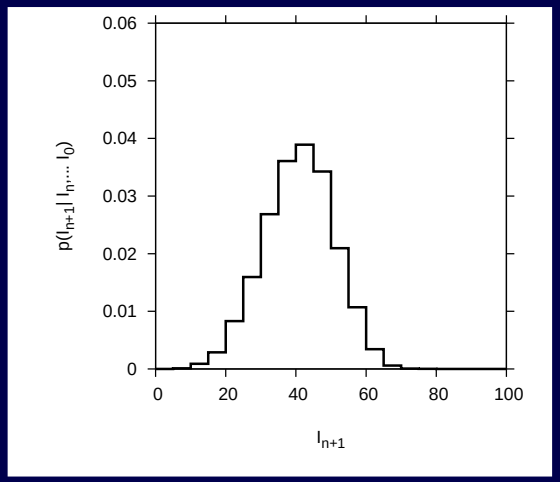

prediction
from various β

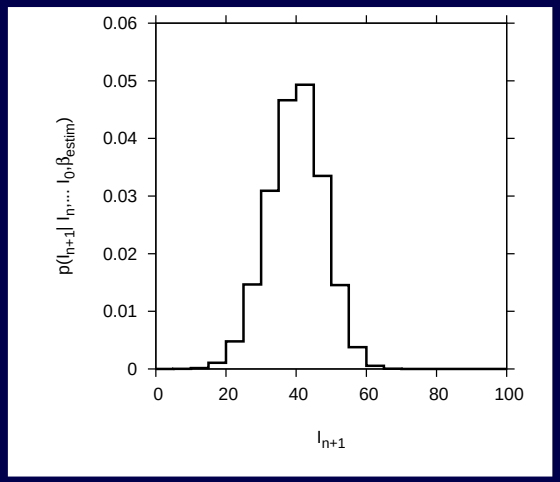

prediction
from estimate $\hat{\beta}$